

ELECTROCATALYTIC AND ANTIBACTERIAL APPLICATIONS OF SANDWICH
TYPE POLYOXOMETALATES

Except where reference is made to the work of others, the work described in this dissertation is my own or was done in collaboration with my advisory committee. This dissertation does not include proprietary, restricted or classified information.

Anand Venkatesh Sankarraj

Certificate of Approval

Vince Cammarata
Associate Professor
Chemistry and Biochemistry

Curtis Shannon, Chair
Professor
Chemistry and Biochemistry

Wei Zhan
Assistant Professor
Chemistry and Biochemistry

Thomas Albrecht-Schmitt
Professor
Chemistry and Biochemistry

George T. Flowers
Interim Dean
Graduate Schools

ELECTROCATALYTIC AND ANTIBACTERIAL APPLICATIONS OF SANDWICH
TYPE POLYOXOMETALATES

Anand Venkatesh Sankarraj

A Dissertation

Submitted to

the Graduate Faculty of

Auburn University

in Partial Fulfillment of the

Requirements for the

Degree of

Doctor of Philosophy

Auburn, Alabama
December 19, 2008

ELECTROCATALYTIC AND ANTIBACTERIAL APPLICATIONS OF SANDWICH
TYPE POLYOXOMETALATES

Anand Venkatesh Sankarraj

Permission is granted to Auburn University to make copies of this dissertation at its discretion, upon request of individuals or institutions and at their expense. The author reserves all publication rights.

Signature of Author

Date of Graduation

VITA

Anand Venkatesh Sankarraj, son of Mrs. Maheswari Sankarraj and Dr. S. Sankarraj was born on Dec 4, 1978 in Shencottah, Tirunelveli, Tamil Nadu, India. He is the eldest in the family with one younger sister, Dr. Anuradha. He obtained his high school diploma from Mahatma Montessori Matriculation School, Madurai in 1996. He gained admission into Central Electrochemical Research Institute (CECRI), a renowned national laboratory in India and graduated with a Bachelor of Technology in Chemical & Electrochemical Engineering in the year 2000. After a brief stint in the Chemical Engineering Department at Auburn University, he entered the Chemistry & Biochemistry Department at Auburn to pursue his Doctoral Degree in Analytical Chemistry in the year 2003 under the tutelage of Dr. Curtis Shannon.

ELECTROCATALYTIC AND ANTIBACTERIAL APPLICATIONS OF SANDWICH
TYPE POLYOXOMETALATES

Anand Venkatesh Sankarraj

Doctor of Philosophy, December 19, 2008
(B.Tech., Central Electrochemical Research Institute,
Madurai Kamaraj University, 2000)

164 Typed Pages

Directed by Curtis Shannon

The primary goal of this dissertation is to study the structure-property relationship of sandwich type polyoxometalates and to employ these versatile molecules in electrocatalytic applications such as oxygen generation and reduction. An attempt has been made to design novel catalysts by a systematic variation of the type of the substituted transition metal in the sandwich type polyoxometalate framework.

Chapter 1 presents an introduction to polyoxometalate structure and chemistry with a detailed literature review of the value added properties responsible for the catalytic activities of these POMs. A brief insight into the phenomenon of electrocatalysis is provided and the suitability of employing POMs as electron transfer mediators is discussed in detail.

Chapter 2 is a detailed outline of the synthesis and structural characterization of sandwich type polyoxometalates. The novel transition metal substituted sandwich type polyoxometalates were synthesized and characterized by the following analytical techniques - FTIR, Raman, UV-VIS, elemental analysis and single crystal XRD.

In chapter 3, a detailed discussion on the electrochemical properties of sandwich type polyoxometalates was provided along with some preliminary electrocatalytic applications.

Chapter 4 deals with the study of electrocatalysis of Ru₂POM for oxygen evolution reaction. In-situ detection of oxygen generated at the gold working electrode was performed with Clark oxygen sensor and rotating ring disc electrode studies. A detailed description of the measurement of oxygen concentration is provided.

Chapter 5 presents the application of electrochemical surface Plasmon resonance spectroscopy in studying the adsorption of sandwich type POMs onto gold electrodes as an elegant complementary technique to electrochemical quartz crystal microbalance method (EQCM) to probe the interfacial processes.

Chapter 6 represents the successful application of transition metal substituted polyoxometalates as co-catalysts for oxygen reduction reaction at several noble metal electrodes, such as gold, palladium and platinum. A simple thermodynamic model has been propounded as the basis for the choice of bimetallic catalysis.

Chapter 7 deals with the application of sandwich type polyoxometalates as antibacterial agents for poultry based pathogens such as Salmonella typhimurium and Listeria monocytogenes.

ACKNOWLEDGEMENTS

I am deeply indebted to my advisor Dr. Curtis Shannon for being such a great motivator and a generous human being, whose penchant for surface science and electrochemistry has fostered a conducive environment for creative research and development. He has been a pillar of support during the many trials and tribulations of my professional career. I would like to offer my sincere gratitude for his many thoughtful suggestions, both at the technical and personal level. I would like to acknowledge the immense contributions from my committee members, Dr. Vince Cammarata, Dr. Thomas Albrecht-Schmitt and Dr. Wei Zhan, in the direction of valuable suggestions and helpful insights in aiding the course of my research. Dr. Vince Cammarata and Dr. Eric Bakker were two of the best teachers during my graduate study at Auburn. I will always hold in fond memory, their dedication to teaching and remarkable ability to impart knowledge to the next generation. Dr. Albrecht-Schmitt had been a constant source of support in providing valuable technical inputs for my research and his group's help in XRD characterization, has been a launching pad for my work. Dr. Omar Oyarzabal of poultry science at Auburn has been a very encouraging presence to provide execution to my anti-bacterial applications. My professors at Central Electrochemical Research Institute (CECRI, India), Dr. K.R. Murali, Dr. Asokan and Dr. John Berchmans have been responsible for setting up the foundation for my research career.

I have received so much support from the faculty, administration assistants, and friends at the Chemistry Department at Auburn. I am very thankful to Mr. Tom Carrington for his helpful suggestions and assistance in setting up analytical instrumentation. My colleagues and friends in our research group have been very helpful at various stages of my study at Auburn and I would like to thank each one of them, Dr. Tsunghsueh Wu, Dr. Ugur Tamer, Dr. Yuming Chen, Dr. Lunsheng Zhang, Dr. Murat Alanyalioglu, Dr. Serdar Abaci, Ms. Junxua Xin, Mr. Chaokang Gu, Ms. Sridevi Ramakrishnan, Ms. Rajakumari Ramaswamy, Ms. Hongxia Zhang, Ms. Weiping Li, Ms. Tanyu Wang, and Ms. Yajiao Yu. I am very thankful to the help provided by Dr. Tyler Sullens, Dr. Travis Bray, Dr. Tatiana Shvareva and Ms. Anna Nelson in XRD analysis of my single crystals. Ms. Kauser Hussain has been very helpful in providing microbiological expertise and assistance for my work.

I would like to pay tribute to all my friends at Auburn, who have been more than a friendly ear or an encouraging word, Mr. Karthik Narayanan, Dr. Shankar Balasubramanian, Dr. Vivek Krishnan, Mr. Raghu Viswanathan, Mr. Narendhiren Pari, Ms. Kavita Arumugam, Mr. Varun Rupela, Dr. Pradeep Prasad, Dr. Ramkumar Krithivasan, Mr. Gopinath Balasubramanian, Mr. Eswar Sabapathy, Dr. Jitto Titus, Ms. Kauser Hussain, Mr. Tony Jefferson, Mr. Rajan Panchapakesan and Mr. Ranjit David. My mentor and good friend, Mr. Sankar Narayanan deserves special mention in shaping the course of my life and being a beacon of hope & encouragement to many more youngsters in India.

I would like to thank my parents and sister for their many sacrifices and for being extra supportive of my education since I was a kid. They have been a source of encouragement and unconditional love and I dedicate my work to their indomitable spirit.

Style manual or journal used: Journal of the American Chemical Society

Computer Software used: Microsoft Word 2003, Microsoft PowerPoint 2003, Microsoft Excel 2003, Origin Pro 7.5 and Endnote 9

TABLE OF CONTENTS

LIST OF TABLES	xii
LIST OF FIGURES	xiii
1. INTRODUCTION	1
1.1 Motivation for research.....	1
1.2 Background of electrocatalysis	2
1.3 Types of electrocatalytic mechanism.....	4
1.4 Polyoxometalate (POM) – Fundamental introduction.....	5
1.5 Sandwich type polyoxometalates.....	10
1.6 Electrochemistry of POMs – Structure/property relationship	12
1.7 Similarity to enzymes and porphyrins	15
1.8 Important value adding properties	16
1.9 References.....	18
2. SYNTHESIS AND STRUCTURAL CHARACTERIZATION OF SANDWICH TYPE POLYOXOMETALATES.....	20
2.1 Introduction.....	23
2.2 Materials and methods	23
2.3 Synthesis of sandwich type polyoxometalates.....	23
2.4 Structural characterization	28
2.5 Single crystal XRD Analysis	33

2.6 References.....	38
3. ELECTROCHEMICAL CHARACTERIZATION OF SANDWICH TYPE	
POLYOXOMETALATES.....	40
3.1 Introduction.....	40
3.2 Literature review.....	41
3.3 Materials and methods.....	44
3.4 Results and discussions.....	45
3.5 References.....	64
4. DIRUTHENIUM SUBSTITUTED POLYOXOMETALATE AS AN	
ELECTROCATALYST FOR OXYGEN GENERATION.....	68
4.1 Introduction.....	68
4.2 Materials and methods.....	72
4.3 Results and discussions.....	70
4.4 Conclusions.....	82
4.5. References.....	84
5. ELECTROCHEMICAL SURFACE PLASMON RESONANCE OF	
POLYOXOMETALATES.....	87
5.1 Introduction.....	87
5.2 Theoretical background on surface plasmon resonance.....	88
5.3 Electrochemical adsorption of Polyoxometalates on electrodes.....	90
5.4 Materials and methods.....	92
5.5 Results and discussions.....	95
5.6 References.....	105

6. POLYOXOMETALATES AS Co-CATALYSTS FOR OXYGEN REDUCTION....	108
6.1 Introduction.....	108
6.2 Materials and methods.....	112
6.3. Results and discussions.....	113
6.4 References.....	124
7. ANTIBACTERIAL APPLICATIONS OF SANDWICH-TYPE POLYOXOMETALATES.....	127
7.1 Introduction.....	127
7.2 Antibacterial properties of polyoxometalates.....	128
7.3 Toxicity.....	130
7.4 Materials and methods.....	131
7.5 Results and discussions.....	134
7.6 References.....	144
8. CONCLUSIONS AND RECOMMENDED FUTURE WORK.....	146

LIST OF TABLES

Table 2.1 Analytical Data for $\text{Na}_n[\text{ZnWM}_2\{\text{ZnW}_9\text{O}_{34}\}_2]$	29
Table 4.1 Literature Overview of Ruthenium Polyoxometalate Synthesis with Respect to the nature of precursor	71
Table 4.2 EDX Analysis of single crystal specimen of Ru_2POM	73

LIST OF FIGURES

Fig 1.1 Schematic of mediated electron transfer	5
Fig 1.2 Ball and stick model of sandwich-type polyoxometalate	12
Fig 2.1 Flowchart for the Synthesis of Ruthenium Substituted Polyoxometalate	25
Fig 2.2 Schematic representation of the central metal belt depicting the lattice position, where the transition metal substitution occurs during the formation of sandwich type bi-Keggin structures.....	26
Fig 2.3 Transmission FTIR data for solid sandwich POMs in a KBr pellet. Na _n [ZnWM ₂ {ZnW ₉ O ₃₄ } ₂], where M=Ru, Ir, Ni, Mn	31
Fig 2.4 Raman spectroscopic analysis of single crystals of Zn ₂ POM and Ru ₂ POM.....	31
Fig 2.5 UV-Vis of sandwich compounds.....	32
Fig 2.6 ORTEP plot (ellipsoids at 40% probability) of the X-ray structure of [Ru ^{III} ₂ Zn ₂ (H ₂ O) ₂ (ZnW ₉ O ₃₄) ₂] ¹⁴⁻	35
Fig 2.7 ORTEP plot of the X-ray structure of Single Crystal Ir ₂ POM.....	37
Fig 3.1 Cyclic voltammogram of 0.2mM Zn ₂ POM in pH=5 buffer solution, with Glassy Carbon as Working Electrode (W.E), Pt mesh as Counter Electrode (C.E) and Ag/AgCl as Reference Electrode (R.E), at a scan rate of 10mV/s	48
Fig 3.2 Cyclic voltammetry of 0.2mM Ru ₂ POM in pH=5 buffer solution.....	50
Fig 3.3 Cyclic voltammetry of Ruthenium oxidation peaks in pH5 acetate buffer solution with 0.2mM Ru ₂ POM	51
Fig 3.4 Cyclic voltammetry of Ir ₂ POM in pH=5 Buffer Solution	53
Fig 3.5 Comparison of L-Cysteine oxidation at iridium substituted sandwich POM and the precursor Zn ₂ POM, with GC as working electrode, Pt mesh as counter electrode and Ag/AgCl as reference electrode.....	54

Fig 3.6 Ascorbic acid oxidation in the presence and absence of iridium substituted sandwich type polyoxometalate.....	55
Fig 3.7 Voltammetric curve showing oxygen reduction reaction at di-iridium substituted sandwich POM at a GC electrode in pH5 acetate solution. Pt mesh as counter electrode and Ag/AgCl as reference electrode	56
Fig 3.8 Cyclic Voltammogram of Fe ₂ POM during the very first scan in 0.2mM solution at WE = GC, CE = Pt mesh.....	57
Fig 3.9 Polarization curves for oxygen generation reaction observed in pH = 5 Buffer solution at a Glassy Carbon (GC) electrode in the presence of different transition metal substituted Polyoxometalates (0.2mM). Counter electrode - Pt mesh and Reference electrode-Ag/AgCl (potential values are reported with respect to NHE).....	58
Fig 3.10 Electrochemical Surface Plasmon Response of Zn ₂ POM solution in 0.5 M Na ₂ SO ₄ corresponding to potential step from -0.2 V (adsorptive) to +0.6 V (desorptive).....	60
Fig.3.11 Cyclic voltammogram of 0.2 mM Zn ₂ POM in 0.1 M HClO ₄ solution.....	61
Fig.3.12 Schematic representation of the breakage of sandwich type clusters and the reasons for the changes to the trivacant lacunary sub-units could be any of the following three - 1. Very low concentration, 2. Low or high pH condition and 3. Species immobilized on electrode surface.....	63
Fig 4.1 pH stability analysis using UV-Vis spectroscopy in 0.5M Na ₂ SO ₄ (pH adjusted by HCl and NaOH).....	74
Fig 4.2 Cyclic Voltammetric studies depicting pH stability in terms of W redox peaks. At pH=9, the “W” reduction peaks are not well-defined, suggesting the breakdown of the compound. WE = Au, CE = Pt mesh, RE = Ag/AgCl, Scan rate 10mV/s.	75
Fig 4.3 Oxygen Evolution Reaction as a function of pH in 0.2 mM Ru ₂ POM. Au as WE, Pt Mesh as CE and Ag/AgCl as RE (represented w.r.t RHE)	76
Fig 4.4 Clark Sensor response for the measurement of electrocatalytic generation of oxygen from A) Au anode, B) Au anode + 2mM Zn ₂ POM, C) Au anode + Ru ₂ POM, D) Au anode and mono RuPOM.....	79
Fig 4.5 Schematic representation of Rotating Disc Electrode (RRDE) Assembly together with the bipotentiostat arrangement. Working electrode = polycrystalline Au electrode, Sensing element – Clark sensor or the Pt ring of the RRDE. Ag wire quasi-reference electrode (QRFE) was employed. The Counter Electrode (CE) was a high surface area platinum mesh. The second figure is the close-up photograph of the	

RRDE assembly	81
Fig 4.6 Electrochemical generation of O ₂ at pH 8 using di-RuPOM catalyst characterized using a Rotating Ring Disc Electrode (RRDE). Disc current (upper trace) and ring current (lower trace) were acquired simultaneously. The rotation rate was 1600RPM and the geometrical area of the disc was 0.27 cm ² . The inset shows an expanded view of one set of pulses.....	82
Fig 5.1 Schematic representation of the experimental set-up showing the modified Spreeta™ as the working electrode, Pt mesh as counter electrode and Ag/AgCl as Reference electrode.....	94
Fig 5.2 a) Spontaneous adsorption from a solution of 0.2 mM Ru ₂ POM in 0.5 M Na ₂ SO ₄ . b) Comparison of SPR response for Ru ₂ POM and Zn ₂ POM on gold electrode.....	97
Fig 5.3 ESPR response in 0.1 M HClO ₄ superimposed with the corresponding cyclic voltammetry	99
Fig 5.4 Electrochemical surface plasmon resonance of 0.2mM Keggin (SiW ₁₂ O ₄₀ ⁴⁻) in pH4 supporting electrolyte (0.1M NaClO ₄ + HClO ₄) solution. The upper graph shows cyclic voltammetry behavior and the bottom graph is the corresponding ESPR response	98
Fig 5.5 ESPR response corresponding to the growth curves shown in Fig 5.6 in 0.4 mM Zn ₂ POM during potential cycling.	102
Fig 5.6 Potential Stability testing of the electro-adsorbed film in 0.4 mM Ru ₂ POM solution in 0.5 M Na ₂ SO ₄	104
Fig 6.1 Schematic diagram depicting the efficiency losses observed during the operation of a typical fuel cell	109
Fig 6.2 Comparison of polarization curves for the oxygen reduction reaction (ORR) on several transition metal substituted sandwich type polyoxometalates at a glassy carbon electrode (3.0mM Diameter). Supporting electrolyte – pH = 5 acetate buffer, Pt mesh as counter electrode, Ag/AgCl as reference electrode. Scan rate – 10mV/s.....	114
Fig 6.3 Thermodynamic correlation between the free energy of M-O bond formation and the E _{1/2} for ORR at the transition metal substituted sandwich POM solutions.....	115
Fig 6.4 Comparison of polarization curves for ORR at different transition metal substituted Wells-Dawson POM solutions at GC (3.0mM Dia) electrode in 0.1M HClO ₄ solution (pH=1). Pt mesh as counter electrode and Ag/AgCl as reference electrode. (Reported in terms of RHE) Scan rate – 10mV/s.....	116

Fig 6.5 Voltammetric scans at an Au electrode immersed in O ₂ saturated 0.1 M HClO ₄ . POM concentrations were [WPOM] = [FePOM] = [RuPOM] = 0.2 mM and [CoPOM] = 0.2 μM. Scan rate: 10 mV/sec. Inset: Plot of maximum observed ORR potential shift, ΔE ^{o'} vs. ΔH ^o _f of the corresponding bulk oxide	117
Fig 6.6 Voltammetric response of a Pd electrode immersed in O ₂ saturated 0.1 M HClO ₄ . POM concentrations were [WPOM] = [FePOM] = [RuPOM] = 0.2 mM and [CoPOM] = 0.2 μM. Scan rate: 10 mV/sec.....	121
Fig 6.7 The voltammetric response of a Pt electrode in O ₂ saturated 0.1 M HClO ₄ as a function of [CoPOM]. Scan rate: 10 mV/sec. Inset: plot of ΔE ^{o'} versus [CoPOM]	122
Fig 6.8 Voltammetric response of a Pt electrode in O ₂ saturated 0.1 M HClO ₄ containing the noted concentrations of PW ₁₂ O ₄₀ ³⁻ and PCoW ₁₁ O ₃₉ ⁵⁻ . Scan rate: 10 mV/sec. Inset: plot of ΔE ^{o'} versus [CoPOM].....	123
Fig 7.1 Cyclic voltammetry comparison of L-cysteine oxidation at V keggin, Zn ₂ POM and V ₂ POM	134
Fig 7.2 Microdisc method of qualitative analysis of bacteriostatic activity for Staphylococcus aureus strain in the presence of silver nanoparticles, V Keggin and V sandwich polyoxometalate.....	136
Fig 7.3 Bacteriostatic activity of the precursor compound Zn ₂ POM, in an agar medium containing a 10 ⁵ to 10 ⁷ CFU/ml of <i>Staphylococcus aureus</i> (S.A).....	137
Fig 7.4 Microdisc method for the study of bacteriostatic effect of Zn ₂ POM on <i>Salmonella typhimurium</i> (S.T).....	138
Fig 7.5 Microdisc method to study the bacteriostatic effect of POMs on 10 ⁵ to 10 ⁷ CFU/ml <i>Salmonella typhimurium</i>	139
Fig 7.6 Microdisc method elucidating the bacteriostatic property of Zn ₂ POM under different concentrations	140
Fig 7.7 Microdisc method to evaluate the bacteriostatic activity of Vanadium POMs and precursor in <i>Listeria monocytogenes</i> agar culture plate	141
Fig 7.8 Time killing assay analysis of <i>Listeria monocytogenes</i> as a function of exposure to V Keggin and V sandwich POMs.....	142
Fig 7.9 Time killing assay analysis of <i>Salmonella typhimurium</i> as a function of exposure to V Keggin and V sandwich POMs.....	142

CHAPTER 1

1. Introduction

1.1. Motivation for Research

In today's world, the energy crisis and global warming are two major challenges facing the scientific community. Industries and common households have become increasingly dependent on energy for even the simplest processes and oil plays the most important role as a driving force for the different economies of the modern world. In this scenario, there are a couple of alternatives available to scientists – one to develop more efficient technologies employing oil based systems and the other to develop alternative systems. From a chemistry standpoint, all the systems – the industrial machinery, the automobiles and the day today home appliances can be envisioned as reactors. In these reactors, the catalyst plays the main role in dictating the efficiency and environmental viability. Hence numerous groups around the world today are striving tirelessly to develop novel and non-conventional catalyst technologies. In this context, we have embarked on a journey to develop novel catalysts for alternative energy systems, i.e. polyoxometalates for fuel cell applications.

Polyoxometalates are a unique class of molecular metal-oxide clusters, which have interesting properties in terms of catalysis. In this work, an effort has been made to design novel polyoxometalate structures to address specific electrocatalytic

applications. Since polyoxometalates are regarded as models for bulk metal oxide catalysts, we have endeavored to replicate the electrocatalytic properties of the latter in the molecular scale of polyoxometalates to achieve distinctive advantages in terms of ease of synthesis, reliability and energy efficiency, amongst others.

1.2. Background of Electrocatalysis

In chemistry, catalysis is defined as the acceleration of rate of chemical reactions by contacting with substances (catalysts), which do not themselves show a permanent chemical change. These catalysts lower the activation energy of the chemical reaction, thus increasing the rate. Depending on the phase of the catalyst and substrate, there are two type of catalysis – heterogeneous (catalyst and substrate are in different phases) and homogeneous (both are in the same phase). In electrocatalysis, the catalytic reactions involve reactant and product species transferring electrons through an electrolyte – catalyst interface. Thus electrocatalysis applies to the influence of electrode material and the state of electrode surfaces on the behavior of chemical-catalyzed steps, which are coupled with electron transfer processes.

The important difference of electrochemistry from other heterogeneous catalytic systems is the use of electrode potential as rate-influencing factor. Changes in electrode potential, over relatively small ranges can cause very large changes in rate for a given reaction, for e.g. about 400 mV can cause three to ten orders of rate increase¹. Such a large change in rate is not possible for reactions occurring in solution, since under isothermal conditions, the only available variable will be concentration change or pressure change for gases. The only parameter exerting this

kind of influence on the reaction rate is temperature, which can be considered as an analog to electrode potential. A temperature perturbation will change the rates of reactions according to their activation energies, however, a variation of ten orders of magnitude will require a temperature increase of several hundred degrees (for processes at higher end of activation energies) Thus at these higher temperatures, side reactions (bond breaking, polymerization) becomes important.

Further for selectivity, (to differentiate chemical steps of varying activation energies), wide variations in temperature are needed, but in electrocatalysis, a mere change in potential will accomplish the effect. The selectivity of rates between different processes will be related to their different potential sensitivities (Difference between their Tafel slopes)

The advantages of electrocatalysis can be summarized as follows¹:

1. Employing the potential variable, there is an ease of control in the rate of reaction and novel routes of synthesis of certain organic materials with high specificity is achieved
2. Due to great specificity at high rates, there is higher energy efficiency than thermal preparation routes
3. There is a possibility of direct energy conversion of free energy of combustion into dc electricity using fuel cells. This process of energy conversion requires the maximum possible reaction rates close to the equilibrium potential for anodic and cathodic reactions.

1.3. Types of Electrocatalytic mechanism

The main objective of catalysis is to increase the rate of a reaction and in this context; electrocatalysis is aimed towards increasing the rate of an electrochemical reaction or in other terms to reduce the overpotential of a given reaction. Electrocatalysis can be divided into two types – Homogeneous electrocatalysis and Heterogeneous electrocatalysis.

In homogeneous electrocatalysis, the catalytic species is in solution and aids in the increased electron transfer between the electrode and substrate. In the case of a reduction reaction, electron transfer occurs between the reduced catalyst and the substrate, thus regenerating the catalyst. Assuming simple reaction schemes, homogeneous electrocatalysis has two mechanistic routes-

- (i) The catalyst behaves purely as an electron mediator between electrode surface and the substrate in solution, where a direct redox electron transfer occurs, and this type of catalysis is termed “redox catalysis”.
- (ii) In the second case, an unstable adduct is formed between the reduced catalyst and substrate, and this adduct undergoes decomposition after reduction in the electrode surface or solution to regenerate the catalyst. This type is termed “chemical catalysis”

In heterogeneous electrocatalysis, the electrocatalyst is immobilized onto the electrode surface and aids in facile electron transfer with the substrate. The usual routes of catalyst immobilization are electrodeposition, polymer encapsulation, physisorption, coating and layer by layer electrostatic methods.

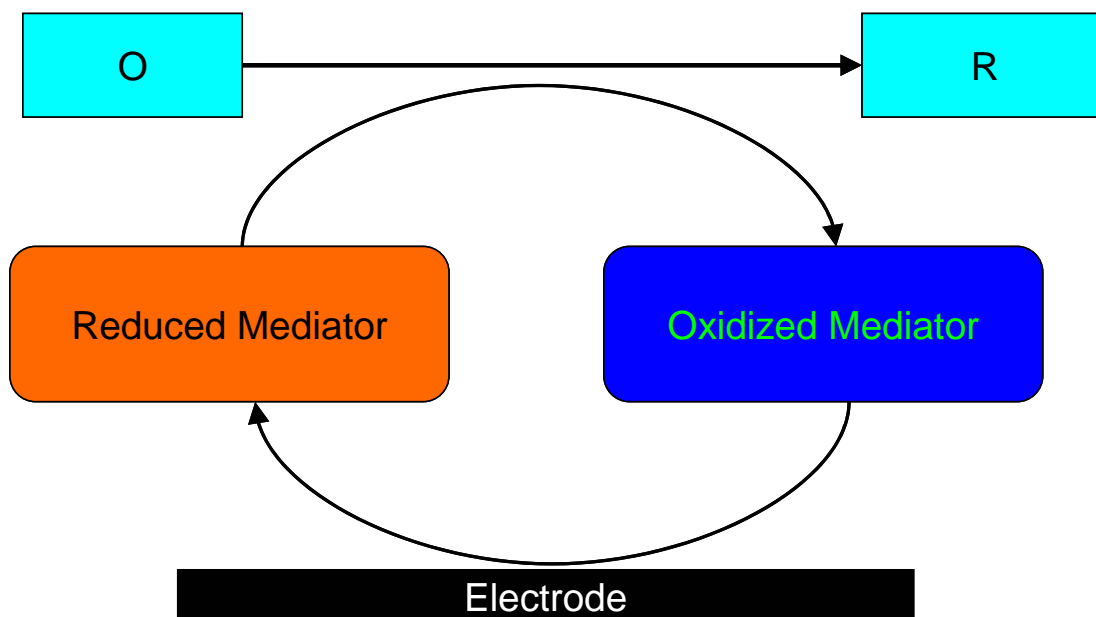


Fig.1.1. Schematic of mediated electron transfer

1.4. Polyoxometalate – Fundamental Introduction

Polyoxometalates (POMs) are discrete nanometer sized metal oxide clusters, which are formed via self assembly of monomeric oxoanions in acidic solutions and are very unique in terms of structure and properties. These inorganic metal-oxygen cluster anions have been studied from the times of Berzelius, Werner and Pauling (1826 – 1929). However, the first structure to be fully characterized by XRD, in the year 1933 by Keggin, and hence these structures, $(\text{H}_3\text{PW}_{12}\text{O}_{40} \cdot 29\text{H}_2\text{O})$, were named after the scientist. The Keggin structures are the best known polyoxometalate structures, which can form many different structures and constitute the most stable and easily available compounds in this class of POMs.

Polyoxometalate metal-oxygen clusters contain highly symmetrical assemblies of MO_x core units, which form a variety of quasi-spherical structures. Usually the formulas of these polyanions are as follows:



According to Pope², metal M is termed as the “addenda atom”, usually the transition metals from group V and VI. There appears to be a natural limitation dictated by a combination of ionic radius, charge and the ability to form dII-pII M-O bonds. There seems to be an abundance of W and Mo clusters in literature, while group V compounds come second and the Ta & Nb compounds are slowly gaining more significance. The atom X, termed as the “heteroatom” does not have any such restrictions and hence almost all the elements in the periodic table can form these heteropolyanions.

In their consideration of polyoxometalate structures, Pope and Muller³ have suggested that almost all these POM structures can be considered to have originated from three highly symmetrical “parent” polyanions; a. with a tetrahedron (Keggin, T_d symmetry), b. with an octahedron (Anderson Evans anion $[\text{XM}_{12}\text{O}_{38}]$, (O_h) and c. with an icosahedron (Dexter Silverton structure, I_h) as the central polyhedron XO_n ($n = 4, 6$ or 12)

Keggin Polyoxometalate Units

Keggin structures are spherical molecules (diameter of $\sim 1.2\text{nm}$), represented by the molecular formula, $[\text{XW}_{12}\text{O}_{40}]^{x-8}$, where X is the heteroatom, x is the oxidation state and M is the addenda atom (W or Mo), with an observed density for $(\text{H}_5\text{O}_2)_3 \cdot [\text{PW}_{12}\text{O}_{40}]$ as 5.6 g cm^{-3} . This well known structure of the POM family has a significant number of derivatives and the rich catalytic properties of these have made

them very relevant in many industrial applications. A central tetrahedron XO_4 surrounded by 12 edge and corner-sharing MO_6 octahedra. Each octahedron is arranged in four M_3O_{13} groups. Each group is formed by three octahedra sharing edges and having a common oxygen atom, which is also shared with the central tetrahedron XO_4 . There is a total association of 40 close-packed oxygen atoms and these can be divided into four types based on their position in the matrix⁴;

- Twelve $M=O$,
- Twelve edge bridging angular $M-O-M$ shared by the octahedral within a M_3O_{13} group
- Twelve corner-bridging quasi-linear $M-O-M$ connecting two different M_3O_{13} groups
- Four internal $X-O-M$ atoms

Each of these oxygen atoms can be individually addressed by ^{17}O NMR and the metal-oxygen bonds provide the signature peaks in the range of 600 to 1100 cm^{-1} in infrared spectroscopy. Each of the M_3O_{13} units can be rotated 60° about its 3-fold axis and forms geometrical isomers – the most common is the α -isomer, and the modification of this structure by means of the number of M_3O_{13} units undergoing rotations gives rise to the new isomers, β -isomer (one M_3O_{13} rotated), γ (two M_3O_{13} rotated) , δ (three M_3O_{13} rotated) , and four M_3O_{13} rotated forms ϵ -isomer. Lacunary Keggin molecules or “Keggin with holes” can be formed from the removal of one or more M atoms. Of the trivacant lacunary structures, if there is a removal of one corner-sharing MO_6 octahedron from each of three bridging M_3O_{13} triads, it is called as A-type and if there is a removal of one entire M_3O_{13} triad, it is called as B-type⁴.

Such lacunary species can assemble into larger polyoxometalate structures, by direct assembly or by the incorporation of metal ion linkers. A significant amount of research has been devoted to the study of trivacant lacunary Keggin moieties because they form the largest possible planar minisurface on the plenary $XW_{12}O_{40}^{n-}$ POM. As mentioned by Finke⁵, the interaction of trivacant lacunary species with different TM atoms can result in structures which could aid in the establishment of POMs as models for bulk metal oxide structures. These structures can form Keggin or Wells-Dawson based sandwich type polyoxometalates. These Keggin units have one terminal oxygen atom $M=O$ per each addenda atom, and hence they can participate in facile redox reactions.

Polyoxometalate structures can accommodate transition metals into their framework and can form the famous transition metal substituted frameworks similar to the organometallic structures. The high negative charges of polyoxometalates are known to stabilize these transition metal atoms. Pope et al⁶ were the first group to show that it was possible to replace one of the tungsten atoms and the terminal oxo-group by a transition metal atom cation. These transition metal cations possess five bridging oxygen atoms and the sixth coordination site has been shown to be occupied by a water molecule.⁷ The sixth coordination site with the labile water molecule is considered to serve as an entry to inner-sphere electron transfer pathways, which are usually inaccessible in the unsubstituted anions. Though they are completely inorganic in nature, these transition metal substituted polyanions have been shown to exhibit catalytic chemistry similar to metalloporphyrins^{8, 9}. The potential for electrocatalytic applications has been very favorable due to the nature of inner-sphere

as well as outer-sphere electron transfer catalysis. Several transition metal-substituted POMs have been synthesized since and the focus towards catalytic applications has been driving this field.

In terms of catalytic applications, transition metal substituted polyanions (TMSP) attract a lot of attention, because they can be systematically modified on the molecular scale; on the basis of size, shape, charge density, acidity, redox activity, stability, solubility, etc ^{2, 3, 10}. All these properties contribute favorably towards interesting chemical properties, leading to versatile catalytic platforms. Of all the commonly occurring TMSP, the class of polyoxotungstates plays a major role in a lot of these catalytic interests because they are structurally more stable than molybdates. Within the Polyoxotungstates, the Keggin anion and its defect fragments are the basis for the structurally diverse molecules³. These defect fragments form mono-, di- and tri-metal substituted derivatives, and together with Dawson substituted derivatives are the most predominant TMSP molecules. The mono substituted Keggin derivatives have been considered to be inorganic analogs of porphyrin structures, and they are unique in being rigid, hydrolytically stable and thermally robust than their organic counterparts⁹. The oxidation resistant tungsten-oxo framework acts as a multidendate ligand for transition metals and hence these TMSPs behave similar to organometallic clusters¹¹, but without the organic framework, which makes them much more stable during catalysis. The main problem observed in metal organic clusters during reactions is auto-oxidation of the framework leading to structural collapse and loss of activity; in this regard the fully inorganic polyanion structure can provide a more stable platform.

1.5. Sandwich Type Polyoxometalates

Among the transition metal substituted polyoxometalates, sandwich type structures are very important in the sense that they are similar in construction to naturally occurring enzymes and cofactors. Keggin and Wells Dawson structures have a predisposition to form these sandwich type structures. Trivacant Keggin fragments, often called as the trilacunary species undergo self-assembly to form the dimeric polyoxometalate framework - the sandwich structure, also called as Weakley or Tourne structures. These sandwich structures formed by the α -B Keggin fragments can be divided into two subgroups¹² –

1. Central heteroatom X with a lone pair of electrons, forms anions of the formula



2. Central heteroatom with no lone pair, forms



Several other anions are reported, where the positions of the transition metal are partially or completely occupied by tungsten atoms¹³, e.g., $[\text{Zn}_3\text{W}(\text{H}_2\text{O})_2(\text{ZnW}_9\text{O}_{34})_2]^{12-}$, and in this structure, $\text{ZnW}_9\text{O}_{34}^{-12}$ is the trivacant lacunary Keggin structure formed by the removal of “ $\text{W}_3\text{O}_6^{6+}$ ” from the Keggin parent $\text{ZnW}_{12}\text{O}_{40}^{-6}$. The removal of three tungsten atoms is the origin to the nomenclature of “trivacant” lacunary. Since the several metal centers in these complexes could be activated independently, there is a need for evaluating the potential of these compounds as electrocatalysts.

The water molecules bonded to the metal atoms can be replaced by other organic solvents or sometimes by chloride ions $[\text{Cd}_4\text{Cl}_2(\text{AsW}_9\text{O}_{34})_2]^{12-}$ ¹⁴. The sandwich compounds, as shown in Figure 1.2 are structurally related to the family of tetranuclear divalent sandwich complexes $[\text{M}^{\text{II}}_4(\text{H}_2\text{O})_2(\text{PW}_9\text{O}_{34})_2]^{10-}$ M= Co, Cu, Zn, Mn, and were first reported by Weakley, Tourne and co-workers¹⁵. These sandwich structures based on the B-Type trivacant derivatives of the parent Keggin compound were later characterized by Finke⁵, Weakley¹⁶ and Gomez-Garcia et al¹⁷. Pope and co-workers¹⁸ have reported a mixed valence $\text{Mn}^{\text{II,III}}$ Keggin sandwich and Craig Hill¹⁹ reported the very first sandwich compound with trivalent metal ions in the center, $[(n\text{-C}_4\text{H}_9)_4\text{N}]_6[\text{Fe}^{\text{III}}_4(\text{H}_2\text{O})_2(\text{PW}_9\text{O}_{34})_2]$. Following these reports, there has been a steady increase in the number of transition metal substituted polyoxometalates. Recently noble metal substituted sandwich type structures are gaining in importance and Neuman et al²⁰⁻²³ have paved the way for the development of ruthenium, palladium and platinum based sandwich type structures.

The incorporation of a variety of metals is an important motivation in polyoxometalate chemistry and this makes it possible to obtain structures with different chemical properties, ultimately providing catalysts with different efficiencies.

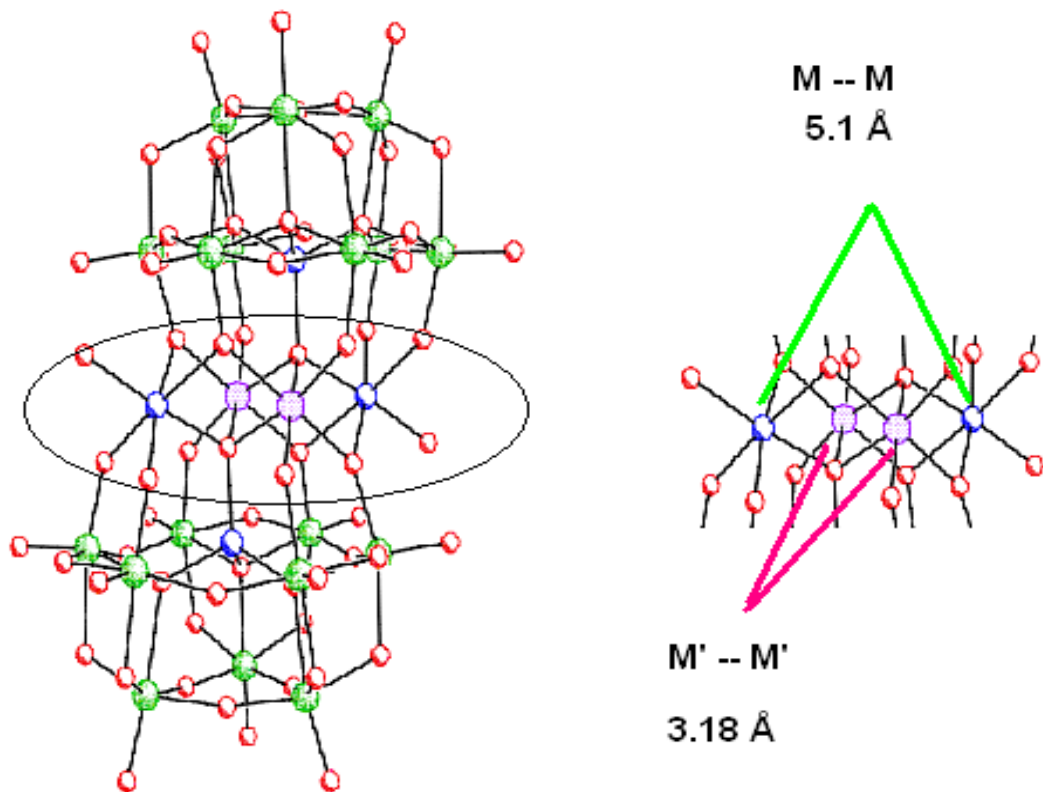


Fig.1. 2. Ball and stick model of sandwich-type polyoxometalate

1.6. Electrochemistry of Polyoxometalates – Structure/Property Relationships

The structure of polyoxometalates, are governed by well-known electrostatic and radius ratio rules observed for extended ionic lattices. All polyoxometalate structures are known to be governed by two general principles, according to Pope²,

1. Each metal atom occupies a MO_x co-ordination octahedra or square pyramid, where the metal atoms are displaced because of M-O π bonding, towards the vertices
2. Structures with MO_6 octahedra with three or more free vertices are not observed (according to Lipscomb²⁴)

According to first principles, the metal atoms M are never located at inversion centers, since they are displaced towards one side. On the basis of the displacement of metal atom within the MO_6 octahedra, polyoxometalates are divided into two types,

1. Type I or Mono-oxo, the metal atom displacement occurs towards one, always terminal oxygen atom, called as mono-oxo compound (C_{4v}), (these compounds can accommodate addenda atoms with d^0 , d^1 and d^2 electronic configuration)
2. Type II or cis-dioxo, the metal atom displacement occurs towards two cis, usually but not always, terminal oxygen atoms, (these compounds can accommodate only d^0 metals)

In the case of the type I POM, there is an absence of in-plane π bonding and the LUMO are normally non-bonding and is metal centered (d_{xy} orbital). Thus the type I Keggin anions are easily reduced to mixed valence species forming colored solutions, commonly called as heteropoly “blues” and “browns”, and these reduced species maintain the overall architecture of oxidized anions. There is a structural affinity to accommodate electrons into the framework and hence the type I Keggin atoms have reversible redox properties. From extended Huckel and $X\alpha$ calculations, the density of states in the LUMO is supposed to increase, and cause the HOMO-LUMO gap to decrease, with the aggregation of MO_6 octahedra. Thus type I compounds have predominantly shown “heteropoly blue” formation in their reduced state. Keggin ($XM_{12}O_{40}$), Dawson ($X_2M_{18}O_{62}$), hexametallate (M_6O_{19}), decatungstate ($W_{10}O_{62}$) and related structures belong to this type I category and form the famous heteropoly blues, and have been historically employed in analytical applications.

For the type II POM, the LUMO is strongly antibonding with respect to terminal M-O bonds. Thus these structures are reduced irreversibly and there is an accompanied structural modification forming complex species, which are yet to be identified. Thus type II compounds such as the Anderson structure ($\text{XMo}_6\text{O}_{24}$), do not form heteropoly blues. The color of the heteropoly blues are the result of the mixed valence species formed due to reduction of MO_6 octahedra, i.e., reduction of the addenda atom. If a substituted transition metal is present in the crystal lattice, and then there is a possibility of a change in the intensity of color change, pertaining to the nature of the transition metal. It has been observed from the redox properties of polyoxometalates - the reducibility is governed by the electronic structure of the individual MO_6 octahedra, and this has been suggested to prove that the bonding in polyanions is not entirely delocalized as seen in organic aromatic systems. As an additional evidence for this difference in delocalization, the possibility of observing the diamagnetic susceptibilities of some select polyanions just by studying the simple building blocks such as MoO_4^{2-} , WO_4^{2-} and of the heteroatom has been provided^{2,25}.

In the type I form, which is more electrochemically active with reproducible redox features, oxidation ability of addenda atoms can be adjusted by the following order $\text{V}(+5) > \text{Mo}(+6) > \text{W}(+6)$. In the case of one electron transfer to a mixed addenda polyoxometalate species, the electron is localized at the more reducible atom at room temperature²⁶. The metals incorporated in the heteropolyanion reside in an octahedral environment, in which one of the coordination sites is occupied by a solvent molecule.

Since these systems are investigated in aqueous solutions, and during electrochemical cycling, the following sequential redox states are possible for the central metal atom: metal (III) with aqua ligand reduced to metal (II) with aqua ligand, which is oxidized to oxometal (III) then to hydroxo metal (IV) , and finally to oxometal (V), for some metals like Re, it is possible to get into (VI) – (VII) oxidation states. The hydroxo metal and oxometal species are important for oxidative synthesis. The formal redox potential depends on a lot of factors, of which the nature of addenda and hetero-ions are important. For example, the redox potential of incorporated metal increases as a function of formal charge on the hetero-ion, A. For a given oxidation state, the redox potential increases with the size and decreasing electronegativity of X. The redox potential of Mn (III/II) increases with X, where $X = B < Zn < Si < Ge < P$. In polar solvents, POMs are deprotonated and could be easily wet-impregnated on modified SiO₂ with methanol as the solvent. Thus POMs can be easily impregnated onto traditional catalytic supports.

1.7. Similarity to Enzymes and Porphyrins

The development of new and efficient catalysts for multi-electron transfer has been one of the reasons for transition metal substituted polyoxometalates (TMSP)² to be employed in electrocatalysis. In this context, these TMSPs have been modeled on transition metal centered organic complexes similar to enzymes available in nature. A number of organometallic compounds have been developed to simulate metalloenzymes and POMs have been identified as viable models²⁷ (biomimesis) for oxidation processes of great biochemical importance.

Galli et al²⁷ have shown that $[\alpha\text{-SiVW}_{11}\text{O}_{40}]^{5-}$ and $[\alpha\text{-SiMnW}_{11}(\text{H}_2\text{O})\text{O}_{39}]^{5-}$ can act as biomimetic simulants of laccases, well-known fungal enzymes belonging to the class of phenol oxidases. Laccases are multi-copper oxidases, which catalyze the one-electron oxidation of phenols in lignins, with a concomitant reduction of dioxygen to water. The authors had matched the redox potential of the POMs with that of the fungal enzyme in aqueous solution to accurately identify the active species. They were successful in performing kinetic studies to determine the mechanism of activity in laccases.

1.8. Important Value Adding Properties of Polyoxometalates – Reasons for Choosing this System of Catalysis

Polyoxometalates exhibit several interesting value adding properties, which make them as ideal candidates for catalytic applications, a summary of these properties along with some industrial applications are provided below:

1. Diverse molecular compositions – Starting from a single structural entity, a variety of molecular compositions can be accomplished by very minimal changes in transition metal and proton concentration (pH changes) – Makes them suitable as models for fundamental applications.
2. Reproducible symmetric structures – All these polyanions are formed by self-assembly in solution and they exhibit a unique nature of reproducibility in terms of symmetry of structures. Symmetry of transition metal placement in TMSP has been responsible for a variety of magnetic and electrochemical applications.

3. They are soluble in aqueous and non-aqueous solvents, they maintain their structural integrity in solution form; thus making them ideal for both homogeneous and heterogeneous catalysis.
4. Ability to accept multiple electrons without structural modification and very good redox reversibility makes them “tailor-made” for electrocatalysis. The possibility of tunable redox potentials by the mere process of replacing the substituted transition metals is also an important reason for interest in electrocatalysis.
5. Strong acidity and inert nature of the metal-oxo bond makes them chemically and to some extent thermally stable – important for considerations in catalysis
6. Relatively low cost and ease of synthesis makes them suitable for development of novel catalytic systems for conventional reactions, e.g. epoxidation of alkenes^{20, 23}.
7. Polyoxometalates can be easily embedded onto support matrices such as carbon, silica and zeolites, thus making them good candidates for heterogeneous catalysis.

Thus, polyoxometalate comprise an elegant class of catalytic metal oxide clusters and the study of these structures in the context of electrocatalysis is explored in the following chapters.

References

1. Appleby, A. J., *Comprehensive Treatise of Electrochemistry* Plenum press: 1983; Vol. 7.
2. Pope, M. T., *Heteropoly and Isopoly Oxometalates*. Springer-Verlag: 1983.
3. Pope, M. T.; Muller, A., *Angew.chem.Int.Ed.Engl.* **1991**, 30, 34-48.
4. Kozhevnikov, I., *Catalysis by Polyoxometalates*. John Wiley and Sons, Ltd: 2002; Vol. 2.
5. Finke, R. G.; Droege, M.; Hutchinson, J. R.; Gansow, O., *J. Am. Chem.Soc* **1981**, 103, 1587-1589.
6. Baker, L. C. W.; Baker, V. E. S.; Eriks, K.; Pope, M. T.; Shibatha, M.; Rollins, O. W.; Fang, J. H.; Kohn.L.L., *J. Am. Chem.Soc* **1966**, 88, 2329.
7. Weakley, T. J. R., *J.Chem.Soc.Dalton Trans* **1973**, 341.
8. Katsoulis, D. E.; Pope, M. T., *J.Am.Chem.Soc* **1984**, 106, 2327.
9. Hill, C. L.; Brown, R. B., *J. Am. Chem. Soc.* **1986**, 108, 536.
10. Keita, B.; Mbomekalle, I. M.; Nadjo, L.; Haut, C., *Electrochemistry Communications* **2004**, 6, (10), 978-983.
11. Li-Hua Bi, U. K., Bineta Keita and Louis Nadjo, *Dalton Transactions* **2004**.
12. Daniel Drewes, M. P. a. B. K., *Journal of Cluster Science* **2006**, 17, (2), 361-374.
13. Tourne, C. M.; Tourne, G. F.; Zonnevjlle, F., *J.Chem.Soc.Dalton Trans* **1991**, (1), 143-155.
14. Hussain F, B. L. H., Rauwald U, Reicke M, and Kortz U *Polyhedron* **2005**, 24, 847.
15. Weakley, T. J. R.; Evans, H. T., Jr; Showell, J. S.; Tourne', G. F.; Tourne', C. M.,

- J. Chem. Soc., Chem* **1973**, 139-140.
16. Weakley, T. J. R.; Finke, R. G., *Inorg. Chem* **1990**, 29, 1235-1241.
17. Go´mez-Garci´a, C. J.; Coronado, E.; Go´mez-Romero, P.; Casan˜-Pastor, N., *Inorg. Chem* **1993**, 32, 3378-3381.
18. Zhang, X. Y.; Jameson, G. B.; O’Connor, C. J.; Pope, M. T.; *Polyhedron* **1996**, 15, 917-922.
19. Zhang, X.; Chen, Q.; C.Duncan, D.; Lachicotte, R. J.; Hill, C. L., *Inorganic Chemistry* **1997**, 36, (20), 4381-4386.
20. Neuman, R.; Khenkin, A. M., *Inorganic Chemistry* **1995**, 34, 5753-5760.
21. Neumann, R.; Dahan, M., *Journal of the American Chemical Society* **1998**, 120, (46), 11969-11976.
22. Neumann, R.; Dahan, M., *Polyhedron* **1998**, 17, (20), 3557-3564.
23. Neumann, R.; Dahan, M., *Nature* **1997**, 388, (6640), 353-355.
24. Lipscomb, W., **1965**, 4, 132.
25. Pacault, A.; Souchay, P., **1949**, D377, (Bull. Soc. Chim. France).
26. Sadakane, M.; Steckhan, E., *Chem. Rev* **1998**, 98, 219-237.
27. Galli, C.; Gentili, P.; Pontes, A. S. N.; Gamelas, J. A. F.; Evtuguin, D. V., *New Journal of Chemistry* **2007**, 31, (8), 1461-1467.

CHAPTER 2

SYNTHESIS AND STRUCTURAL CHARACTERIZATION OF TRANSITION METAL SUBSTITUTED SANDWICH-TYPE POLYOXOMETALATES

2.1. Introduction

There are numerous synthetic procedures directed towards the development of novel polyoxometalate structures and the literature has well documented evidence for synthesis in aqueous and non-aqueous solvents¹, incorporation of organometallic moieties², hydrothermal synthesis and to produce giant polyanions using small building blocks of pre-formed oxides or synthons³⁻⁵. Before getting into the basics of synthesis of different types of polyoxometalate structures, a brief overview of the structure of these compounds is presented.

The basic heteropolyanion can be viewed as a structure containing numerous oxygen atoms (sometimes hydrogen atoms) and fewer atoms of two more elements in positive oxidation states. Due to this arrangement, these structures are considered to resemble discrete fragments of metal oxide structures possessing unique sizes and shapes⁶. Thus they have been employed as molecular models of bulk metal oxide catalysis. The first step in the chemical characterization of any compound is to identify its precise chemical composition or stoichiometry. In the case of metal oxides, even with single crystals or with polycrystalline samples confirmed as single phase, an exact value

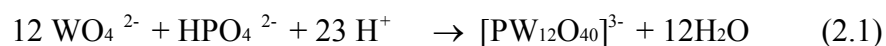
of composition is difficult to obtain. Apart from difficulties and inaccuracies in analytical procedures, the phenomenon of non-stoichiometry (e.g. $\text{Na}_{0.7}\text{WO}_3$) and the difficulty in determining oxygen content changes with synthetic method and this contributes toward uncertainty in fundamental properties of some metal oxide systems. The many disputes regarding metallic versus non-metallic properties or the existence of magnetic moments on transition metal atoms, suggests that different research groups are not studying the same compound (particularly differing oxygen content)⁷. In this regard, polyoxometalates represent thermodynamically relatively stable structures and hence could account for reproducible catalytic properties and better mechanistic understanding. Although, mainly in the case of polytungstates, the formation is often under kinetic control rather than thermodynamic control⁸. Another characteristic feature of these POMs is that they maintain their structural integrity in aqueous and non-aqueous solutions as well as in ionic crystals.

In the polyoxometalate compounds, predominantly W, Mo and V in their highest oxidation state act as the “addenda atoms” (less frequently Ta^{5+} , Nb^{5+} , Re^{7+} , I^{7+}) and over 60 other elements can function as “heteroatoms”. The addenda atoms have some unique characteristics⁸ –

1. They can change their co-ordination with oxygen from 4 to 6 as they polymerize in solution upon acidification
2. They have high positive charges and are some of the smaller atoms that fall within the radius range for octahedral packing with oxygen atoms. Further the ability to form addenda atoms has been known to increase if these atoms form double bonds with unshared oxygen of their MO_6 octahedra, by p Π –d Π interaction. The

formation of a heteropoly complex involves the polymerization of addenda polyhedra around a heteroatom

The reason for the existence of these small discrete heteropoly complexes is due to the polymerization of the addenda atoms and the driving force for this process is a mechanism involving the attachment of protons to oxygen atoms. Once the structure of the heteropoly species is attained (self-assembly), the strong inward polarization of the exterior oxygen atoms terminates any further polymerization. Thus the POMs form in solutions containing simple oxoanions and the necessary heteroatoms by the self-assembly process on acidification. The following is an example of such process:



The catalytically active species of Keggin structures are very well known and hence they are commercially available, while the rest of the POM structures have to be synthesized in-house. The preparation techniques are numerous and are dependent on the type of POM to be synthesized. If there is a common trend in the synthetic procedure, it should follow the sequence: (i) Precursor compounds of metal ions dissolved in water in a ratio corresponding to the final stoichiometry, (ii) Acidification of the solution achieved by addition of mineral acids such as HCl, HClO₄ or HNO₃. Some groups have employed acidic ion-exchange resins (e.g. Amberlyst-15) or electrolysis^{6, 9}, (iii) a subsequent heat treatment after the addition of heteroatom, either in the presence or absence of air, (iv) The heteropoly anions are isolated by addition of an appropriate counter cation – an alkali metal, ammonium or tetra-alkylammonium. Usually, Li and Na salts are more water soluble than K, Rb and Cs. Tetrabutylammonium salts are insoluble in water and can be recrystallized from acetonitrile or acetone⁶, (v) Recrystallization from the

appropriate solvent should yield pure compounds to be characterized using XRD, FTIR and other analytical techniques such as UV-VIS, Cyclic Voltammetry etc.

Several other methods of synthesis have been seen in literature, such as electro dialysis, hydrothermal and photochemical.

2.2. Materials and Methods

2.2.1. Chemicals

Millipore-Q purified distilled water (18M Ω) was used throughout. All of the chemicals were of high-purity grade and were used as received without further purification. The precursors Na₁₂[WZn₃(H₂O)₂(ZnW₉O₃₄)₂].48H₂O (Zn₂POM) and *cis*-Ru[(CH₃)₂SO]₄Cl₂ were prepared according to published methods^{10, 11}.

2.2.2. Equipment and Apparatus

UV-Vis spectra were recorded on a Perkin Elmer spectrometer. All FTIR analysis was done on Ru₂POM sandwich loaded transparent KBr pellets on a Shimadzu spectrometer. Single crystal X-ray diffraction studies were performed using G. M. Sheldrick, SHELXTL NT/2000, Version 6.1, Bruker AXS, Inc.: Madison, WI 2000.

2.3. Synthesis of Sandwich Type Polyoxometalates

2.3.1. Preparation of Zinc Precursor Na₁₂[WZn₃(H₂O)₂{ZnW₉O₃₄}₂]:

The synthetic procedure developed by Tourne et al¹⁰, was employed for the preparation of the zinc precursor compound, which was the base molecule for the subsequent transition metal substituted compounds. A solution of Na₂WO₄.2 H₂O (32 g) in water (87.5ml) was treated with nitric acid (14N, 0.5 ml) at 80-85° C with vigorous stirring, until the initial precipitate dissolved completely to form a dark yellow solution. Then a solution of zinc nitrate (7.5g) in water (25ml) was added very slowly in small

aliquots (1-2ml), accompanied by continuous stirring and heating at 90-95°C (without boiling). During the initial addition of zinc nitrate, a white precipitate was formed, which re-dissolved immediately, and after about 2/3 addition, the precipitate started to dissolve more slowly and hence the solution was added in a drop-wise manner, so that the mixture remained clear till the end. This addition requires about 2-3 hours and the final pH was about 7.5. On moderate cooling to about 40 °C, a first batch of fine needles were crystallized. The liquid was evaporated to half the volume and was left unstirred overnight. More white needle-like crystals were formed and separated by filtration. The resulting cold filtrate was treated with an equal volume of acetone to produce two separate layers. The dense lower layer was further diluted and heated to 50 °C & maintained at this temperature overnight to extract more products. The total yield was about 75-80%. The entire collected product was subjected to recrystallization from water to yield a uniformly hydrated product.

2.3.2. Preparation of Di-Ruthenium Substituted Sandwich $\text{Na}_{14}[\text{Zn}_2\text{Ru}_2(\text{H}_2\text{O})_2\{\text{ZnW}_9\text{O}_{34}\}_2]$:

Preparation of $\text{Ru}(\text{DMSO})_4\text{Cl}_2$ as precursor

Five grams of $\text{RuCl}_3 \cdot 6\text{H}_2\text{O}$ was mixed with 5 ml of anhydrous DMSO solution and the mixture was heated to 80°C for 30 minutes in the presence of an Ar gas blanket. After heating under continuous stirring, the mixture was let to cool to produce clear orange red crystals of $\text{Ru}(\text{DMSO})_4\text{Cl}_2$ (yield 50%). The compound was further subjected to recrystallization from DMSO solution and tested with FTIR for purity.

To a solution of $\text{Na}_{12}[\text{WZn}_3(\text{H}_2\text{O})_2\{\text{ZnW}_9\text{O}_{34}\}_2]$ (Zn_2POM precursor, 4.5g in 10ml water), maintained at 90°C, under a blanket of Ar gas, was added 1.5g of

$\text{Ru}(\text{DMSO})_4\text{Cl}_2$. After heating at 90°C for about 18hrs, the mixture was slowly cooled and when the temperature is near 45°C , the solution was exposed to atmospheric air and a concentrated solution of KCl is added. An orangish brown solution was formed, signifying the formation of Ru substituted POM. This step of atmospheric exposure is known to be responsible for the formation of $\text{Ru}^{(\text{III})}$ from $\text{Ru}^{(\text{II})}$ present in the ruthenium solvate. On cooling an orangish brown precipitate was obtained (yield 50%). On subsequent recrystallization with water, needle-shaped single crystals were obtained. The sodium salt $\text{Na}_{14}[\text{Zn}_2\text{Ru}_2(\text{H}_2\text{O})_2\{\text{ZnW}_9\text{O}_{34}\}_2]$, was prepared by dissolving the potassium salt from the previous step in 0.5 M solution of NaCl .

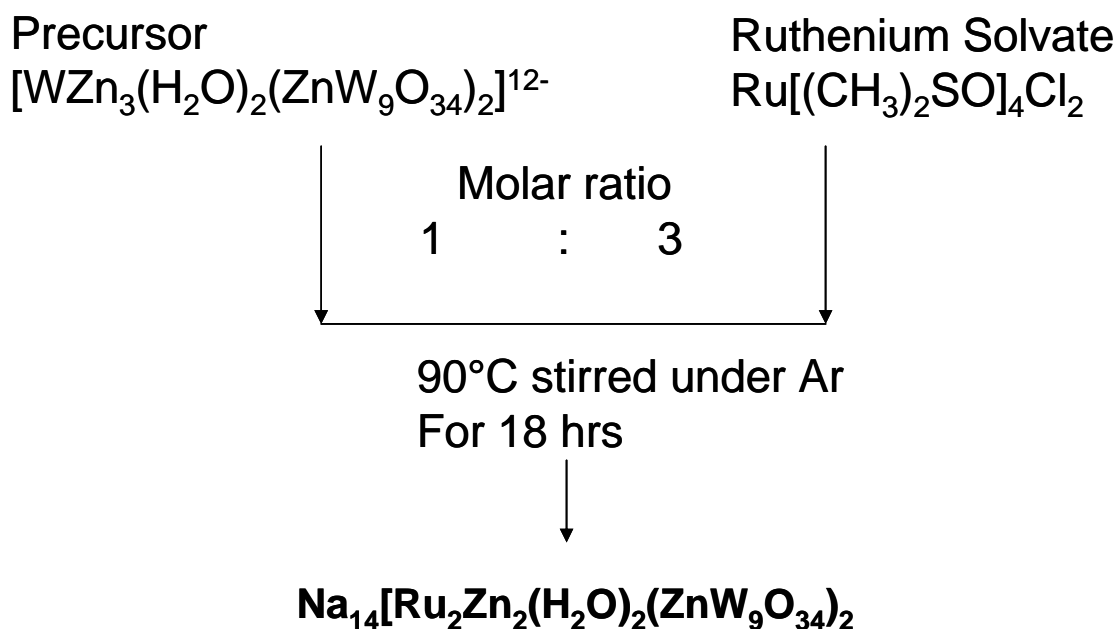


Fig. 2.1. Flowchart for the Synthesis of Ruthenium Substituted Polyoxometalate

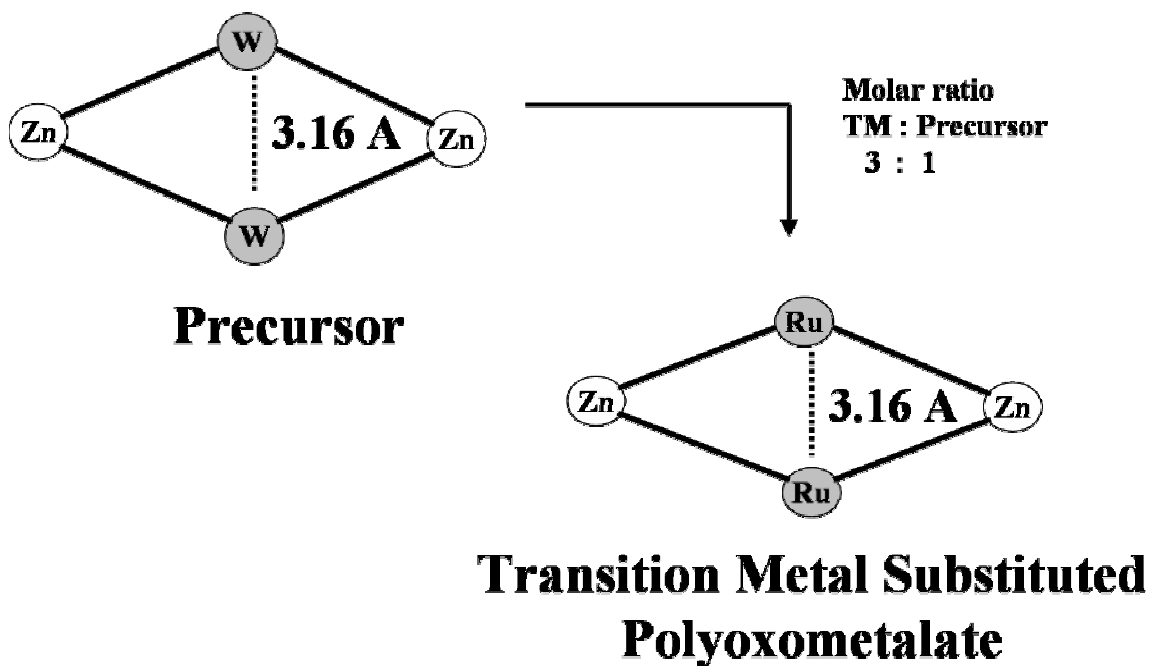


Fig. 2.2. Schematic representation of the central metal belt depicting the lattice position, where the transition metal substitution occurs during the formation of sandwich type bi-Keggin structures.

2.3.3. Preparation of Ir^(IV) substituted Sandwich POMs (Ir₂POM)

Noble metal substituted polyoxometalates, such as iridium substituted polyoxometalates have been employed as organic oxidation catalysts for the C-H activation process¹². A number of mono-iridium substituted polyoxometalate structures exist in literature, Keggin¹³, Wells-Dawson¹⁴ and organo-polyoxometalate hybrids^{15, 16}, but to our knowledge, a di-iridium substituted sandwich polyoxometalate has not been synthesized. In this context, we have been successful in substituting iridium in the sandwich type structure (Weakley structure), first synthesized by Tourne et al¹⁰. Di-iridium substituted polyoxometalate Na₁₂ [Ir₂Zn₂(H₂O)₂(ZnW₉O₃₄)₂] (Ir₂POM), has been synthesized according to the following procedure.

To a solution of Zn₂POM (4.5 g in 10ml water) was added 1.5g of anhydrous Ir(III) chloride (purchased from Alfa Aesar) and the solution was heated at 90°C for 18 hours under Ar atmosphere. A dark brown solution was obtained. On subsequent cooling, needle shaped crystals of the dark brown coloration was obtained. The crystals were subjected to recrystallization with water to obtain uniform water of hydration.

2.3.4 Preparation of Fe^(III) substituted sandwich POMs (Fe₂POM)

The di-substituted iron (III) heteropolyanion was prepared by following Tourne's¹⁰ method of synthesis. In short, a solution of Fe(NO₃)₃.9H₂O was added in a drop wise manner to a stirred solution of precursor Zn₂POM (molar ratio of Transition Metal : Precursor at 3:1) at 90°C. To the resulting light yellow solution was added solid sodium acetate and then methanol to obtain a turbid yellow liquid. The sodium salt of Fe₂POM was obtained by crystallization at 0°C, overnight. Despite forming well-defined needle like crystals, this compound could not be characterized by single crystal XRD due to formation of twinned crystals. (Data could not be solved due to this “twinning” phenomenon. Since these structures have already been solved, we have used vibrational spectroscopy and elemental analysis as structural characterization methods.

2.3.5. Preparation Mn^(II) sandwich POMs

To a solution of Zn₂POM precursor, maintained at 80° C and under continuous stirring, manganese nitrate solution was added in the molar ratio of 3:1. A yellowish brown solution was obtained after heating for 18 hrs. On cooling a powdery precipitate was obtained and it was subjected to recrystallization in water. A concentrated solution of potassium nitrate was added to crystallize the potassium salt of the POM. A subsequent

addition of concentrated sodium nitrate solution produced dark brown needle-like crystals for single crystal XRD analysis.

2.4. Structural Characterization

2.4.1. Elemental Analysis

Chemical composition measurements were performed on single crystals of sandwich type compounds using SEM-EDX analysis and in some cases by ICP-AAS analysis. Analytical data for Zn₂POM (precursor), Ru₂POM, Ir₂POM, Fe₂POM and Mn₂POM are listed in Table 1. The analytical data are consistent with the formulation $[\text{Zn}_2\text{M}_2\{\text{ZnW}_9\text{O}_{34}\}_2]^{12-}$ and there is indication towards M(H₂O) type arrangement for the substituted transition metal. (Also confirmed by single crystal XRD studies)

Table 2.1. Analytical Data for $\text{Na}_n[\text{ZnWM}_2\{\text{ZnW}_9\text{O}_{34}\}_2]$

Complex	Na	Zn	M
			Experimental (Calculated)
$\text{Na}_{14}[\text{Ru}^{\text{III}}_2\text{Zn}_2(\text{H}_2\text{O})_2\{\text{ZnW}_9\text{O}_{34}\}_2]$.	5.8 (6.17)	7.92 (5.01)	3.79 (3.88)
$\text{Na}_{12}[\text{Ir}^{\text{IV}}_2\text{Zn}_2(\text{H}_2\text{O})_2\{\text{ZnW}_9\text{O}_{34}\}_2]$	6.6 (6.4)	6.3 (6.18)	9.11 (9.09)
$\text{Na}_{16}[\text{Ni}^{\text{II}}_2\text{Zn}_2(\text{H}_2\text{O})_2\{\text{ZnW}_9\text{O}_{34}\}_2]$	7.5 (8.0)	6.15 (6.53)	3.02 (2.93)
$\text{Na}_{16}[\text{Mn}^{\text{II}}_2\text{Zn}_2(\text{H}_2\text{O})_2\{\text{ZnW}_9\text{O}_{34}\}_2]$	7.68 (8.01)	6.24 (6.54)	3.01 (2.74)
$\text{Na}_{14}[\text{Fe}^{\text{III}}_2\text{Zn}_2(\text{H}_2\text{O})_2\{\text{ZnW}_9\text{O}_{34}\}_2]$.	5.2 (6.0)	7.0 (5.01)	4.2 (3.8)

2.4.2 Vibrational spectroscopic studies of selected sandwich polyoxometalates

Infrared spectroscopy is the first characterization tool in determining the structural integrity of the synthesized polyoxometalate. Fig.2.3 shows the FTIR characteristics of different transition metal (Ru, Ir, Ni, Mn) substituted sandwich compounds. These studies reveal the substituted compounds to be isostructural with the precursor molecule Zn_2POM and clear evidence for the presence of transition metal substitution is not seen as the number of heavy tungsten atoms far exceeds the number of TM atoms, since FTIR is

an averaging technique. Thus the starting material Zn_2POM and the transition metal substituted compounds exhibit similar signature peaks, with very minimal shifts, attributed to the transition metal substitution:

927 cm^{-1}	-----	W=O _t (Terminal oxo group)
881 cm^{-1}	-----	W-O-W (Corner sharing WO ₆ octahedra)
777 cm^{-1}	-----	W-O-W (Edge sharing octahedra)
576 cm^{-1}	-----	W-O-W (Edge sharing mixed or maybe noble metal-oxo

Stretch

Further Raman spectroscopic analysis of the single crystal of Zn_2POM and Ru_2POM in Fig.2.4 have revealed that the common Keggin features were observed and there were some other additional peaks, which could be attributed to the sandwich moiety. More elaborate work is needed to comprehend the difference between Keggin and sandwich type structures.

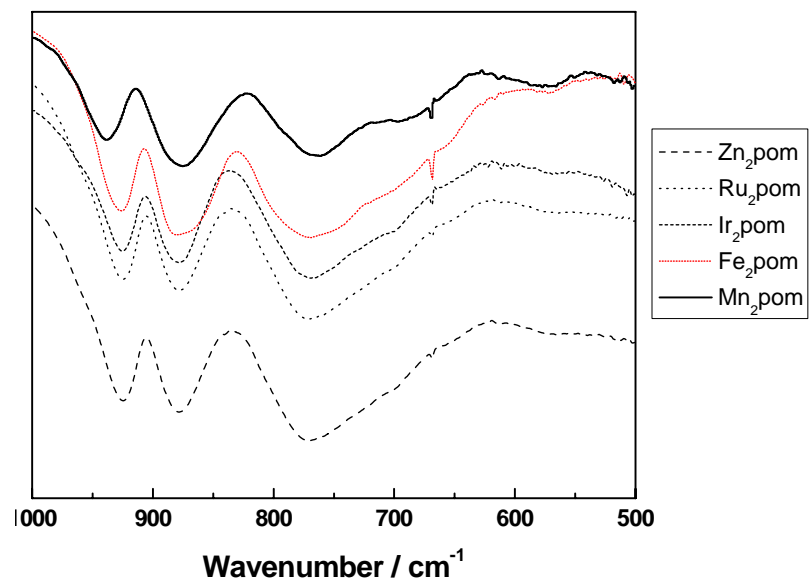


Fig.2.3 Transmission FTIR data for solid sandwich POMs in a KBr pellet.

$\text{Na}_n[\text{ZnWM}_2\{\text{ZnW}_9\text{O}_{34}\}_2]$, where M=Ru, Ir, Ni, Mn

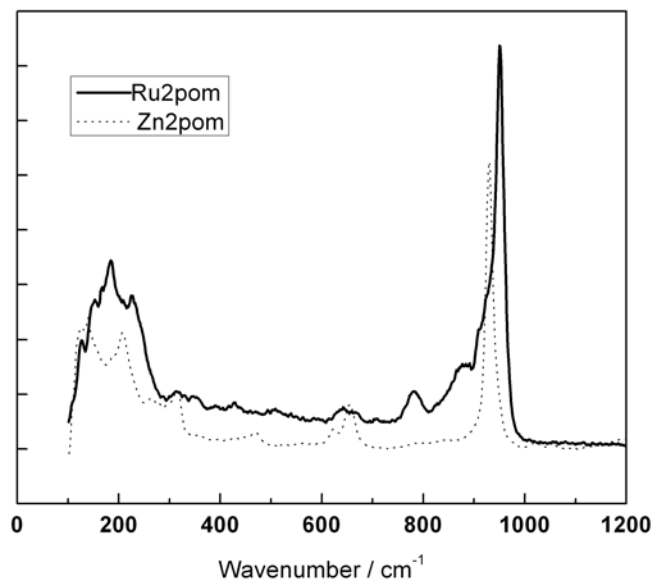


Fig. 2.4. Raman spectroscopic analysis of single crystals of Zn_2POM and Ru_2POM

2.4.3. UV-Vis Spectroscopy

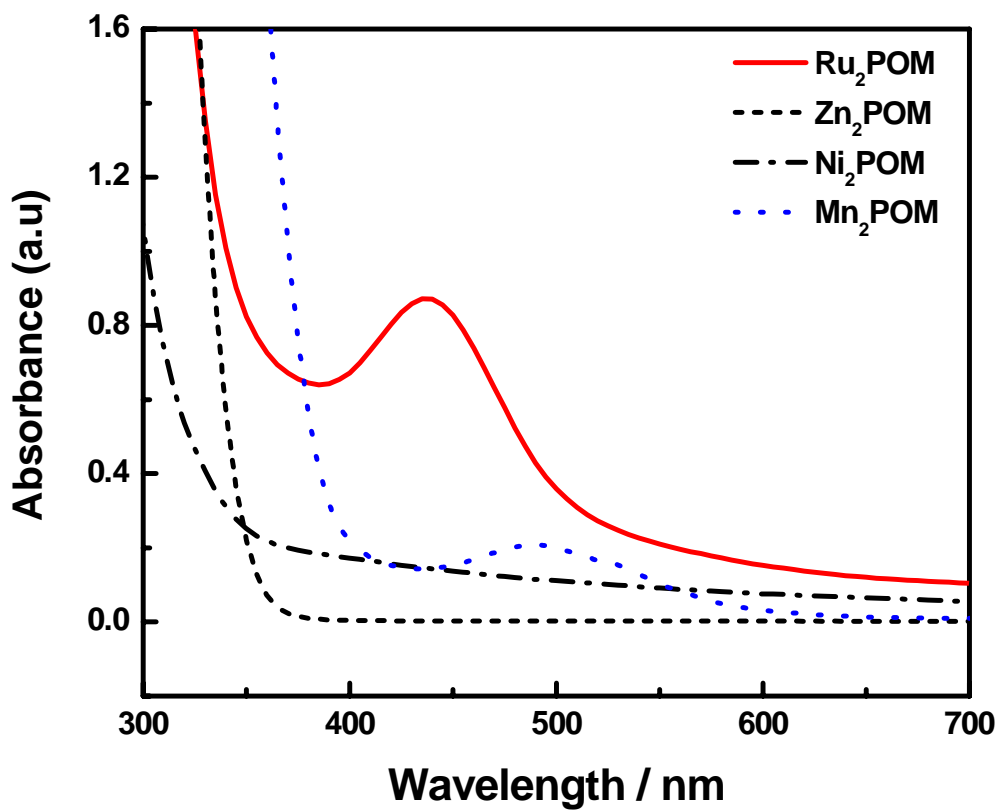


Fig. 2.5. UV-Vis of sandwich compounds

In the case of sandwich type polyoxometalates, the UV-Vis spectrum reveals the presence of an intense, broad absorption band (below 350nm, not shown for sake of clarity) attributed to the usual oxygen to tungsten charge transfer band of Keggin based derivatives. For unsubstituted Zn₂POM precursor and Ni₂POM, only W-O-W charge transfer bands are seen. Ru₂POM reveals a strong absorption band at 435 nm, which is

attributed to the oxygen to Ru charge transfer band. Mn₂POM reveals a broad absorption peak centered around 500 nm and from the work done by Tourne^{10, 17, 18}, these could correspond to a mixture of Mn(II) and Mn(III) species.

2.5. Single Crystal XRD Analysis

Zn₂POM Precursor

White needle shaped single crystals were obtained by recrystallization from aqueous solutions. Careful harvesting of single crystals was performed and mounted onto the glass fiber and reproducible results were obtained.

Ru₂POM

Single crystals containing the sodium and zinc salt of the polytungstometalate cluster $[W_{0.92}Ru_{1.08}Zn_2(H_2O)_2(ZnW_9O_{34})_2]^{12-}$ (Ru₂POM) were grown via slow evaporation from aqueous solution. Single crystal X-ray diffraction studies revealed two α -B-[ZnW₉O₃₄]¹²⁻ units linked by a four metal atom belt as shown in Figure 2.6. Not shown in this figure are four [Zn(H₂O)₅]²⁺ cations that are bound to the periphery of the cluster by the terminal oxo atoms from the polytungstometalate. The two lobes of the cluster are related through a center of inversion. The four atom belt consists of two zinc centers that are five coordinate to the two α -B-[ZnW₉O₃₄]¹²⁻ fragments, and in their six site by a coordinating water molecule. W and Ru atoms that are disordered by the inversion center occupy the remaining two positions. In addition, refinement on the occupancy of this site reveals a small, but non-negligible, excess of Ru in the belt. This reveals that there must be some compositional variation in the clusters and that some diruthenium clusters exist in the product mixture. Similar compositional variations were

observed in $[\text{WMZn}_2(\text{H}_2\text{O})_2(\text{ZnW}_9\text{O}_{34})_2]^{12-}$ (M = Co, Zn) where slight excesses of Co and Zn were found¹⁰.

Crystallographic Data:

$\text{Na}_{14}\{[\text{Zn}(\text{H}_2\text{O})_5]_4[\text{Zn}(\text{H}_2\text{O})]_2\text{W}_{0.92}\text{Ru}_{1.08}(\text{ZnW}_9\text{O}_{34})_2\} \cdot 28\text{H}_2\text{O}$: yellow prism, dimensions 0.106 x 0.132 x 0.400 mm, triclinic, $P\bar{1}$, $Z = 2$, $a = 12.4771(6)$, $b = 13.7096(7)$, $c = 16.6901(8)$ Å, $V = 2460.1(4)$ Å³ (T = 193 K), $\mu = 24.238$ cm⁻¹, $R_1 = 0.0497$, $wR_2 = 0.1533$.² Bruker APEX CCD diffractometer: $\theta_{\text{max}} = 56.58^\circ$, MoK α , $\lambda = 0.71073$ Å, 0.3° ω scans, 24234 reflections measured, 11886 independent reflections all of which were included in the refinement. The data was corrected for Lorentz-polarization effects and for absorption (SADABS), the structure was solved by direct methods, followed by a refinement of F^2 by full-matrix least-squares with 668 parameters and one restraint. Anisotropic displacement parameters were included for all heavy atoms and all but four oxygen atoms.

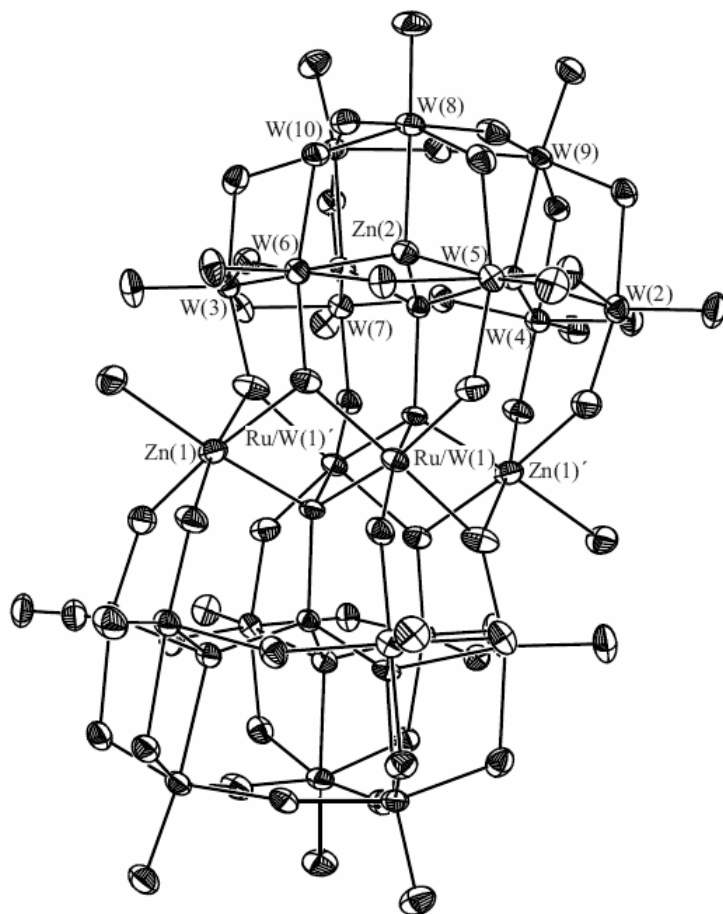


Fig.2.6. ORTEP plot (ellipsoids at 40% probability) of the X-ray structure of $[\text{Ru}^{\text{III}}_2\text{Zn}_2(\text{H}_2\text{O})_2(\text{ZnW}_9\text{O}_{34})_2]^{14-}$.

Ir₂POM

The elemental composition performed by EDX and ICP-AAS revealed a formulation of $\text{Na}_{12} [\text{Ir}^{\text{IV}}_2\text{Zn}_2(\text{H}_2\text{O})_2\{\text{ZnW}_9\text{O}_{34}\}_2]$, which corresponds to an oxidation state of +4 for iridium. X-ray structure analysis reveals the formation of a sandwich type polyoxometalate similar to the Ru₂POM structure. The ORTEP plot in Fig.2.7, reveals a Zn₂Ir₂ ring between the two α -B-[ZnW₉O₃₄]¹²⁻ units. The large thermal coefficients

observed for Ir atoms suggest that this position is labile and there seems to be degree of disorder between Ir and W atoms, suggesting that there is a mixture of di-substituted and mono-substituted single crystal structures. These results suggest that the iridium atom substitutes the place of W-atoms in the central metal belt of the precursor molecule $[\text{WZn}_3(\text{H}_2\text{O})_2(\text{ZnW}_9\text{O}_{34})_2]^{12-}$. Unfortunately, it is difficult for the refinement of occupancy between Ir and W, as performed in Ru_2POM , due to the reason that X-ray diffraction cannot categorically differentiate between Ir and W, since they are very close in the periodic table (negligible differences in atomic weight). Thus the real composition of this species has been compared with EDX and ICP-AAS to confirm the stoichiometric iridium substitution in the lattice. The exact set of single crystals, which were tested with single crystal XRD were subjected to the elemental analysis.

An important feature about the XRD results was that the iridium substitution occurred on the W-atom position of the precursor, and that interatomic distance between the Ir atoms was 3.18 Å. Neuman and Tourne^{10, 17-19} have reported that the transition metal substitution occurs at the Zn atom position at the farthest ends of the central metal belt at an interatomic distance of 5.1 Å. We believe that there has been some discrepancy in the crystallographic data analysis and hence we performed some control experiments with other transition metal substitutions such as Fe and Mn. We were able to get good diffraction quality crystals from Mn_2POM and crystallographic analysis reveals that the transition metal substitution does indeed occur at the nearest ends of the central metal belt, at an interatomic distance of 3.18 Å.

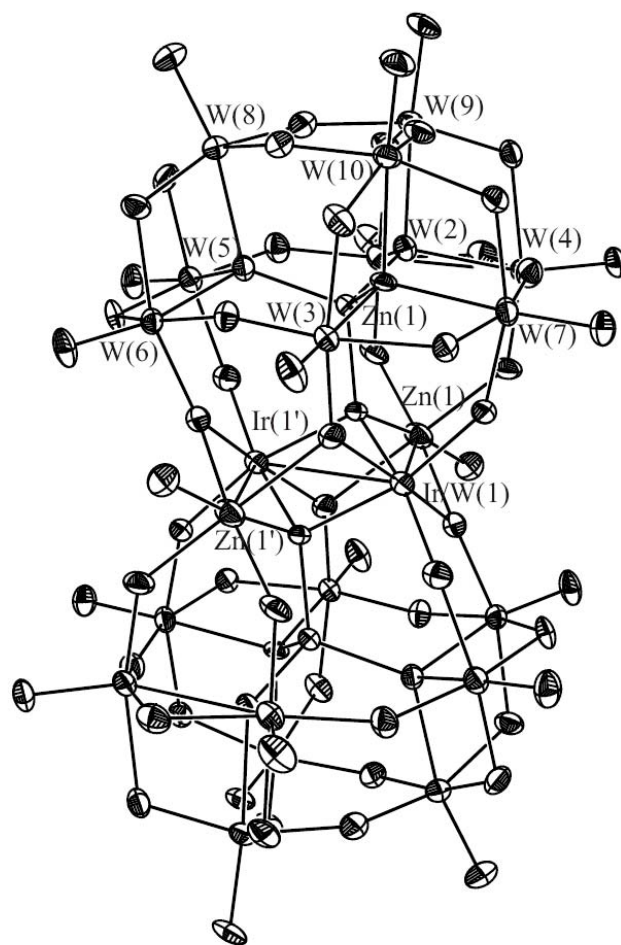


Fig.2.7. ORTEP plot of the X-ray structure of Single Crystal X ray structure of Ir₂POM

Conclusions

Synthesis of the transition metal substituted sandwich type polyoxometalates has been established and the traditional structural characterization of these compounds has been accomplished. In case of a lack of literature record, single crystal XRD analysis was performed to prove the uniqueness of crystal structure.

References

1. Errington, R. J., *Polyoxometalate Chemistry from Topology via Self-Assembly to Applications*. Kluwer: 2007; p 7.
2. Gouzerh, P.; Proust, A., *Chem. Rev* **1998**, 98, 77.
3. A.Muller; F.Peters; M.T.Pope; D.Gatteschi, *chem. Rev* **1998**, 98, 239.
4. A.Muller; P.Kogerler; C.Kuhlmann, *Chem. Commun* **1999**, 1347.
5. O.Delgado; A.Dress; A.Muller, *Polyoxometalate Chemistry from Topology via Self-Assembly to Applications*. 2001; p 69.
6. Pope, M. T., *Heteropoly and Isopoly Oxometalates*. Springer-Verlag: 1983.
7. Cox, P. A., *Transition Metal Oxides*. Oxford Science Publications: 1992.
8. C.W.Baker; D.C.Glick, *Chem. Rev* **1998**, 98, 3-49.
9. G.M.Maksimov, *Russ. Chem. Rev* **1995**, 64, 445.
10. Tourne, C. M.; Tourne, G. F.; Zonnevillje, F., *J.Chem.Soc.Dalton Trans* **1991**, (1), 143-155.
11. Evans, I. P.; Spencer, A.; G, W., *J. Chem. Soc., Dalton Trans* **1973**, 204-209.
12. Siedle, A. R.; Newmark, R. A.; Brownwensley, K. A.; Skarjune, R. P.; Haddad, L. C.; Hodgson, K. O.; Roe, A. L., *Organometallics* **1988**, 7, (9), 2078-2079.
13. Liu, H. Z.; Sun, W. L.; Yue, B.; Jin, S. L.; Deng, J. Q.; Xie, G. Y., *Synthesis and Reactivity in Inorganic and Metal-Organic Chemistry* **1997**, 27, (4), 551-566.
14. Sun, W. L.; Yang, F.; Liu, H. Z.; Kong, J. L.; Jin, S. L.; Xie, G. Y.; Deng, J. Q., *Journal of Electroanalytical Chemistry* **1998**, 451, (1-2), 49-57.
15. Lin, Y.; Nomiya, K.; Finke, R. G., *Inorganic Chemistry* **1993**, 32, (26), 6040-6045.
16. Ishida, K.; Lockledge, S. P.; Klemperer, W. G., *Abstracts of Papers of the American*

Chemical Society **1993**, 206, 347-INOR.

17. Howard T Evans, C. M. T., Gilbert F Tourne, Timothy J R

Weakley,*J.Chem.Soc.Dalton Trans* **1986**, (1), 2699-2705.

18. Weakley, T. J. R.; Evans, H. T., Jr; Showell, J. S.; Tourne', G. F.; Tourne', C. M., *J.*

Chem. Soc., Chem **1973**, 139-140.

19. Neuman, R.; Khenkin, A. M.,*Inorganic Chemistry* **1995**, 34, 5753-5760.

CHAPTER 3

Electrochemical Characterization of Sandwich-Type Transition Metal Substituted Polyoxometalate Structures

3.1. Introduction

As discussed earlier, transition metal substituted polyoxometalates (TMSP) have been employed in many catalytic applications, where, they have replaced bulk metal oxides, porphyrins and enzymes. There is a plethora of chemical applications involving the oxidation/reduction of the heteroatoms and the addenda ions. Electrochemical analysis of these heteropolyanions serves two purposes, one to identify novel redox active species and the other to understand the reactivity and mechanism of these species as redox reagents and catalysts^{1, 2}. The unique properties of TMSPs, such as high stability of redox states, tunability of redox potentials, variability of transition metal centers and multiple electron transfers³ makes them promising candidates for several efficient and clean electrocatalytic processes⁴. Several unique applications of polyoxometalates (POMs) as electrocatalysts have appeared in the literature and a couple of good reviews^{3, 4} illustrate the state of the art in today's scientific world. Nadjo⁵⁻¹¹ and Hill^{8, 10, 12, 13} groups have made several noteworthy contributions to this field. Of all the POMs available, Keggin and Wells Dawson based structures form the bulk of electrocatalytically active species. Literature review shows that polyoxometalates are active in both electrocatalytic oxidation and reduction reactions, provided the right POM

and conditions are chosen⁴. This chapter deals with a short review of the electrochemical properties of TMSPs and basic electrochemical characterization of the sandwich type polyoxometalates comprising the two Keggin units connected by a belt of four transition metals in the center. $\text{Na}_n(\text{M}_2\text{Zn}_2[\text{ZnW}_9\text{O}_{34}]_2)$, where M is the substituted transition metal atom. Electrochemical characterization of sandwich POMs has been performed to identify and understand the nature of the electroactive species to shed some light on the electrocatalytic properties of these structures.

3.2. Electrochemical Properties of Transition Metal Substituted Polyoxometalates – Literature Review

As described in the first chapter, polyoxometalates can be classified into two groups, “mono-oxo” (type I) and “cis-oxo” (type II), based on their redox properties¹. This classification is predominantly based on the number of terminal oxygen atoms attached to the addenda atom, tungsten or molybdenum. It has been shown that only type-I POMs are easily reduced and hence can form reversible mixed valence species, without any major changes in the structure. These redox properties are further enhanced when different transition metals are substituted in these frameworks. Depending on the final application, POMs were chosen with favorable thermodynamics and kinetics for the redox transformations. In this regard, POMs have been employed as oxidation catalysts for clean synthesis of organic substances in the industrial world.

In TMSP, the presence of the sixth coordinated water molecule on the transition metal contributes to the possible entry point for inner-sphere electron transfer⁸. Further, the inorganic nature of the cluster combined with their resistance to conventional degradation processes, has been attractive properties for electrocatalysis. The potential

for both inner-sphere and outer sphere electron transfer phenomena has contributed to the substantial volume of research in the literature of electrocatalysis of POMs. Since, efficient electrocatalysis of multiple electron transfer reactions is important in many industrial reactions, the stable and reversible multiple electron transfer properties of POMs are particularly conducive. Usually the POMs are employed to replace conventional transition metal complexes (capable of only single electron transfer), which are the metalloporphyrins and organometallic complexes, and these compounds are frequently susceptible to degradation (oxidation) by reactive intermediates formed during the process (ref). When there is a possibility of multiple electron transfer (up to five electrons) as in POM, the formation of highly reactive radical intermediates is avoided, given that numerous oxygen ligands of POMs are inherently inert towards oxidizing environments.

Large number of polyoxometalates undergoes a series of reversible one or two electron reductions. These reactions are typically substantiated using cyclic voltammetry which provides electrochemical fingerprints for these structures. It has been found that, if the substituted transition metal atoms are not reduced, then the $E_{1/2}$ or redox potential of TMSPs will be very similar to their precursors. In these cases, the reduction process and the structure of the polyanions are considered to be the same as the precursor molecules. If the substituted transition metal atoms are reduced, then the reduction process and the number of reduction waves will undergo changes corresponding to the nature of the substituted metal.

Another desirable property in POM based electrocatalysis is the ability to fine-tune the redox potential of transition metal center over a wide range by altering the

identity of the heteroatom located in the center of the tungsten-oxide cage¹⁴⁻¹⁸. This property has been described as “tuning by synthesis”. This particular aspect of POM electrocatalysis has been employed as a diagnostic tool to study the mechanisms of electron transfer reactions during the catalysis.

General Understanding of POM electrochemistry

In the case of POMs, the unique symmetry in structures contributes to the equivalence of several metal centers of a given framework. However, during electron transfer in a Keggin molecule, such as $\text{PW}_{12}\text{O}_{40}^{3-}$, a step-wise reduction of the tungsten centers takes place⁸. EPR experiments have revealed that an added electron undergoes delocalization over all of the twelve tungsten centers and this has been observed has the general trend for all unsubstituted and highly symmetrical Keggin anions. Introduction of lower symmetry by substitution of transition metal atoms creates substantial modifications in this degree of valence trapping.

POMs have been used as model systems to mimic the electronic properties of metal oxides at the molecular level (ref). In general, the fully oxidized anions are known to have a simple electronic structure with a set of doubly occupied orbital's, which are centered at the oxo-ligands and are well separated from the occupied orbitals¹⁹ (centered at metal atoms). Fully oxidized POMs are easily reduced in solution and this is achieved because the lowest unoccupied molecular orbital (LUMO) of POM, which is a symmetry-adapted non-bonding orbital (d_{xy} -like), is always low in energy²⁰. In the case of one of the addenda atoms, W^{VI} or Mo^{VI} being replaced by another early transition metal such as V^{V} , Nb^{V} or Ti^{IV} , the redox properties of these compounds have been well understood in terms of both theory²¹ and experiment²². However, the incorporation of a transition metal

(TM) in a lower oxidation state such as Fe^{III} , Co^{II} , Ni^{II} etc onto the POM framework is not well understood and hence several hypotheses are prevalent and more experimental investigations are needed. In the case of TM substitution in Keggin and Wells-Dawson derived sandwich-type polyoxometalates, which have been employed in numerous applications in catalysis, medicine, pharmaceutical etc, the interaction of the substituted transition metal with the POM structure and its influence on the electron transfer behavior is also very interesting.

3.3. Materials and Methods

3.3.1. Polyoxometalates and Reagents

All sandwich type polyoxometalate structures were synthesized as described in the previous chapter. BAS glassy carbon electrode or BAS gold disc electrode were employed as working electrodes. Supporting electrolyte solutions were unbuffered 0.5M Na_2SO_4 (pH~ 6) and buffered acetate solutions at pH 5.

3.3.2. Electrochemical Measurement Set-up

The solutions were thoroughly deaerated with pure Ar gas for 20 minutes and kept under positive pressure of this gas during all electrochemical experiments. All cyclic voltammetric measurements were performed on a 20ml glass vial with a home made mounting head to place the electrodes at constant inter-electrode distances. The electrochemical set-up was a three electrode arrangement and driven by a BAS-Epsilon workstation. All experiments were performed with Ag/AgCl/KCl (satd.) reference electrode, unless otherwise stated. In order to prevent contamination by polyoxometalate, a salt bridge filled with 0.1M NaClO_4 was employed. The counter electrode was platinum gauze of a large surface area. The experiments were performed at laboratory temperature.

3.3.3. Cyclic Voltammetry of Transition Metal Substituted Sandwich type Polyoxometalate

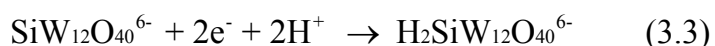
Glassy carbon was employed as the working electrode, Pt mesh as counter electrode and Ag/AgCl as reference electrode. In order to prevent contamination, a salt bridge containing the pure electrolyte was used for housing the reference electrode and was placed very close to the working electrode. GC electrode was subjected to polishing with alumina nanoparticles and then tested for consistent electrochemical characteristics in 0.1M HClO₄. The concentration of Zn₂POM and Ru₂POM was maintained at 0.2mM and the corresponding cyclic voltammetric measurements were made, first by cycling from negative potential to positive. An initial scan was performed at 100mV/s (not always shown) and then exploratory scans were performed at slow scan rates of 10mV/s, with the potential window being expanded as necessary.

3.4. Results and Discussion:

3.4.1. Electrochemical Behavior of Sandwich POM Structures

In our attempt to understand the electrochemical behavior of the sandwich type polyoxometalates, it will be an imperative step to discuss the well-established electrochemistry of Keggin type polyoxometalates, for example SiW₁₂O₄₀⁴⁻. In 1 M HCl solution, there are five reduction peaks with the approximate electron ratios of 1:1:2:8:12. The characteristic signature of Keggin molecule has been known to be comprised of the first three redox peaks, which are well-defined and reversible in nature. The origin of these redox features have been attributed to the addition and removal of electrons from primarily non-bonding orbital's within the four tungsten oxide triads (W₃O₁₃) within the Keggin polyanion. The fourth and fifth reduction waves are accompanied by chemical

reactions of the cluster contributing to adsorption of tungsten compounds onto the electrode surface. The first two one electron redox peaks were essentially unaltered under condition of $\text{pH} < 5$. The third wave, consisting of two electron reduction has been shown to move to more negative potentials by about 59mV/pH unit. The three redox waves can be described by the following equations,



$$1 < \text{pH} < 5$$

For the case of the monolacunary Keggin atom, $\text{SiW}_{11}\text{O}_{39}^{8-}$, with one tungsten cation missing, the electrochemical response comprises of two waves caused due to two electron transfer reactions and the formal potentials have been shown to be significantly more negative than the parent Keggin polyanion.

In our study, the electrochemical behavior of $\text{Na}_n(\text{M}_2\text{Zn}_2[\text{ZnW}_9\text{O}_{34}]_2)$, a sandwich type polyoxometalate was studied by employing cyclic voltammetry to identify the electroactive species in solution and to evaluate the feasibility for electrocatalysis. Traditionally, the stability of these sandwich type POM structures has been evaluated by monitoring the UV-VIS spectra under different pH conditions to determine the ideal medium for electrochemical analysis. The reproducibility of the UV-VIS response, in terms of absorption spectra and wavelength positions have been known to provide the stability conditions between pH 4 and 9 and this has been shown to be a good starting point for reliable cyclic voltammetry. Outside of this range, the cyclic voltammograms of these anions were ill-defined and the heteropolyanions were unstable with respect to

degradation. In this chapter, the electrochemical behavior of transition metal substituted sandwich type structures (Zn₂POM, Fe₂POM, Ni₂POM, Cu₂POM, V₂POM, Mn₂POM, Ir₂POM and Ru₂POM) were studied to understand the effect of transition metals as heteroatoms in the sandwich polyoxometalate framework. The series of transition metal substituted sandwich compounds were expected to exhibit not only the step-wise reduction processes of the addenda atom (W), but also some of the redox features of the substituted transition metal atoms. In this regard, the electrochemical behavior of these sandwich POM structures could have some similarity to the transition metal substituted Keggin type structures, as described by the groups of Pope^{1, 23-25}, Keita^{4, 26-28} and others²⁹⁻³². In some cases, for the sake of simplicity and clarity, the electrochemical behavior of the respective W atoms and the substituted central metal atoms are described separately in the following sections. We have understood from literature that transition metal substitution causes a change in the position of tungsten redox peaks; there is a common observation of these peaks to be shifted to even more cathodic potentials in Keggin structures.

As we have seen before, the sandwich type structures, Na_n[Zn₂M₂{ZnW₉O₃₄}₂] are formed by the assembly of two trivacant Keggin molecules onto a central metal belt comprising four transition metal atoms in a rhombus-like arrangement. Since the trivacant lacunary B-ZnW₉O₃₄¹²⁻ molecules are not known to exist in the isolated solid state,¹ (they are difficult to isolate from solution), all electrochemical measurements have been compared with the literature data for trivacant lacunary fragments of phosphotungstate (α -[PW₉O₃₄]ⁿ⁻). The effect of substitution of each transition metal (V, Mn, Fe, Ni, Cu, Ir, Ru) on the electrochemical behavior of the sandwich compounds have

been studied and the results have been summarized in the following section.

Zn₂POM (Precursor) Na₁₂[WZn₃(H₂O)₂{ZnW₉O₃₄}₂]

The sodium salt of the Zn₂POM precursor in a pH 5 buffer solution has been studied by cyclic voltammetry and the predominant redox features obtained during a steady state condition has been shown in Fig.3.1. No other peaks are visible in the higher anodic potential region, signifying the absence of Zn redox features. This voltammogram shows the fingerprint features analogous to those observed for [PW₉O₃₄]ⁿ⁻ based sandwich type structures^{33,34}.

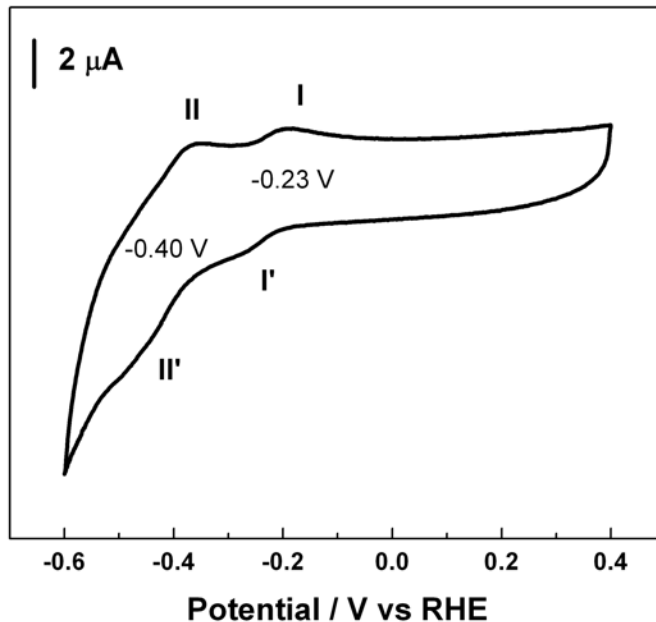


Fig.3. 1 Cyclic Voltammogram of 0.2mM Zn₂POM in pH=5 buffer solution, with Glassy Carbon as Working Electrode (W.E), Pt mesh as Counter Electrode (C.E) and Ag/AgCl as Reference Electrode (R.E), at a scan rate of 10mV/s.

From Fig.3.1, two sets of redox peaks are clearly visible at the formal potentials, $E_{1/2}$ of -0.23V and -0.4 V. The difference between E_{pa} (I,II) and E_{pc} (I',II') was generally in the range of 0.059 to 0.074 V, where E_{pa} and E_{pc} are the anodic and cathodic peak

potentials. Both the peak potentials were independent of potential scan rates in the range from 10 to 100mV/s. These results have suggested that the electrode reactions of the Zn₂POM precursor compound are reversible or quasi-reversible. From the previous studies²⁹⁻³¹ on the phosphotungstate sandwich compounds, we can correlate the two redox peaks observed in Fig.3.1 to the tungsten (VI) redox peaks. These peaks are pH dependent and they exhibit a reversible nature until a pH of 9 in the alkaline direction. After this, the redox behavior becomes ill-defined in high pH conditions, and hence no further studies were performed in this direction.

Further, each redox peak current has been found to be proportional to the two thirds power of the scan rate and this signifies that the redox features are surface-active in nature³⁵. It has been well-established that the two-thirds power scan rate dependence of peak current corresponds to a two-dimensional phase transition or a nucleation and two-dimensional growth mechanism.^{36, 37}

Ru₂POM sandwich, Na₁₄[Ru^{III}₂Zn₂(H₂O)₂{ZnW₉O₃₄}₂]

The diruthenium substituted sandwich type polyoxometalate has been synthesized by the reaction of cis-Ru(dmsO)₄Cl₂ with the Zn₂POM precursor, as described in the second chapter. In earlier studies, Keita et al^{27, 33, 38} have prepared several Ru supported POMs such as [Ru(dmsO)₃(H₂O)-XW₁₁O₃₉]ⁿ⁻, where X=Si or Ge, using similar organic ruthenium solvates as precursors together with lacunary species of the kind [A-XW₉O₃₄]¹⁰⁻, in aqueous acidic media. The presence of the organic component of the Ru precursor in the polyoxometalate framework was a common trend in all of the studies conducted by this group. In our compound, detailed elemental analysis and single crystal studies have revealed the absence of the DMSO fragment. Thus, the diruthenium

substituted sandwich compound was completely inorganic in its structural composition.

The steady state voltammetry of 0.2mM Ru₂POM at a glassy carbon electrode reveals some interesting differences when compared to the Zn₂POM characteristics. As shown in Fig.3.2, a pair of redox couples at the most negative potentials corresponding to W(VI) were observed at formal potentials $E_{1/2}$ at -0.30 V and -0.42 V. The slight negative shift of these redox peaks in comparison to those of the parent Zn₂POM, has been observed in literature and is a consequence of transition metal substitution^{29, 31}. There is an additional redox couple at $E_{1/2}$ of -0.15 V could be attributed to the redox state of the substituted Ru metal centers. From Fig.3.2, we can identify the redox features of W cage and the first redox couple of ruthenium metal centers. A small ill-defined shoulder of a redox peak is visible at the $E_{1/2}$ of +0.12 V.

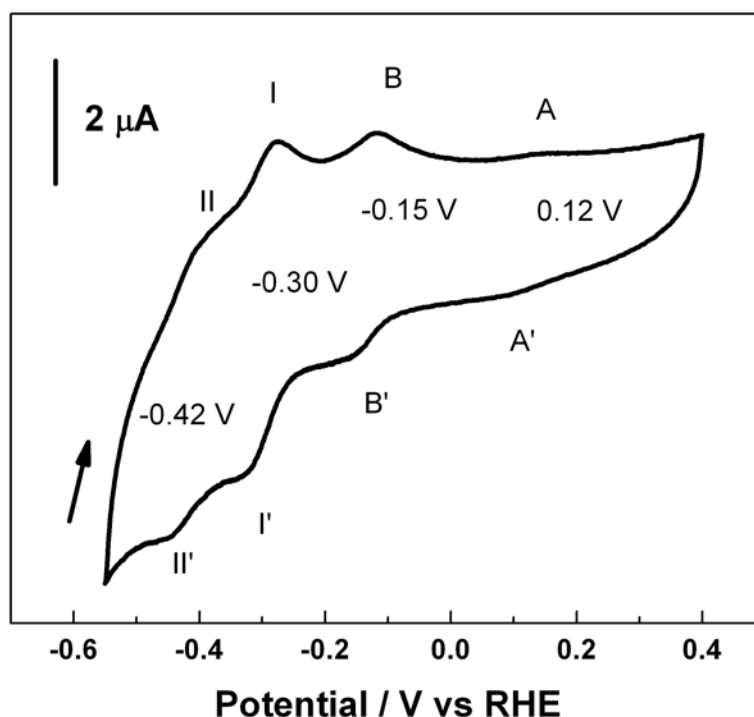


Fig.3. 2 Cyclic voltammetry of 0.2mM Ru₂POM in pH=5 buffer solution

From comparison with previous ruthenium substituted polyoxometalate structures containing Ru(III) centers by Pope³⁹, Keita^{27, 33, 38} and Hill, the redox features correspond to the stepwise reduction of the ruthenium metal centers. Further analysis of the cyclic voltammogram in the positive direction as shown in Fig.3.3 reveals the presence of one Ru oxidation peak ($E_{1/2} = 0.95\text{V}$), one irreversible oxidative peak (1.2V) and one irreversible reduction peak at 0.7V.

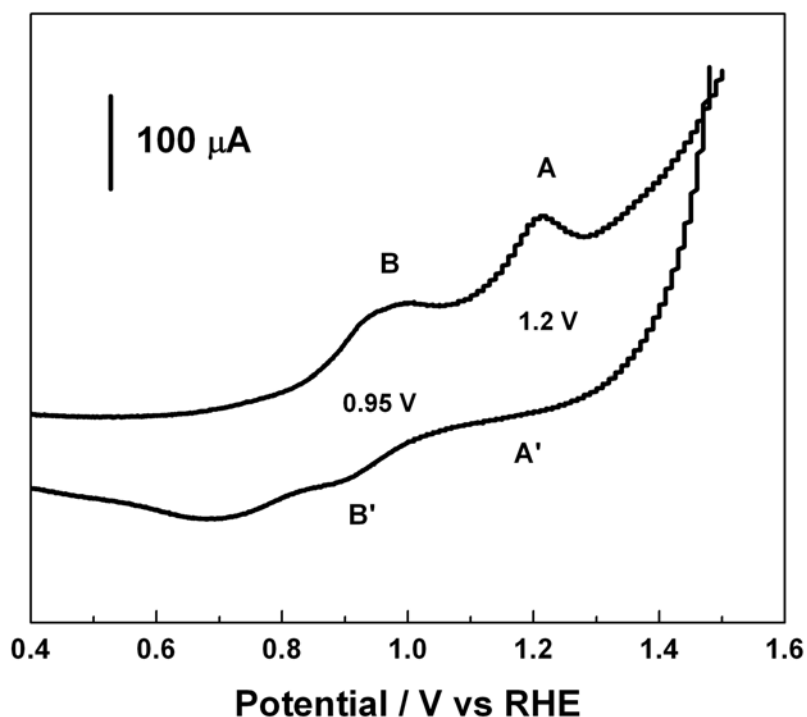


Fig.3.3. Cyclic voltammetry of Ruthenium oxidation peaks in pH5 acetate buffer solution with 0.2mM Ru₂POM

Ir₂POM sandwich

Electrochemical investigations have been performed to establish the iridium substitution in the framework. The electrocatalytic effect of this compound has been tested for oxidation and reduction reactions, i.e., oxidation of water (oxygen generation

reaction), oxidation of L-cysteine & ascorbic acid and oxygen reduction were studied. According to our knowledge, this is the very first time that a bifunctional electrocatalytic nature has been experimentally tested on a di-iridium substituted sandwich polyoxometalate. It has been well established in literature that the mono-substituted Iridium Keggin and Wells-Dawson structures are very good electrocatalysts for nitrite reduction in acidic medium⁴⁰⁻⁴².

In this work we have concentrated on the electrocatalytic applications in near neutral conditions. Our interest in novel applications of transition metal substituted polyoxometalates had prompted us to explore amino acid oxidation, which is very important in neutral medium and hence, can be employed in biosensing systems. Keita et al^{11, 43} have developed Vanadium substituted Wells-Dawson structures to be efficient electrocatalysts for L-cysteine oxidation. Of all the transition metal compounds tested, the vanadium based system was the most efficient in their studies. Ascorbic acid oxidation is also an important reaction occurring at near neutral conditions and several groups have explored polyoxometalate based electrocatalysis^{31, 44} for this reaction.

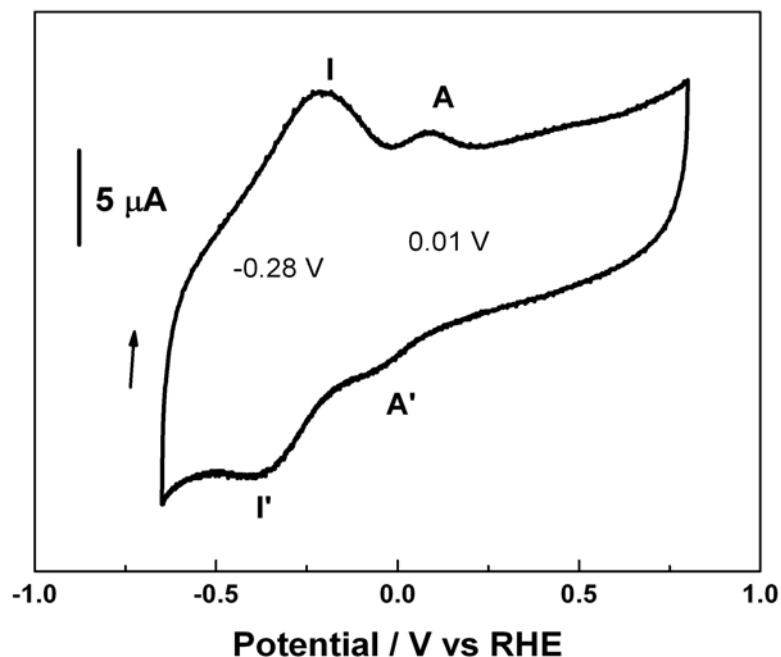


Fig.3. 4 Cyclic Voltammetry of Ir₂POM in pH=5 Buffer Solution

In the case of Ir₂POM (Fig.3.4), the cage features are very similar to the Zn₂POM redox waves and similarities with Ru₂POM can be made. A slight shift in the Ru₂POM cage feature can be attributed to the difference in their valencies (Ru^(III) and Ir^(IV)).

L-cysteine oxidation occurs at very high overpotentials in glassy carbon electrode at neutral pH conditions^{43, 45}, despite this fact, L-cysteine sensing plays an important role as a biological marker molecule¹¹. In this regard, the stability of sandwich type structures in neutral conditions is an important advantage and hence the application of Ir₂POM has been explored. Fig.3.5 reveals the linear scan voltammogram of 0.2mM Zn₂POM and Ir₂POM solutions, in the presence of L-cysteine (0.05mM).

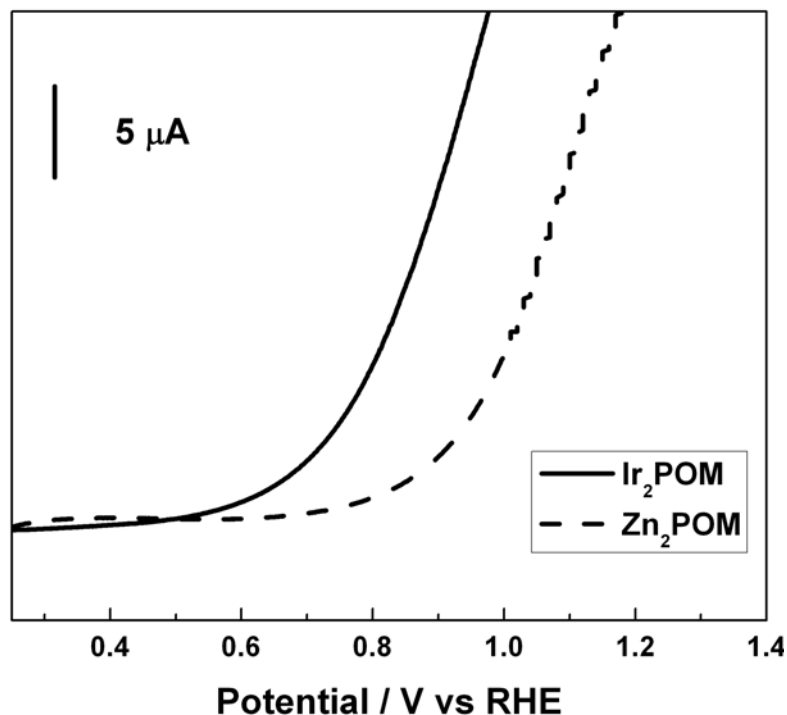


Fig.3.5. Comparison of L-Cysteine (10 μ M) oxidation at iridium substituted sandwich POM and the precursor Zn₂POM, with GC as working electrode, Pt mesh as counter electrode and Ag/AgCl as reference electrode.

The precursor Zn₂POM shows an oxidation peak, which begins at about 0.80V. Ir₂POM on the other hand exhibits an oxidation peak very early at about 0.45V. Since the cysteine oxidation peak begins just after the iridium oxidation peak, which is centered on 0.01V under these pH conditions, the transition metal plays an important role in this oxidation reaction. It has been shown in literature^{40, 42} that Ir substituted polyoxometalates exhibit some unique reductive electrocatalytic properties. In this work, the presence of a di-iridium substitution has provided improved oxidative capability.

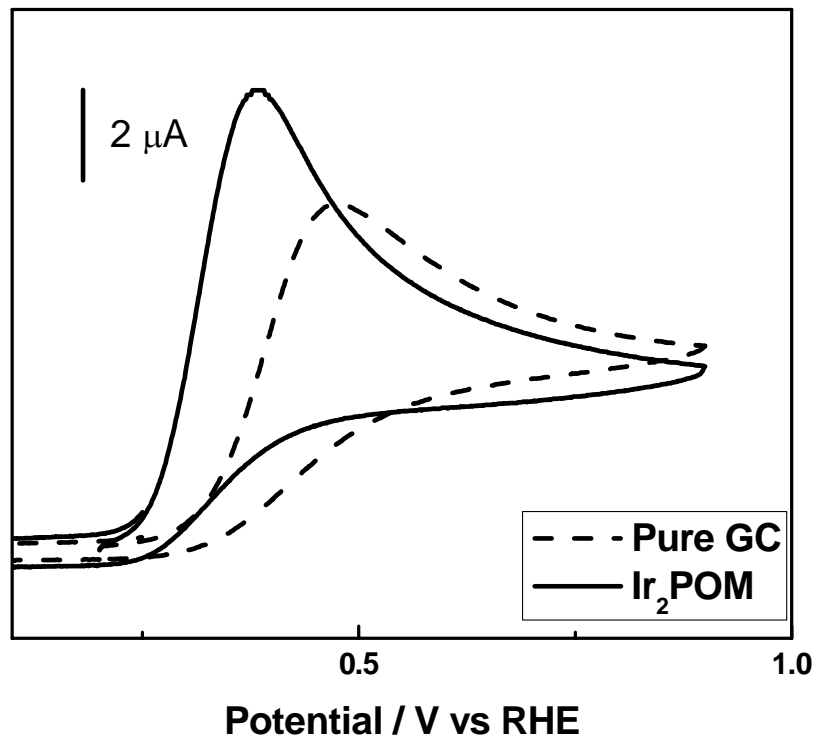


Fig.3.6. Ascorbic acid (10 μM) oxidation in the presence and absence of iridium substituted sandwich type polyoxometalate.

In a similar direction, the performance of di-iridium for ascorbic acid oxidation has also been evaluated. As shown in Fig.3.6, the oxidation reaction of ascorbic acid occurs about 0.1V to the left of the pure glassy carbon electrode. This behavior is unique to the di-iridium substituted species and not shown in the Zn_2POM precursor molecule. Further explorations are needed to identify the mechanism of oxidation of organic molecules to understand the role played by the iridium substituted onto the Zn_2POM . In this regard, iridium substituted sandwich can be considered as similar to vanadium substituted sandwich compounds as described by Keita et al^{5,46,47}.

Further studies on the reduction side of Ir_2POM voltammetry, revealed an interesting behavior in the presence of oxygen in solution. It has been well established

that polyoxometalates catalyze the reduction of oxygen. In our case, as shown in Fig. 3.7, in a pH=5 acetate buffer, there is a steady increase in current, exactly after the iridium reduction peak. This has been attributed to oxygen reduction by the iridium metal center.

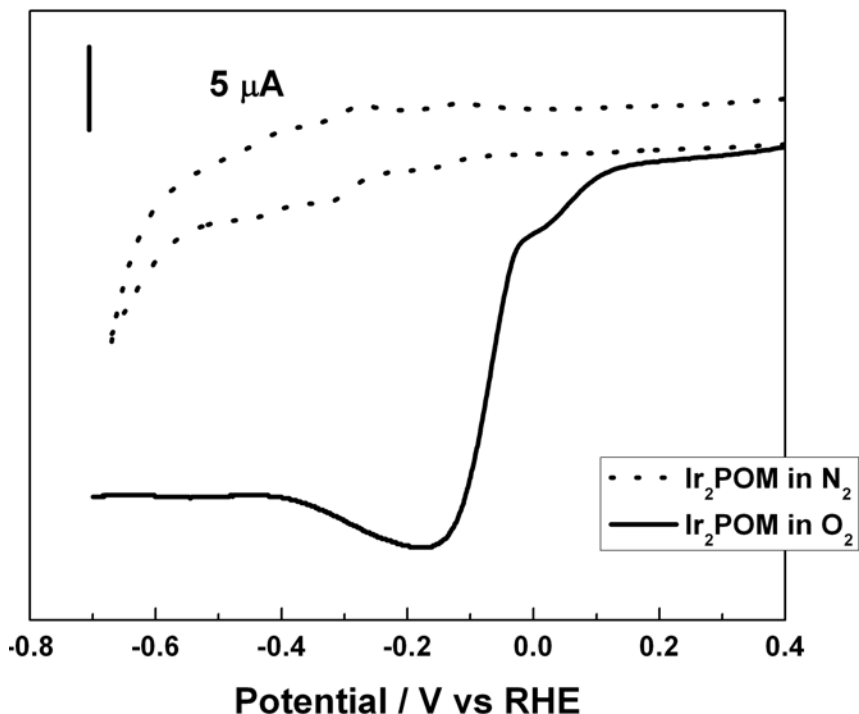


Fig.3.7. Voltammetric curve showing oxygen reduction reaction at di-iridium substituted sandwich POM at a GC electrode in pH5 acetate solution. Pt mesh as counter electrode and Ag/AgCl as reference electrode.

The electrolyte solution was bubbled with oxygen for more than 30 minutes and the oxygen concentration was considered to be constant and equivalent to saturated values at the given atmospheric conditions.

Fe₂POM Sandwich {Na₁₄[Fe^{III}₂Zn₂(H₂O)₂{ZnW₉O₃₄]₂}

Iron substituted polyoxometalates have been extensively studied due to their unique electrocatalytic property directed towards H₂O₂ reduction, nitrate reduction etc.

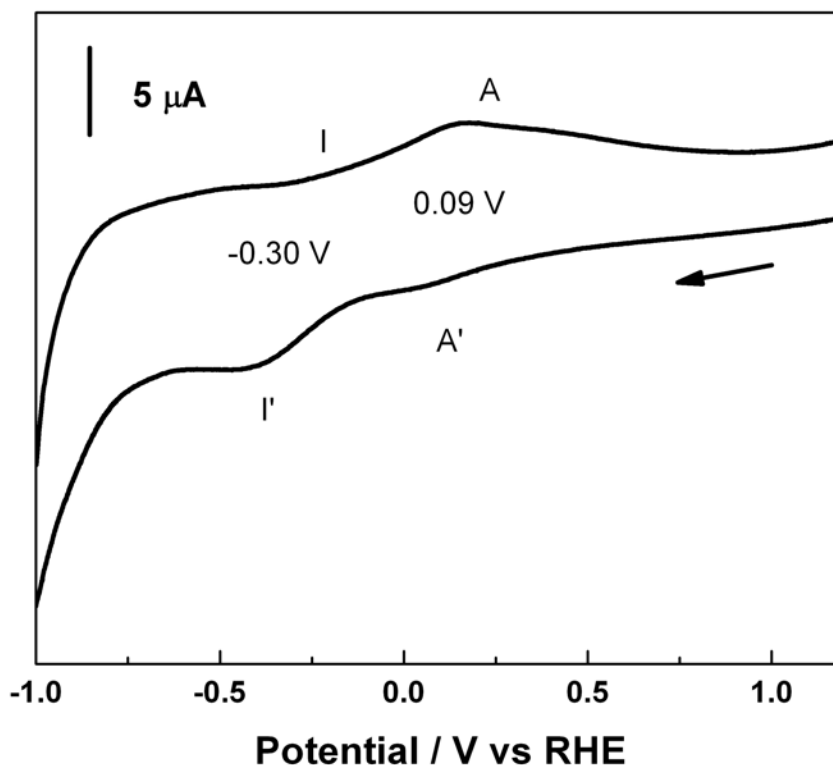


Fig.3. 8 Cyclic Voltammogram of Fe₂POM during the very first scan in 0.2mM solution at WE = GC, CE = Pt mesh

The cyclic voltammogram of Fe₂POM solution as shown in Fig.3.8 exhibits the usual tungsten (VI) reduction peak at -0.30 V and an additional peak at +0.09V in the anodic region. From previous studies, this peak could be assigned to Fe^{3+/2+} redox peak. The poorly-defined redox peaks observed during the initial cycling is a consistent trend in these sandwich compounds, and is also observed in the Zn₂POM. Electrocatalytic activity of Fe₂POM for oxygen reduction will be discussed in subsequent chapters.

3.5. Electrocatalytic oxygen generation at transition metal substituted sandwich type polyoxometalates

In order to evaluate the electrocatalytic property of these TMSP sandwich

compounds, oxygen generation through water oxidation was selected as the model reaction. Glassy carbon was chosen and a near neutral pH (~5) was chosen for study as shown in Fig.3.9. This qualitative cyclic voltammetry establishes the fact that diruthenium substituted sandwich compound is the most active complex in glassy carbon electrode. Following Tourne's method⁴⁸, Fe, Mn and Ni substituted sandwich type POMs were also synthesized.

As observed from the polarization curve in Fig.3.9, the Ru₂POM solution exhibits the very best performance followed by Ni, Mn and Fe. For the Ru₂POM, the onset of oxygen evolution occurs at 0.94 V, which matches with the thermodynamic potential corresponding to oxygen evolution at pH=5 solution.

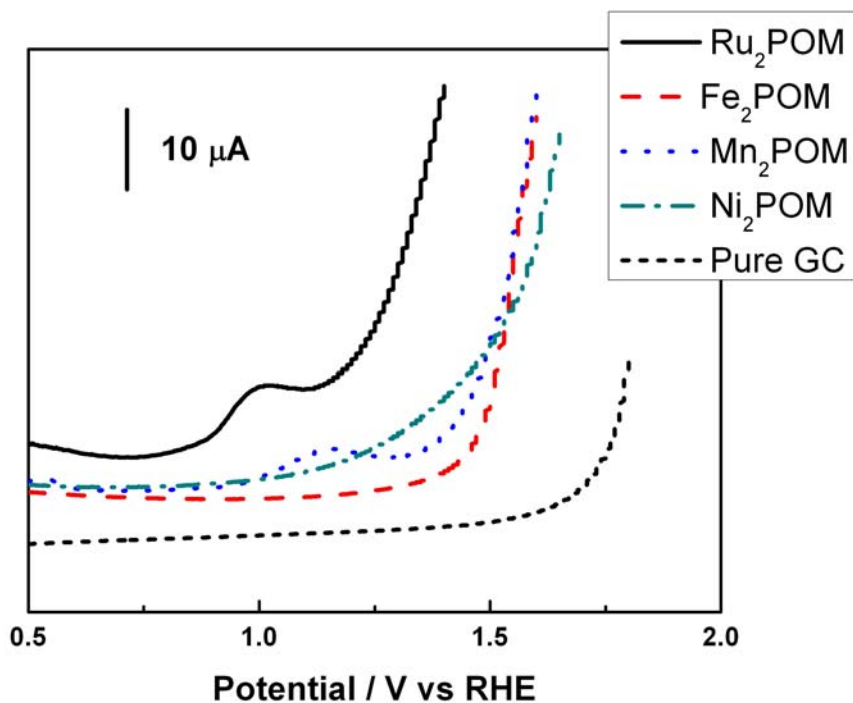


Fig.3.9 Polarization curves for oxygen generation reaction observed in pH = 5 Buffer solution at a Glassy Carbon (GC) electrode in the presence of different transition metal substituted polyoxometalates (0.2mM). Counter electrode - Pt mesh and Reference

electrode-Ag/AgCl (potential values are reported with respect to NHE)

3.6. Stability of transition metal substituted sandwich polyoxometalate thin films

Films of sandwich type polyoxometalates are formed as a result of delicate self assembly under very precise conditions of pH and concentration. In this regard, we believe that there is a dynamic equilibrium exists between the integral sandwich compounds and their precursor molecules in solution during potential cycling also. There could also be an effect of localized pH variation in a non-buffered electrolyte. There is a possibility of derivatization of the electrode surface during the initial cycling procedure, in the case of Zn₂POM. Keita et al^{33, 34} have shown that extending the potential window of trivalent lacunary phosphotungstate species to more cathodic regions (> -0.7 V) results in the deposition of a film and this film has been described to render the voltammogram featureless. Keeping these concepts in mind, we have explored the behavior of Zn₂POM sandwich as unique structures. As an example for adsorption on the surface of electrodes, we have performed electrochemical surface plasmon resonance studies of Zn₂POM. An elaborate exploratory study has been performed in the chapter 5. Here we present a representative plot of the behavior of Zn₂POM solution in the presence of a potential step. The Fig.3.10 show the response of ESPR, an interface exploratory technique, which shows changes in optical properties with increase in interfacial activity.

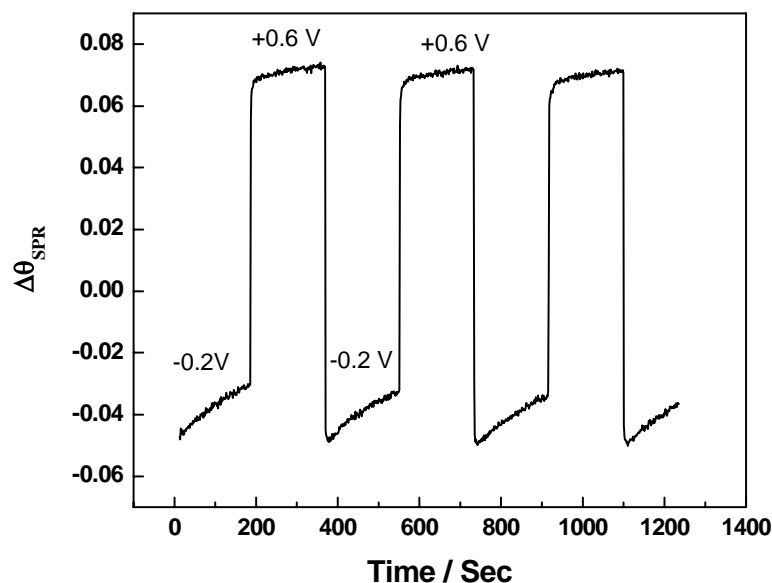


Fig.3.10 Electrochemical Surface Plasmon Response of Zn_2POM solution in 0.5 M Na_2SO_4 corresponding to potential step from -0.2 V (adsorptive) to +0.6 V (desorptive)

It has been shown that at very high pH conditions, the whole polyanion undergoes decomposition via the OH^- ion attack. From UV-Vis studies of these compounds, it has been established that the sandwich POMs have a stability window from pH 4 to pH 9³³. In order to understand the decomposition of sandwich type structures, we have deliberately acidified a solution of Zn_2POM and subjected it to electrochemical characterization. A single investigative cyclic voltammogram was recorded for this Zn_2POM precursor in an acidic medium (ca. 0.1M HClO_4), as shown in Fig.3.11. The three redox couples in 0.1M HClO_4 solution can be labeled by a preliminary comparison with the redox peaks of a monolacunary Keggin structure³ ($\text{ZnW}_{11}\text{O}_{39}^{10-}$). The first two reduction peaks (I' and II') could be equated to the two one-electron waves seen in Keggin structures and the third peak (III') could be equated to the two electron reduction

accompanied by proton addition. The number of electrons transferred have been calculated using constant potential electrolysis and by comparison of the magnitude of current in the case of one electron reduction of potassium ferricyanide solution at a glassy carbon electrode with the same geometric area. The position of the redox peaks in Fig.3.11 reveals a similarity to the characteristic tungsten redox features of the corresponding zinco-tungstate monolacunary Keggin molecule, $\text{ZnW}_{11}\text{O}_{39}^{10-}$. This observation, coupled with the fact that the stability of these sandwich compounds reside in the range of pH 4 to 9, points to the phenomenon of the fragmentation of the sandwich into lacunary Keggin-like structures.

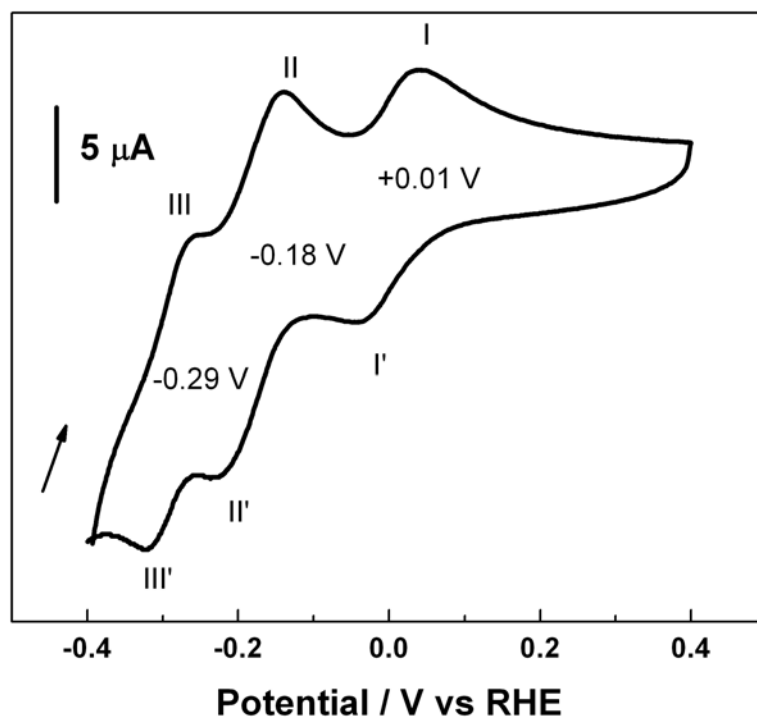


Fig.3. 11 Cyclic voltammogram of 0.2 mM Zn_2POM in 0.1 M HClO_4 solution

At this juncture, it will be interesting to discuss the nature of the fragmentation of clusters in the acidic medium. As mentioned earlier, these sandwich compounds are made

of two trivacant lacunary Keggin units attached by a central metal belt comprising four transition metals. Hence a natural candidate for the fragment will be the trivacant lacunary structure, $ZnW_9O_{34}^{12-}$. These trivacant lacunary species have been described previously, but its structural characterization had always been based on indirect methods, since these species are known to exist in solution at a relatively low half-life during the pH dependent equilibria with the monolacunary species (ca. $PW_{11}O_{39}^{7-}$) and other units. Finke et al⁴⁹, were the first group to identify conditions to stabilize these trivacant Keggin units using an M^{2+} substitution, by titration with Co^{2+} . When these structures were subjected to crystallographic investigations, it was found that the $PW_9M_2O_{34}^{5-}$ species had dimerized to form a saturated heteropolytungstate $P_2W_{18}M_4(H_2O)_2O_{68}^{10-}$. This is the tetra metal substituted version of the sandwich complex under investigation in our study $[(M_2Zn_2[ZnW_9O_{34}]_2)^{n-}]$. Finke's group was successful in developing an alternative synthetic route for these sandwich compounds. This finding presents strong evidence towards the presence of a bimetal substituted trivacant lacunary species in solution during the decomposition or cluster breakage as shown in Fig.3.12.

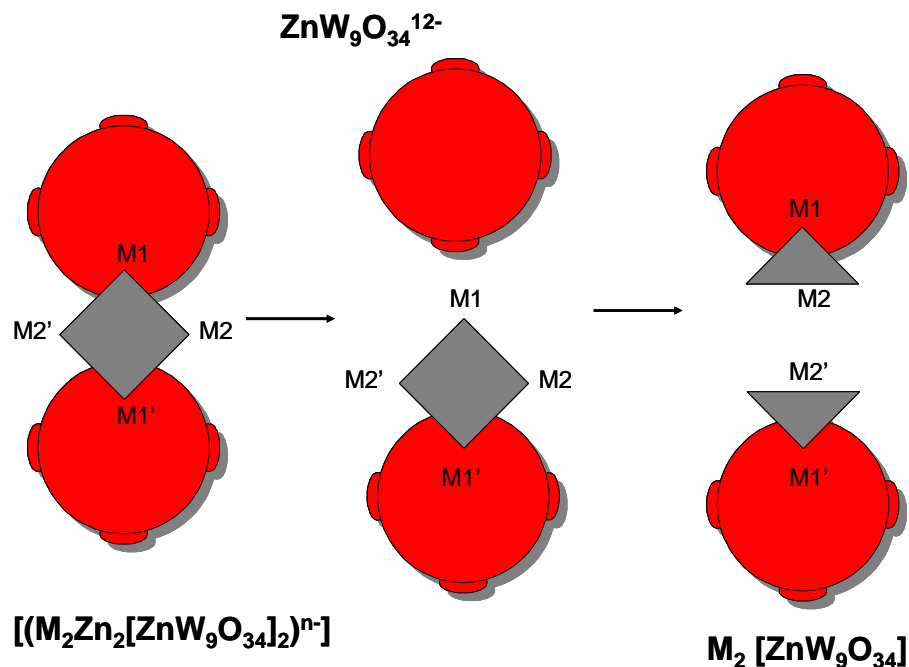


Fig.3.12 Schematic representation of the fragmentation of sandwich type clusters and the reasons for the changes to the trivalent lacunary sub-units could be any of the following three: 1. Very low concentration, 2. Low or high pH condition and 3. Species immobilized on electrode surface.

A comparison of the behavior of Zn_2POM in acidic medium (Fig.3.11) and at $\text{pH}=5$ (Fig.3.2), reveals another important feature that the redox peaks in $\text{pH}=5$ are not well-defined and they do not exhibit diffusion limitation, unlike the peaks observed under acidic conditions. This behavior shows that these redox peaks could be the result of surface active species, and subsequent studies have been performed to elucidate this observation. The presence of two trivalent lacunary Keggin molecules and the possibility of a surface active species, in the sandwich compound could be cited as the reason for the lack of well-defined redox peaks.

Finally, there seems to be a dynamic equilibrium which dictates the identity of the

polyoxometalate species at any given condition of concentration, pH and whether the species is in solution or on a surface.

References:

1. Pope, M. T., *Heteropoly and Isopoly Oxometalates*. Springer-Verlag: 1983.
2. Pope, M. T.; Muller, A., *Angew.chem.Int.Ed.Engl.* **1991**, 30, 34-48.
3. Sadakane, M.; Steckhan, E., *Chem. Rev* **1998**, 98, 219-237.
4. Keita, B.; Nadjo, L., *Journal of Molecular Catalysis a-Chemical* **2007**, 262, (1-2), 190-215.
5. Keita, B.; Mbomekalle, I. M.; Nadjo, L.; Haut, C., *Electrochemistry Communications* **2004**, 6, (10), 978-983.
6. Ruhlmann, L.; Nadjo, L.; Canny, J.; Contant, R.; Thouvenot, R., *European Journal of Inorganic Chemistry* **2002**, (4), 975-986.
7. Keita, B.; Abdeljalil, E.; Nadjo, L.; Contant, R.; Belgiche, R., *Electrochemistry Communications* **2001**, 3, (2), 56-62.
8. Keita, B.; Mbomekalle, I. M.; Lu, Y. W.; Nadjo, L.; Berthet, P.; Anderson, T. M.; Hill, C. L., *European Journal of Inorganic Chemistry* **2004**, (17), 3462-3475.
9. Keita, B.; Abdeljalil, E.; Nadjo, L.; Contant, R.; Belgiche, R., *Langmuir* **2006**, 22, (25), 10416-10425.
10. Keita, B.; Mbomekalle, I. M.; Nadjo, L.; Anderson, T. M.; Hill, C. L., *Inorganic Chemistry* **2004**, 43, (10), 3257-3263.
11. Keita, B.; Contant, R.; Mialane, P.; Secheresse, F.; De Oliveira, P.; Nadjo, L., *Electrochemistry Communications* **2006**, 8, (5), 767-772.
12. Anderson, T. M.; Fang, X. K.; Mbomekalle, I. M.; Keita, B.; Nadjo, L.; Hardeastle,

- K. I.; Farsidjani, A.; Hill, C. L., *Journal of Cluster Science* **2006**, 17, (2), 183-195.
13. Duncan, D. C.; Hill, C. L., *Journal of the American Chemical Society* **1997**, 119, (1), 243-244.
14. MeEvoy, A. J.; Gratzel, J., *J. Electroanal. Chem* **1986**, 209, 391.
15. B. Keita; L. Nadjo, *Chem. Phys* **1989**, 22, 77.
16. Keita, B.; Nadjo, L., *Curr. Top. Electrochem* **1993**, 2, 77.
17. Keita, B.; Nadjo, L.; Belhouari, A.; Constant, R., *J. Electroanal. Chem* **1995**, 381, 243.
18. Toth, J. E.; Anson, F. C., *Journal of Electroanalytical Chemistry* **1988**, 256, (2), 361-370.
19. Ritorto, M. D.; Anderson, T. M.; Neiwert, W. A.; Hill, C. L., *Inorganic Chemistry* **2004**, 43, (1), 44-49.
20. Romo, S.; Jorge, F.; Miquel, M. J.; Keita, B.; Nadjo, L.; Coen, G.; Josep, P., *Inorg. Chem* **2007**, 46, 4022.
21. Lopez, X.; Bo, C.; Poblet, J. M., *J. Am. Chem. Soc.* **2002**, 124, 12574.
22. Cadot, E.; Fournier, M.; Teze, A.; Herve, G., *Inorg. Chem.* **1996**, 35, 282.
23. Rong, C. Y.; Pope, M. T., *J. Am. Chem. Soc.* **1992**, 114, 2932.
24. Baker, L. C. W.; Baker, V. E. S.; Eriks, K.; Pope, M. T.; Shibatha, M.; Rollins, O. W.; Fang, J. H.; Kohn, L. L., *J. Am. Chem. Soc* **1966**, 88, 2329.
25. Zhang, X. Y.; Jameson, G. B.; O'Connor, C. J.; Pope, M. T.; *Polyhedron* **1996**, 15, 917-922.
26. Keita, B.; Lu, Y. W.; Nadjo, L.; Contant, R., *European Journal of Inorganic Chemistry* **2000**, (12), 2463-2471.
27. Bi, L. H.; Kortz, U.; Keita, B.; Nadjo, L., *Dalton Transactions* **2004**, (20), 3184-3190.

28. Li-Hua Bi, U. K., Bineta Keita and Louis Nadjo, *Dalton Transactions* **2004**.
29. Cheng, L.; Dong, S., *Journal of Electroanalytical Chemistry* **2000**, 481, (2), 168-176.
30. Liu, J. Y.; Cheng, L.; Li, B. F.; Dong, S. J., *Langmuir* **2000**, 16, (19), 7471-7476.
31. Liu, J. Y.; Cheng, L.; Dong, S. J., *Chemical Journal of Chinese Universities-Chinese* **2001**, 22, (10), 1641-1644.
32. Cheng, L.; Niu, L.; Gong, J.; Dong, S. J., *Chemistry of Materials* **1999**, 11, (6), 1465-1475.
33. Bi, L. H.; Kortz, U.; Dickman, M. H.; Keita, B.; Nadjo, L., *Inorganic Chemistry* **2005**, 44, (21), 7485-7493.
34. Constant, R., *Canadian Journal of Chemistry-Revue Canadienne De Chimie* **1987**, 65, 568.
35. Demir, U.; Shannon, C., *Langmuir* **1996**, 12, 6091-6097.
36. Sanchez-Maestre, M.; Rodriguez-Amaro, R.; Munoz, E.; Ruiz, J.; Camacho, L., *Journal of Electroanalytical Chemistry* **1994**, 373, 31.
37. Bosco, E.; Rangarajan, S. K., *Journal of Electroanalytical Chemistry* **1981**, 129, 25.
38. Bi, L. H.; Chubarova, E. V.; Nsouli, N. H.; Dickman, M. H.; Kortz, U.; Keita, B.; Nadjo, L., *Inorganic Chemistry* **2006**, 45, (21), 8575-8583.
39. Rong, C. Y.; Pope, M. T., *Journal of the American Chemical Society* **1992**, 114, (8), 2932-2938.
40. Liu, H. Z.; Sun, W. L.; Yue, B.; Jin, S. L.; Deng, J. Q.; Xie, G. Y., *Synthesis and Reactivity in Inorganic and Metal-Organic Chemistry* **1997**, 27, (4), 551-566.
41. Sun, W. L.; Yang, F.; Liu, H. Z.; Kong, J. L.; Jin, S. L.; Xie, G. Y.; Deng, J. Q., *Journal of Electroanalytical Chemistry* **1998**, 451, (1-2), 49-57.

42. Wenliang Sun, H. L., Jilie Kong, Gaoyang Xie, Jiaqi Deng, *Journal of Electroanalytical Chemistry* **1997**, 437, 67-76.
43. Keita, B.; Mbomekalle, I. M.; de Oliveira, P.; Ranjbari, A.; Justum, Y.; Nadjo, L.; Pompon, D., *Journal of Cluster Science* **2006**, 17, (2), 221-233.
44. Geletii, Y. V.; Bailey, A. J.; Cowan, J. J.; Weinstock, I. A.; Hill, C. L., *Canadian Journal of Chemistry-Revue Canadienne De Chimie* **2001**, 79, (5-6), 792-794.
45. Raof, J. B.; Ojani, R.; Beitollahi, H., *Electroanalysis* **2007**, 19, (17), 1822-1830.
46. Keita, B.; Zhang, G. J.; Dolbecq, A.; Mialane, P.; Secheresse, F.; Miserque, F.; Nadjo, L., *Journal of Physical Chemistry C* **2007**, 111, (23), 8145-8148.
47. Keita, B.; Essaadi, K.; Nadjo, L.; Desmadril, M., *Chemical Physics Letters* **1995**, 237, (5-6), 411-418.
48. Tourne, C. M.; Tourne, G. F.; Zonnevjlle, F., *J.Chem.Soc.Dalton Trans* **1991**, (1), 143-155.
49. Finke, R. G.; Droege, M.; Hutchinson, J. R.; Gansow, O., *J. Am. Chem.Soc* **1981**, 103, 1587-1589.

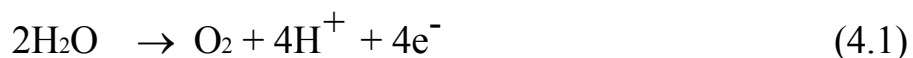
CHAPTER 4

DIRUTHENIUM SUBSTITUTED POLYOXOMETALATE AS AN INORGANIC ELECTROCATALYST FOR OXYGEN GENERATION

4.1. Introduction

Electrocatalytic oxygen generation is a very important reaction in electrochemistry and it plays an important role in wide ranging applications from industrial metallurgy to regenerative fuel cell applications¹. Oxygen evolution reaction is a very demanding reaction and hence it is highly sensitive to the nature and structure of electrocatalysts. The very early oxygen electrodes were based on nickel and nickel oxides², and subsequently RuO₂, IrO₂, perovskites and mixed oxide systems were employed³. These oxides have been employed as anodes of water electrolyzers, in metal electrowinning processes, cathodic protection, in electro-organic reductions etc.

The importance of oxygen evolution during the light-assisted decomposition of water has been a major driving force in the direction of alternative and clean energy systems based on solar energy. In this regard, a lot of attention has been devoted to homogeneous water oxidation complexes in the scientific community to mimic the oxygen evolving center (OEC) of photosystem II (PS-II), present in green plants. The active component for this water oxidation reaction has been identified as a polynuclear Ca-Mn₄ complex with dimeric di- μ -oxo Mn units⁴.



Though very ubiquitous in nature, this energy intensive reaction [$E^{\circ} = 1.23$ V (vs SHE) at pH = 0.0], has tremendous molecular complexity from a mechanistic perspective, since it involves the transfer of four electrons to an oxidant, coupled with the release of four protons and ultimately the formation of an O-O bond. In this scenario, there are very few well-defined complexes that can oxidize water to dioxygen in a homogeneous phase and in the absence of light, such as the one occurring in the PS-II system. Several di- and tetra nuclear metal complexes have been synthesized and tested as models of the OEC complex, and four electron oxidation of water has been achieved with only very few complexes, namely about two Mn complexes (not very stable) and a number of Ru complexes (more robust). From the review by Llobet et al, of all the Ru complexes employed for water oxidation, there are two distinctive types, complexes containing Ru-O-Ru bridging group and those without this oxo-bridge⁵⁻⁷.

Till date only a very few totally inorganic catalysts^{8, 9} for oxygen evolution are known, and of these, transition metal substituted polyoxometalate clusters are the most predominant group of compounds¹⁰. The chemistry of transition metal substituted polyoxometalate is highly developed and much of the interest in recent years is driven by their prospects as “green” oxidation catalysts and as model transition metal oxide surfaces¹¹⁻¹⁴.

Within the transition metal substituted polyoxometalates, the sandwich type structures, described in the earlier chapters are very important. The sandwich type polyoxotungstates consisting of two trivacant Keggin units connected by a central metal belt of four transition metals (WZn_3), first synthesized by Tourne et al¹⁵ have been employed in many catalytic applications via the substitution of different transition metals.

Recently Neuman et al¹⁶ synthesized a di-Ru substituted compound, $[\text{WZnRu}_2(\text{OH})(\text{H}_2\text{O})(\text{ZnW}_9\text{O}_{34})_2]^{11-}$ to be employed as organic oxidation catalyst under different solvent conditions.

Ruthenium substituted polyoxometalates have a special importance because of the unique redox and catalytic activities of the element, ruthenium¹⁷. Until now, only a few ruthenium based polyoxotungstates have been studied for their catalytic and electrocatalytic properties¹⁸⁻²⁸. The main reason for the scarcity of well-defined ruthenium substituted structures is that the synthesis of these structures is not straightforward. This is due to the lack of a pure, well characterized precursor which is water-soluble, air stable and also labile to release the Ru atoms in solution to be available for substitution. Of the compounds available commercially, $\text{RuCl}_3 \cdot n\text{H}_2\text{O}$ has been employed extensively. However, this compound is actually a mixture of mono and polymetallic oxides, hydroxides and chlorides of ruthenium in the +3 and +4 oxidation states^{29, 30}. Table 4.1 shows the collection of ruthenium polyoxometalates and their corresponding precursor molecules observed from literature results.

Table 4.1 Literature Overview of Ruthenium Polyoxometalate Synthesis with Respect to the nature of precursor

Ru Precursor	Polyoxometalate Precursor	Ru-substituted Compound	Literature
$\text{RuCl}_3 \cdot n\text{H}_2\text{O}$	$[\text{SiW}_{11}\text{O}_{39}]^{8-}$	$[\text{Ru}^{\text{III}}(\text{H}_2\text{O})\text{SiW}_{11}\text{O}_{39}]^{5-}$	Neuman et al ³¹⁻³³
$\text{RuCl}_3 \cdot n\text{H}_2\text{O}$	$[\text{P}_2\text{W}_{17}\text{O}_{61}]^{10-}$	$[\text{O}\{\text{Ru}^{\text{IV}}\text{Cl}(\alpha_2\text{-P}_2\text{W}_{17}\text{O}_{61})\}_2]^{16-}$	Finke et al ³⁴
$[\text{Ru}^{\text{II}}(\text{H}_2\text{O})_6][\text{C}_7\text{H}_7\text{SO}_3]_2$	$[\text{PW}_{11}\text{O}_{39}]^{7-}$	$[\text{Ru}^{\text{III}}(\text{H}_2\text{O})\text{PW}_{11}\text{O}_{39}]^{4-}$	Pope et al ³⁵
$[\text{Ru}^{\text{II}}(\text{H}_2\text{O})_6][\text{C}_7\text{H}_7\text{SO}_3]_2$	$[\text{P}_2\text{W}_{17}\text{O}_{61}]^{10-}$	$[\alpha_2\text{-Ru}^{\text{III}}(\text{H}_2\text{O})\text{P}_2\text{W}_{17}\text{O}_{61}]^{7-}$	Pope et al ³⁵
$\text{Ru}(\text{acac})_3$, hydrothermal	$[\text{SiW}_{11}\text{O}_{39}]^{8-}$	$[\text{Ru}^{\text{III}}(\text{H}_2\text{O})\text{SiW}_{11}\text{O}_{39}]^{5-}$	Higashijima ³⁶
$\text{Ru}(\text{acac})_3$, hydrothermal	$[\text{SiW}_{11}\text{O}_{39}]^{8-}$	$[\text{SiW}_{11}\text{O}_{39}\text{-Ru}^{\text{IV}}\text{ORu}^{\text{III}}\text{SiW}_{11}\text{O}_{39}]^{11-}$	Sadakane ³⁷
<i>cis</i> - $\text{Ru}(\text{dmsO})_4\text{Cl}_2$	$[\text{WZn}_3(\text{H}_2\text{O})_2(\text{ZnW}_9\text{O}_{34})_2]^{12-}$	$[\text{WZnRu}^{\text{III}}_2(\text{OH})(\text{H}_2\text{O})(\text{ZnW}_9\text{O}_{34})_2]^{11-}$	Neuman et al ¹⁶
Same as above		$[\alpha_2\text{-Ru}^{\text{III}}(\text{H}_2\text{O})\text{P}_2\text{W}_{17}\text{O}_{61}]^{7-}$	Nomiya et al ²²
Same as above Microwave assisted hydrothermal	$[\text{PW}_{11}\text{O}_{39}]^{7-}$	$[\text{Ru}^{\text{II}}(\text{dmsO})\text{PW}_{11}\text{O}_{39}]^{5-}$	Bonchio et al ³⁸
Same as above		$[\text{HW}_9\text{O}_{33}\text{Ru}^{\text{II}}_2(\text{dmsO})_6]^{7-}$	Li-Hua Bi ³⁹
Same as above		$[\text{Ru}(\text{dmsO})_3(\text{H}_2\text{O})\text{XW}_{11}\text{O}_{39}]^{6-}$	Li-Hua Bi ²⁸

General Considerations

From an electrochemical perspective, the anodic reaction of oxygen evolution has a rather high overvoltage on most electrode materials. In comparison to the often studied

four electron reduction of molecular oxygen (as in fuel cells), there are no strong oxygen-to-oxygen bond scission involved during water oxidation. From the review by Yeager et al⁴⁰, some very interesting aspects about the oxygen evolution reaction can be listed as follows.

- i. Oxygen evolution reaction occurs from either OH^- or H_2O in aqueous solutions
- ii. Oxygen evolution reaction in aqueous solutions occur in the potential regime where most metal electrodes are not corrosion resistant and hence the need for novel electro-catalytic materials
- iii. It is extremely difficult to detect the intermediates of water oxidation such as H_2O_2 or the corresponding HO_2^- , since they are very unstable in the potential regime of oxygen generation
- iv. In the case of metal based electrocatalysis, an intermediate step of metal oxide formation is always observed before oxygen evolution reaction

4.2. Materials and Methods

Diruthenium substituted sandwich type polyoxometalate was prepared according to methods described in previous chapters. Oxygen generation experiments were performed with gold as working electrode, Pt mesh as counter electrode and Ag wire as quasi-reference electrode. The supporting electrolyte is phosphate buffer solution at pH=8.

4.3. Results and Discussion

4.3.1. Elemental analysis

Elemental analysis determinations were made using energy dispersive X-ray (EDX) spectroscopy carried out on the same single crystals that were used for the XRD

measurements discussed above. For each single crystal sample, three iterations were performed and the results for all samples were pooled. Quantitation was carried out for Na, Ru, Zn and W. In the table below, averaged experimental data are compared to values calculated using the formulation $\text{Na}_{14}[\text{Ru}^{\text{III}}_2\text{Zn}_2(\text{H}_2\text{O})_2(\text{ZnW}_9\text{O}_{34})_2]$.

Table 4.2 EDX Analysis of single crystal specimen of Ru2POM

Element	Calc weight %	Exptl weight %	Exptl mol %
Na	6.17	5.80	25.22
Ru	3.88	3.79	3.75
Zn	5.01	4.92	7.52
W	66.40	64.03	34.84

The experimental W/Zn and Zn/Ru molar ratios are 4.63 and 2.01, respectively. These compare well with the above formulation, for which W/Zn = 4.50 and Zn/Ru = 2.00. The predicted W/Zn molar ratio for Neuman's formulation¹⁶ ($\text{Na}_{11}[\text{ZnWRu}_2(\text{OH})(\text{H}_2\text{O})(\text{ZnW}_9\text{O}_{34})_2]$) is 6.33, while the Zn/Ru molar ratio is 1.5.

4.3.2. UV-VIS Spectroscopy for pH Stability

The UV-Vis electronic spectroscopy of the compounds in neutral conditions, shows the general absorption at 300 nm (attributable to all Keggin systems), caused by the W-O-W charge transfer bands¹⁶. In addition, the ruthenium substituted Ru2POM exhibits a strong peak at 435nm as shown in Fig.4.1, attributable to the oxygen to ruthenium charge transfer band. Effect of change in pH has been studied via the UV-VIS spectroscopy, as shown in Fig.4.1, shows that the 435 nm peak does not undergo major changes and this shows that from pH 4 to 8, the compound exhibits a stable structure.

UV-Vis electronic spectroscopy has been extensively used in polyoxometalate research to establish the stability of transition metal substituted POMs under different pH conditions. Since the W-O-W charge transfer bands are characteristic features of Keggin based units, the presence of these strong absorption bands can be useful for determining the structural integrity of that particular compound in a given solution. UV-VIS can also be employed to determine the degree of completion of a given reaction, by observing the charge transfer bands of the POMs.

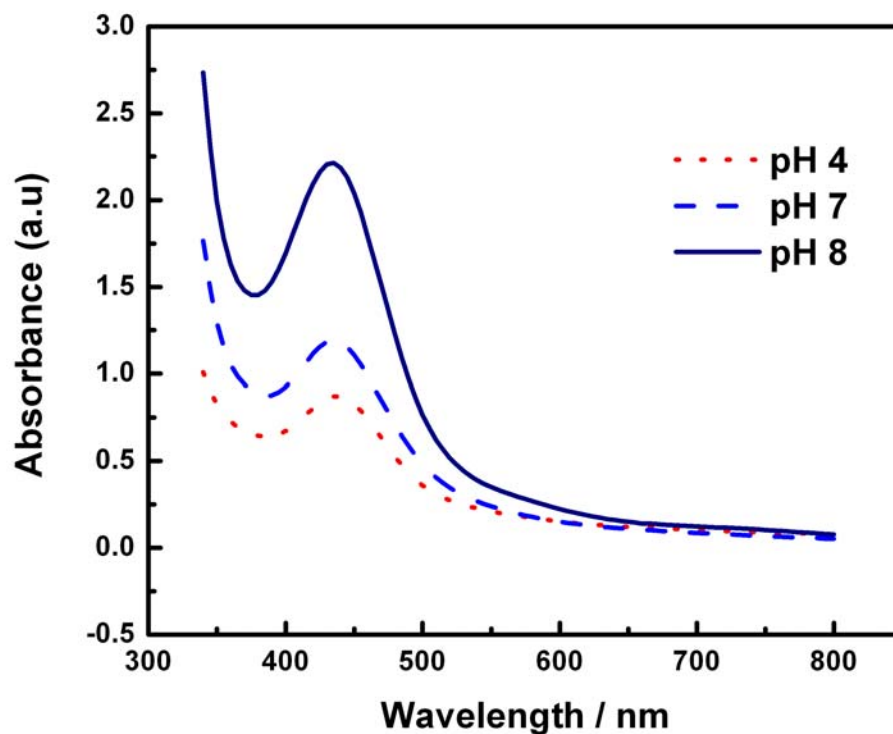


Fig.4. 1 pH stability analysis using UV-Vis spectroscopy in 0.5M Na₂SO₄ (pH adjusted by HCl and NaOH)

4.3.3. Electrochemical Characterization

Cyclic Voltammetric Measurement as an Evidence for pH Stability

Au electrodes were employed as working electrodes, together with Pt mesh and a Ag/AgCl reference electrode. Ru₂POM was dissolved in Ar saturated 0.5M Na₂SO₄ at a concentration of 0.2mM and this solution was employed as the electrolyte under a positive pressure of Ar. A non-buffered 0.5 M Na₂SO₄ was chosen to determine the effect of pH changes. Addition of H₂SO₄ and NaOH was performed to achieve the required pH condition.

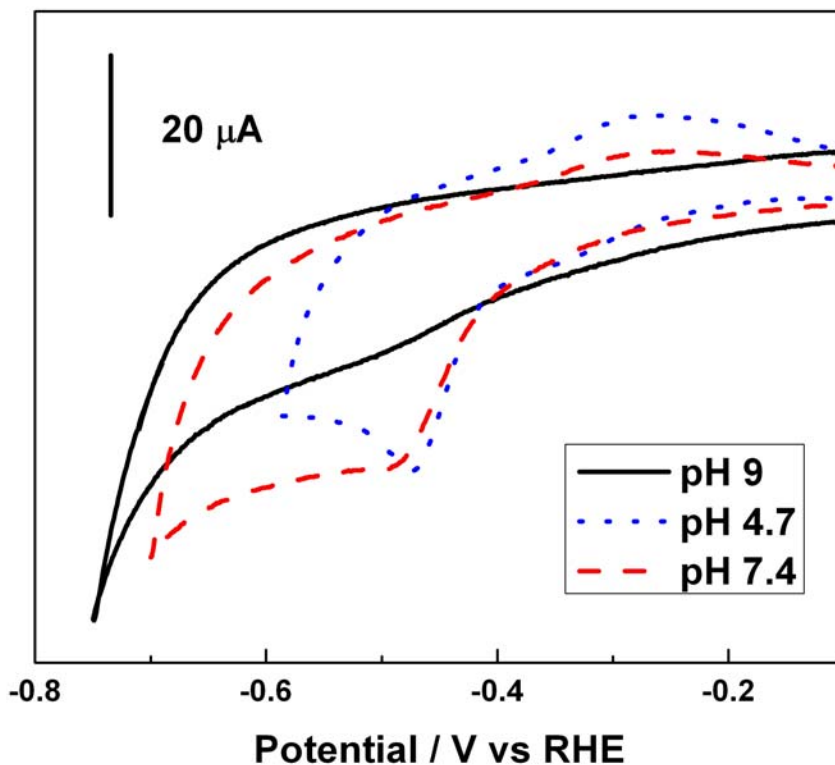


Fig.4. 2 Cyclic Voltammetric studies depicting pH stability in terms of W redox peaks. At pH=9, the “W” reduction peaks are not well-defined, suggesting the breakdown of the compound. WE = Au, CE = Pt mesh, RE = Ag/AgCl, Scan rate 10mV/s.

Cyclic voltammetry has been employed to determine the redox features of Ru₂POM as a function of pH. From Fig.4.2, the two tungsten redox peaks seen at -0.33mV and -0.48 mV are well-defined in the pH conditions of 4 and 7.4. In the case of pH 9, the reduction peaks have lost their shape and this can correspond to some decomposition of the compound. As seen by Tourne, the stability window for these sandwich compounds^{15, 41} is usually from pH 4 to 8, and our electrochemical data shows that in the case of Ru₂POM, we might be reaching the limits of stability at pH of 9.

4.3.4. Electrocatalysis for Oxygen Generation Reaction

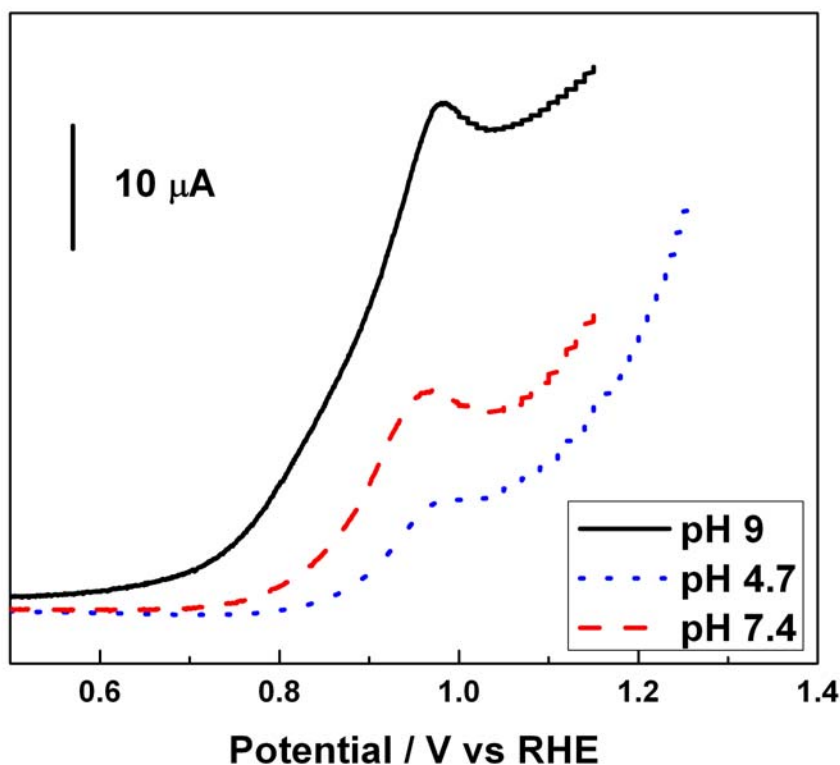


Fig.4. 3 Oxygen Evolution Reaction as a function of pH in 0.2 mM Ru₂POM. Au as WE, Pt Mesh as CE and Ag/AgCl as RE (represented w.r.t RHE)

From Fig.4.3 we can identify the effect of pH variation with the onset of the oxygen evolution reaction. The last Ru oxidation peak coincides with the oxygen generation curve.

Electrochemical generation of O₂ was investigated using pulsed voltammetry. In the first set of experiments, the amount of O₂ produced was measured using a Clark sensor fabricated with a 500 μm diameter Pt disk. The sensor assembly was separated from the test solution with an oxygen-permeable Teflon membrane and held in close physical proximity to a polycrystalline Au anode. The Clark sensor and Au anode served as dual working electrodes in a four-electrode electrochemical cell in which a Pt wire was the counter electrode and a Ag wire served as a quasi-reference electrode (QRFE). The potentials of the Clark sensor and the Au anode were controlled using a conventional bipotentiostat circuit. The potential of the Ag QRFE was calibrated against a standard hydrogen electrode (SHE), and all potentials are referenced to the H⁺/H₂ couple.

The supporting electrolyte was a pH 8 phosphate buffer in which the analytical concentration of phosphate was 0.10 M. O₂ generation experiments were carried out in solutions that had been purged with ultrahigh purity N₂ for at least 30 min, and that were maintained under a N₂ atmosphere during all subsequent measurements. The Au anode was stepped from a rest potential of +0.2 V (vs. H⁺/H₂) to a series of increasingly positive potentials. The duration of each voltage pulse was 5 sec; after each pulse, the potential was stepped back to +0.2 V to re-establish the baseline response of the O₂ sensor. The amperometric response of the Clark electrode was measured continuously as the Au anode was subjected to this potential program, and is plotted as a function of time in Fig.4.4. Trace A shows the response of the Au anode (no catalyst present) to a series of

voltage pulses. No measurable O₂ generation is observed from naked Au until a potential of greater than +1.05 V is applied (not shown), consistent with the known behavior of Au anodes. The narrow current spikes that are observed in this data set are due to capacitive charging that occurs when the working electrode is subjected to a voltage step, and are not faradic. Trace B shows the response of the system to an identical potential program after the addition of the un-substituted di-ZnPOM (formal concentration 2 μM) to the electrochemical cell. The behavior of this system is identical to the behavior of the Au anode alone, indicating that the di-ZnPOM is not catalytically active for O₂ generation. Trace C shows the response of the Clark sensor after the addition of the di-RuPOM (2 μM formal concentrations) to pure electrolyte.

Electrochemically driven generation of O₂ by this system is clearly observed as negative-going current spikes in phase with the applied potential pulses. Negative changes in current correspond to O₂ generation and positive-going currents correspond to a decrease in the amount of O₂ at the sensor. It is clear that O₂ generation is only observed when the working electrode potential is stepped positive from the rest potential; when the potential is stepped back to +0.2 V, the response of the Clark sensor returns rapidly to its baseline value. Finally, trace D shows the response of the Clark sensor in a solution containing a mono-substituted RuPOM catalyst, [PW₁₁O₃₉Ru^{III}(H₂O)]⁴⁻, a compound first synthesized by Pope and co-workers that exhibits a ‘lacunary’ Keggin-type structure³⁵. Interestingly, no catalytic activity for O₂ generation is observed for this compound. These findings are consistent with a reaction mechanism involving oxygen-containing species bound to adjacent Ru sites combining to form molecular oxygen.

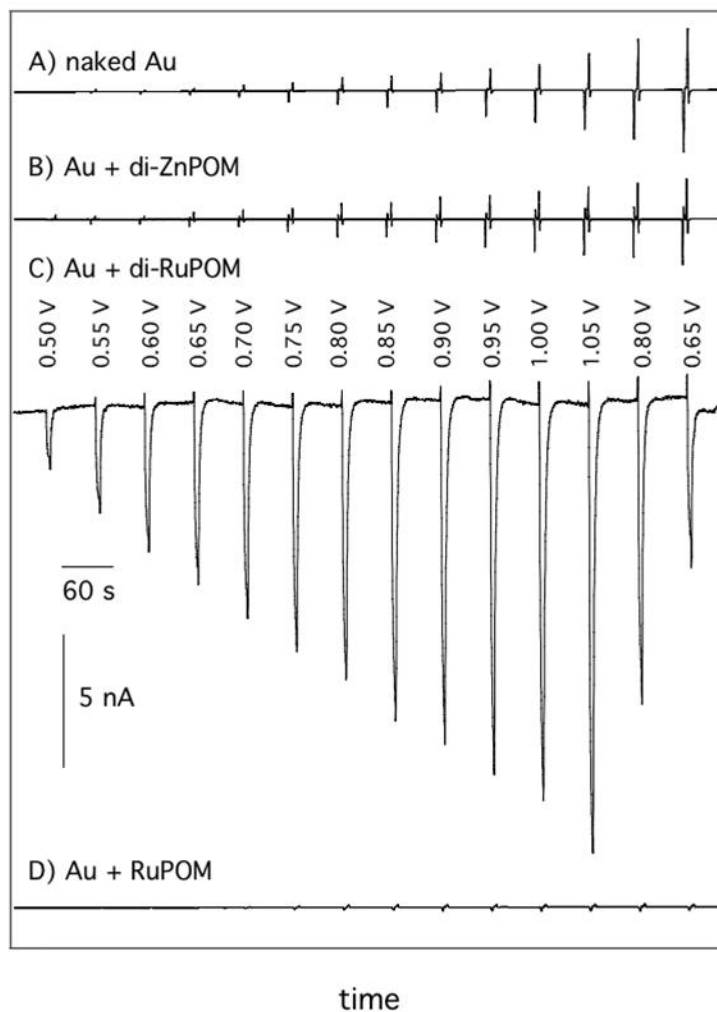


Fig.4. 4 Clark Sensor response for the measurement of electrocatalytic generation of oxygen from A) Au anode, B) Au anode + 2mM Zn_2POM , C) Au anode and Ru_2POM , D) Au anode and mono Ru substituted Keggin POM

Further characterization of this system was undertaken using a rotating ring disk electrode assembly, Fig.4.6. The Pt ring was maintained at a constant potential of -0.20 V while the potential of the Au disk was stepped to increasingly positive voltages (pulse duration, 5 s). O_2 generated at the Au disk was collected at the Pt ring. Mass transport from the disk to the ring was controlled by the electrode rotation rate. The disk response

consists of an initial rapid positive (*i.e.*, anodic) increase in current, followed by a slower, quasi-Cottrell (*i.e.*, $i \propto t^{-1/2}$) decrease (inset). The current-time response is similar to that of a stationary electrode because the voltage pulses were kept shorter than the time required to establish a steady state current in order to prevent the accumulation of excess oxygen.

When the potential is stepped back to its base value, a negative-going current is observed that is due to reduction of O₂ in the double layer. The response of the Pt ring to this voltage program is shown in the lower trace; the pulse shapes are qualitatively similar to those seen for the disk. A small but noticeable dip in the ring response occurs at the same time point as the cathodic disk current reaches its maximum value, and is due to the disk shielding the ring.

An approximate $E_{1/2}$ for the electrocatalytic generation of O₂ of +0.750 V was calculated from the disk current-potential data, and is consistent with the thermodynamics of oxygen generation ($E^\circ = +0.760$ V vs. SHE at pH 8) and with the redox properties of the di-RuPOM electrocatalyst.

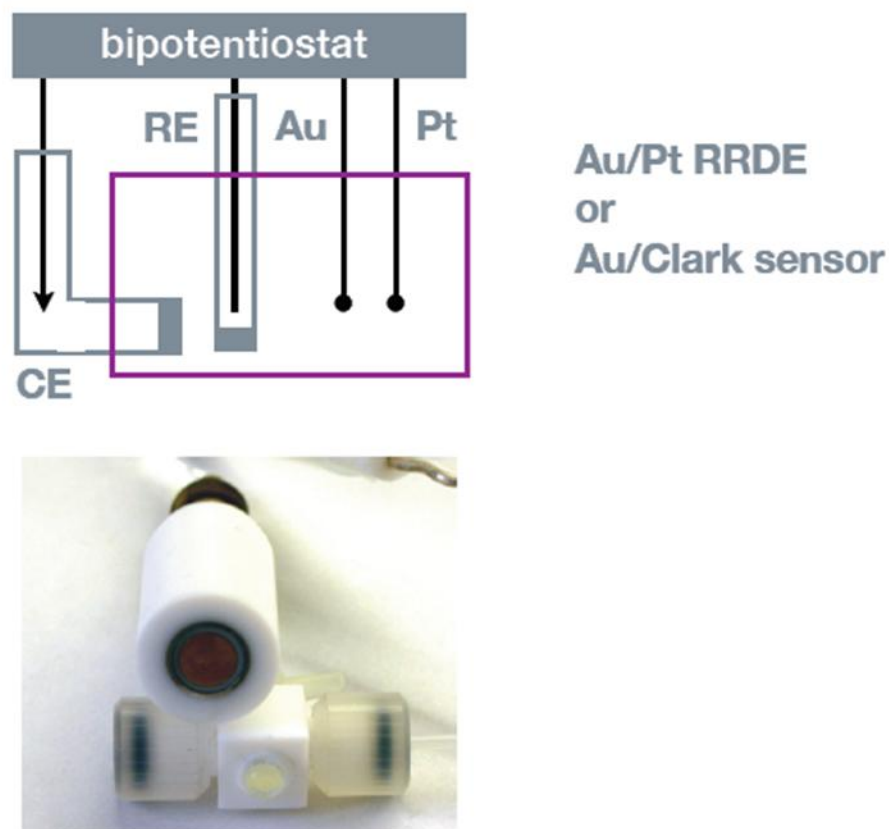


Fig.4. 5 Schematic representation of Rotating Disc Electrode (RRDE) Assembly together with the Bipotentiostat arrangement. Working electrode = polycrystalline Au electrode, Sensing element – Clark sensor or the Pt ring of the RRDE. Ag wire Quasi-reference electrode (QRFE) was employed. The Counter Electrode (CE) was a high surface area platinum mesh. The second figure is the close-up photograph of the RRDE assembly.

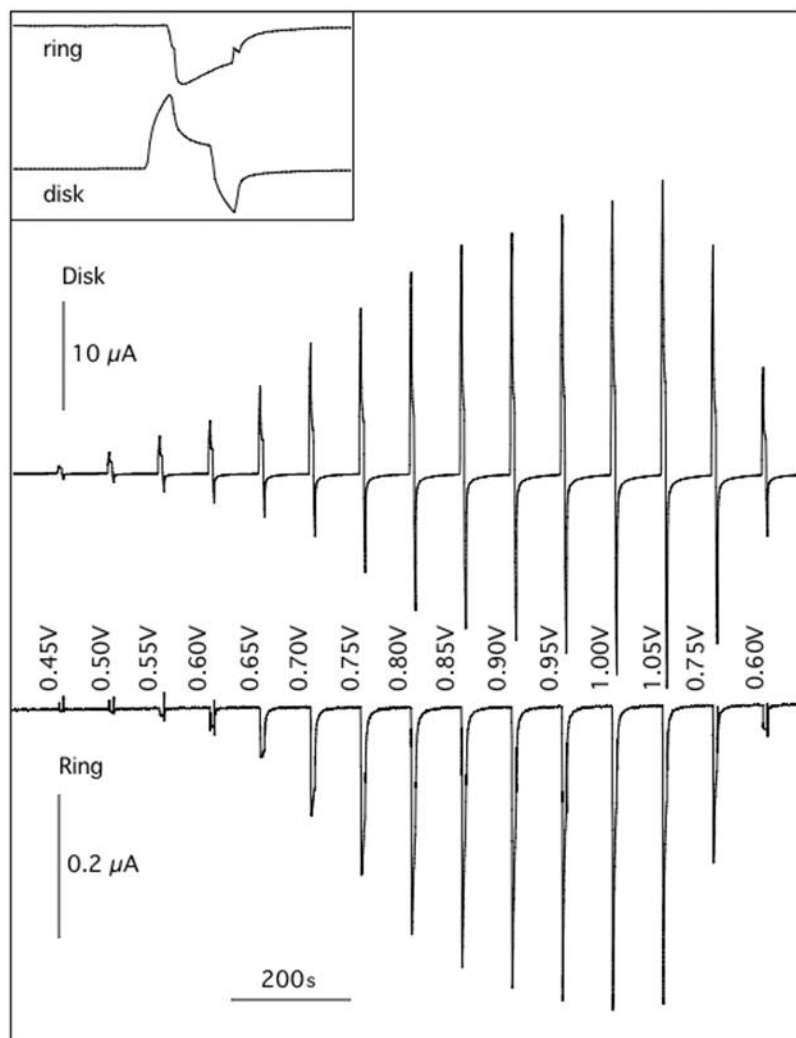


Fig.4. 6 Electrochemical generation of O₂ at pH 8 using Ru₂POM catalyst, which is characterized using a Rotating Ring Disc Electrode (RRDE). Disc current (upper trace) and ring current (lower trace) were acquired simultaneously. The rotation rate was 1600RPM and the geometrical area of the disc was 0.27 cm². The inset shows an expanded view of one set of pulses.

4.5. Conclusion

In conclusion, we have demonstrated that the di-Ru-substituted POM $\{[\text{Zn}_2\text{Ru}_2(\text{OH})(\text{H}_2\text{O})](\text{ZnW}_9\text{O}_{34})_2\}^{11-}$ functions as a catalyst for the electrochemical

generation of O₂. The structural stability of Sandwich type structures have been tested both by electronic spectroscopy and electrochemistry. Our results indicate that adjacent Ru sites are necessary to observe O₂, which points to a reaction pathway involving two Ru-bound oxygen species combining to form O₂. The observed kinetics are similar to those found previously for perovskite materials, suggesting that adsorbed monolayers of this POM would serve as robust models of bulk oxide electrodes.

References

1. Chen G; Delafuente D; Sarangapani S; Mallouk T, *Catal. Today* **2001**, 67, 341.
2. Justi, E. W. W., E. A., *Kalte Verbrennung-fuel Cells*. Franz Steiner Verlag, Wiesbaden, : 1962; p 248.
3. Damjanovic, A., in: Bockris, J.O'M.; Conway, B.E. (Eds), *Modern Aspects of Electrochemistry*, . Plenum Press, New York, : 1969; Vol. 5, p 369.
4. Yachandra V K; De Rose V J; Latimer M J; Mukerji I; Sauer K; Klein M P, *Science* **1993**, 260, 675.
5. Romero, I.; Rodriguez, M.; Sens, C.; Mola, J.; Kollipara, M. R.; Francas, L.; Mas-Marza, E.; Escriche, L.; Llobet, A., *Inorganic Chemistry* **2008**, 47, (6), 1824-1834.
6. Rodriguez, M.; Romero, I.; Sens, C.; Llobet, A., *Journal of Molecular Catalysis a-Chemical* **2006**, 251, (1-2), 215-220.
7. Sens, C.; Romero, I.; Rodriguez, M.; Llobet, A.; Parella, T.; Benet-Buchholz, J., *Journal of the American Chemical Society* **2004**, 126, (25), 7798-7799.
8. Yagi, M.; Yamaguchi, T.; Kaneko, M., *Journal of Molecular Catalysis a-Chemical* **1999**, 149, (1-2), 289-295.
9. Ogino, O.; Nagoshi, K.; Yagi, M.; Kaneko, M., *Journal of the Chemical Society-Faraday Transactions* **1996**, 92, (18), 3431-3434.
10. Sartorel, A.; Carraro, M.; Scorrano, G.; De Zorzi, R.; Geremia, S.; McDaniel, N. D.; Bernhard, S.; Bonchio, M., *Journal of the American Chemical Society* **2008**, 130, (15), 5006-+.
11. Baker, L. C. W.; Glick, D. C., *Chem. Rev.* **1998**, 3, 98
12. Hill, C. L.; Prosser-McCartha, C. M., *Coord. Chem. Rev* **1995**, , 143, 407.

13. Sadakene, M.; Steckhan, E., *Chem. Rev.* **1998**, 98, 219.
14. Kim, J.; Gewirth, A. A., *Langmuir* **2003**, 19, 8934.
15. Tourne, C. M.; Tourne, G. F.; Zonnevrijle, F., *J.Chem.Soc.Dalton Trans* **1991**, (1), 143-155.
16. Neuman, R.; Khenkin, A. M., *Inorganic Chemistry* **1995**, 34, 5753-5760.
17. Naota T; Takaya H; Murahashi S, *Chem. Rev.* **1998**, 98, 2599.
18. Bi, L. H.; Kortz, U.; Keita, B.; Nadjo, L., *Dalton Transactions* **2004**, (20), 3184-3190.
19. Khenkin, A. M.; Shimon, L. J. W.; Neumann, R., *Inorganic Chemistry* **2003**, 42, (10), 3331-3339.
20. Qi, J. Y.; Qiu, L. Q.; Lam, K. H.; Yip, C. W.; Zhou, Z. Y.; Chan, A. S. C., *Chemical Communications* **2003**, (9), 1058-1059.
21. Cheng, L.; Cox, J. A., *Chemistry of Materials* **2002**, 14, (1), 6-+.
22. Nomiya, K.; Torii, H.; Nomura, K.; Sato, Y., *Journal of the Chemical Society-Dalton Transactions* **2001**, (9), 1506-1512.
23. Bagno, A.; Bonchio, M.; Sartorel, A.; Scorrano, G., *European Journal of Inorganic Chemistry* **2000**, (1), 17-20.
24. Neumann, R.; Dahan, M., *Journal of the American Chemical Society* **1998**, 120, (46), 11969-11976.
25. Neumann, R.; Dahan, M., *Polyhedron* **1998**, 17, (20), 3557-3564.
26. Neumann, R.; Dahan, M., *Nature* **1997**, 388, (6640), 353-355.
27. Neumann, R.; Khenkin, A. M.; Dahan, M., *Angewandte Chemie-International Edition in English* **1995**, 34, (15), 1587-1589.
28. Li-Hua Bi, U. K., Bineta Keita and Louis Nadjo, *Dalton Transactions* **2004**.

29. Seddon, E. A.; Seddon, K. R., *The Chemistry of Ruthenium*. Elsevier, New York: 1984; p 156.
30. Rard, J. A., *Chem. Rev.* **1985**, 85, 1.
31. Neumann, R.; Abu-Gnim, C. J., *J. Chem. Soc., Chem. Commun* **1989**, 1324.
32. Neumann, R.; C. J. Abu-Gnim, *J. Am. Chem. Soc.* **1990**, 112, 6025.
33. Filipek, K., *Inorg. Chim. Acta* **1995**, 231, 237.
34. W. J. Randall; T. J. R. Weakley; R. G. Finke, *Inorg. Chem.* **1993**, 32, 1068.
35. Rong, C. Y.; Pope, M. T., *J. Am. Chem. Soc.* **1992**, 114, 2932.
36. Higashijima, M., *Chem. Lett.* **1999**, 1093.
37. Sadakane, M.; M. Higashijima, *J. Chem. Soc., Dalton Trans* **2003**, 659.
38. A. Bagno; M. Bonchio; Sartorel, A.; Scorrano, G., *Eur. J. Inorg. Chem* **2000**, 17.
39. L. Bi; F. Hussain; U. Kortz; Sadakane, M.; Dickman, M. H., *Chem. Commun* **2004**, 1420.
40. Tarasevich, M. R.; sadkowski, A.; Yeager, E., 1983; Vol. 7, p 301.
41. Jabbour, D.; Keita, B.; Israel-Martyr; Mbomekalle; Nadjo, L.; Kortz, U., *European Journal of Inorganic Chemistry* **2004**, 2004, (10), 2036-2044.

CHAPTER 5

ELECTROCHEMICAL SURFACE PLASMON RESONANCE STUDIES TO EVALUATE POLYOXOMETALATE ADSORPTION ON GOLD ELECTRODES

5.1. Introduction

In the previous chapters, we have seen the unique properties and catalytic applications of sandwich type polyoxometalates. The application of polyoxometalates as homogenous redox mediators has been very well established and in order to achieve industrial relevance in fuel cells, batteries or other electrosynthetic uses, there is a need to transfer the catalytic properties of polyoxometalates onto solid surfaces. In this regard, entrapment of POMs in polymer matrices and direct electrodeposition onto electrodes has been successfully performed^{1, 2}. Several studies of Keggin adsorption onto gold electrodes during electrochemical cycling have been reported³⁻⁵. In all these studies, the adsorption of POM species has been monitored using electrochemical quartz crystal microbalance (EQCM) method. Using this method, many important insights have been made about the behavior of polyoxometalates in the presence of an electric field.

In the present work, we are interested in the application of electrochemical surface plasmon resonance as an elegant complementary technique to study polyoxometalate behavior. In recent years, surface plasmon resonance (SPR) has been identified as a potential technique for the analysis and characterization of ultra-thin films, interfaces and kinetic processes at surfaces⁶. When combined with electrochemistry, the

electrochemical surface plasmon resonance (ESPR) technique has been demonstrated as a powerful technique for the simultaneous characterization and manipulation of electrode/electrolyte interfaces⁷⁻⁹. Electrochemical and optical properties of nanometer-scale films can be studied simultaneously using the gold sensing substrate as a working electrode.

5.2. Theoretical Background on Surface plasmon resonance

Surface plasmon resonance (SPR) has been used as a sensitive technique for detecting analytes adsorbed onto a metal surface¹⁰. It has been widely employed as an analytical tool in biomedical and pharmaceutical applications to screen and identify biological and chemical reagents. SPR has been defined¹¹ as an optical phenomenon, which occurs when TM-polarized light undergoes total internal reflection at certain angles of incidences (resonance angle) at an interface between two media of differing refractive indices and resulting in the production of an evanescent wave. Surface plasmons are a result of collective oscillations of free electrons in the metal film. When these plasmons undergo resonance with the incident light beam, they absorb part of the energy of the beam. This phenomenon of resonance produces the evanescent wave, which propagates perpendicular to the surface of the metal film. Usually in a SPR set-up, the interface is modified with a thin layer of metal (either Au or Ag ~ 50 nm) and a monochromatic p-polarized light is used as a photonic source. In this arrangement, for a given thickness of metal in the interface, a corresponding minimum in reflectivity is observed at the resonance angle. The resonance angle (or position of the minimum) is very sensitive to even minute changes in the refractive index (R.I) of the adjacent medium, which is ultimately a function of the change in surface concentration of

interacting species at the interface. During a typical SPR experiment, the change in refractive index is continuously monitored as a function of time. There is a relationship between the change in refractive index and the corresponding change in surface analyte concentration. For proteins, a value of 1000 RIU (refractive index units) or 0.1° change in angle of total internal reflection, is equated to 1ng/mm² change in surface concentration¹². Thus, Surface plasmon resonance (SPR) is one of the most sensitive methods for detection of analyte binding events – protein adsorption on functionalized surfaces, metal deposition from solution, adsorption of thiol molecules etc. Using SPR, the surface coverage concentration of adsorbed layer can be calculated using the following equation 5.1.

$$d_a = \left(\frac{l_d}{2} \right) * \left[\frac{(n_{eff} - n_b)}{(n_a - n_b)} \right] \quad (5.1)$$

- Where d_a - Thickness of adsorbed layer
 l_d - Characteristic decay length (~307nm)
 n_{eff} - Effective RI of adlayer (from SPR)
 n_b - Refractive index of electrolyte
 n_a - Refractive index of Polyoxometalates (~2)

Electrochemical surface plasmon resonance (ESPR) is a relatively novel approach to evaluate the behavior of an interface in the presence of an electrical field. The applied electric field modulates the observed SPR response as follows:

$$\frac{\Delta\theta}{\Delta V} = c_1\left(\frac{\Delta n}{\Delta V}\right) + c_2\left(\frac{\Delta d}{\Delta n}\right) + c_3\left(\frac{\Delta\sigma}{\Delta n}\right) \quad (5.2)$$

where θ is the reflected light intensity where SPR occurs, n corresponds to the dielectric constant of the adsorbed film, d is the thickness of the film, σ is the surface charge density of the gold surface and c_1 , c_2 & c_3 are constants. Here, θ and σ are wavelength dependent while last two terms are wavelength independent. Because of its sensitivity to the applied electric field, electrochemical-SPR was largely exploited for investigating interfacial reactions. Several studies have been performed to target the detection of heavy metal ions^{10, 13-15} and more particularly a combined technique of anodic stripping voltammetry (ASV) and surface plasmon resonance¹⁰ has been developed. Wang et al¹⁶ have employed catalyzed metal deposition onto the gold sensing surface of the SPR set-up to produce selective surfaces for heavy metal ions. The insensitivity of ESPR to background currents due to presence of dissolved oxygen and other gases has been claimed as an advantage over the traditional anodic stripping voltammetry. An elegant approach to modify self-assembled monolayers using electrochemical potential has been studied using ESPR¹¹. Further considerable insights into electropolymerization of conductive polymers such as polyaniline¹⁷⁻¹⁹ and polypyrrole have been obtained using electrochemical SPR.

5.3. Electrochemical Adsorption of Polyoxometalates on electrodes

Due to the high solubility of polyoxometalates in water, there is a need to immobilize the catalytically active species on a solid substrate – carbon, metal nanoparticles or inert alumina or silica. For electro-active species contributing to

catalysis, there is a possibility of employing electrodeposition to transfer catalytic activity from solution to solid substrates. The early evidence for electrodeposition of polyoxometalates onto metal and glassy carbon surfaces was provided by Profs. Keita and Nadjo²⁰⁻²⁴. Since then several other studies have been performed to elucidate the mechanism of electrodeposition of POMs. It has been shown that in the case of Keggin molecules, when the potential is scanned until the value corresponding to the eight and twelve electron reduction peaks, there is a formation of an adherent film²³. These films have been shown to have good electrocatalytic properties towards hydrogen evolution reaction. Despite forming well-ordered two dimensional arrays (via AFM and STM studies²⁵), the exact chemical nature of these films have not yet been identified. The electrode modification has been claimed to have been formed by electrodecomposed Keggin structures³. Electrochemical quartz crystal microbalance method has been employed to demonstrate that oxidized form of the polyoxometalates ($\text{SiW}_{12}\text{O}_{40}^{4-}$, $\text{P}_2\text{W}_{18}\text{O}_{62}^{6-}$ and $\text{H}_2\text{W}_{12}\text{O}_{40}^{6-}$) undergo adsorption on gold electrodes. Surprisingly, there is an absence of adsorption of species formed during the first two or three tungsten redox peaks of these compounds. Protonation of the reduced product has been cited as the reason for this observation. An increase in potential beyond the initial redox waves and reaching the realm of $6e^-$ reduction has been shown to form thick tungstate films on the metal electrode. Some of the basic understandings from their studies are as follows:

1. To obtain a persistent and adherent film, there is a necessity to fix more than six electrons per molecule in the case of $[\text{P}_2\text{Mo}_{18}\text{O}_{62}]^{6-}$, i.e. the electrodeposition occurs only when the potential is cycled towards more negative potentials corresponding to almost six electron reduction⁴

2. It has been demonstrated that electrodeposition of catalyst at -1.2 V in acidic solutions exhibits good electrocatalytic property for hydrogen evolution reaction, but then they do not necessarily maintain the same Keggin or Dawson structure of the parent compounds
3. At very mild pH and potential conditions, composite films of new electroactive oxides have been deposited, when the starting materials are molybdenum containing tungsten frameworks or fully molybdic species
4. During electrodeposition, there is a possibility of forming new electroactive catalytic species by decomposition and/or polymerization reactions of heteropolyanions
5. Molybdenum based species exhibit more propensity to undergo electrodeposition than tungsten based complexes
6. It has been demonstrated that (W^{VI} , W^V) or (Mo^{VI} , Mo^V) mixtures can be considered as good catalysts and electrocatalysts

There has been a dearth of studies of electrochemical adsorption of sandwich type polyoxometalates in the literature and hence this is an attempt made to illustrate the same with electrochemical surface plasmon resonance spectroscopy.

5.4. Materials and Methods

5.4.1 Polyoxometalates and Reagents

The precursor sandwich type Zn_2POM and Ru_2POM structures were prepared as described in previous chapters and $SiW_{12}O_{40}^{4-}$, the Keggin compound was purchased

from Alfa Aesar. Two different electrolytes were chosen, 0.5M Na₂SO₄ and 0.1M NaClO₄. Keggin based experiments were performed in pH=4 medium (0.1M NaClO₄ + HClO₄).

5.4.2. Electrochemical Surface Plasmon Resonance Set-up

Spreeta™ units developed by Texas Instrument (TI) were employed as sensors for our experiments. Advantages such as robust design, ease of handling and relatively lower cost (US25\$) have made us choose these Spreeta™ units for our application. The sensitivity of these units is in the range of $\sim 3 \times 10^{-6}$ R.I, and they are very well suited to address extremely low surface concentrations (Specifically monolayer concentrations in our case). For the purpose of adding electrochemical capability to these systems, the following modification to the sensor has been performed. A Ni wire (Alfa Aesar, 0.001 mm thickness) has been attached to the gold sensing surface using silver epoxy (Alfa Aesar) to provide a conductive contact. This current collector was glued on to one corner of the rectangular gold sensing area, so that there is no hindrance to the regular signal generation during sensor operation. A layer of silicone sealant was placed on top of this Ag epoxy contact to ensure mechanical stability during experimentation. The sealant was allowed to cure overnight and then the system was subjected to pre-treatment of the gold surface. A complete experimental set-up is shown in Fig.5.1.

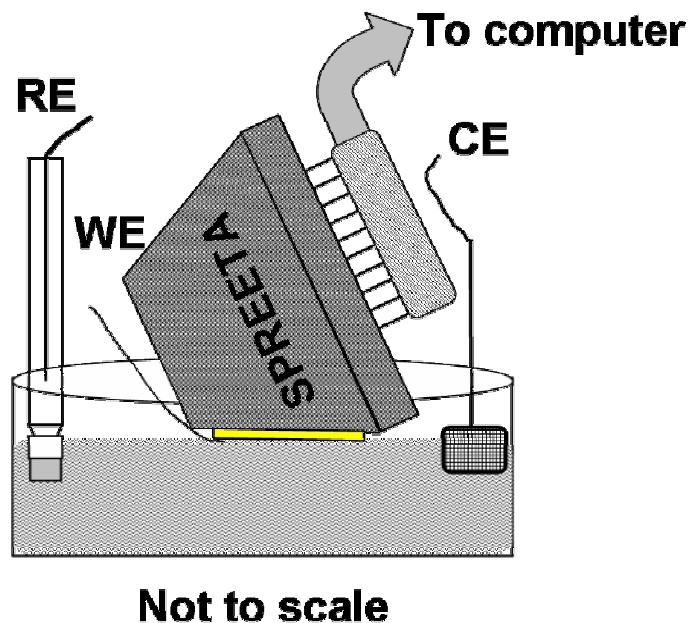


Fig.5. 1 Schematic representation of the experimental set-up showing the modified Spreeta™ as the working electrode, Pt mesh as counter electrode and Ag/AgCl as Reference electrode.

5.4.3. Pre-treatment of gold electrode

The gold sensing surface of the Spreeta™ set-up, which was used as the working electrode was rinsed with piranha solution (3:1 ratio of conc. H_2SO_4 and 30 wt% H_2O_2), with utmost care as to not damage the polymer outer walls. After thorough rinsing with de-ionized water, the electrode was electrochemically tested for consistent gold oxidation and reduction peaks in 0.1M HClO_4 solution, by cycling from 0.0 V to 1.6 V.

5.4.4. Electro-adsorption by Potential Cycling of Polyoxometalate Solutions

The phosphotungstate species containing Keggin structure was initially subjected to electrochemical cycling in the modified ESPR set-up. The electrodeposition of Keggin structures have been previously studied by Nadjo et al²⁰⁻²⁴ using electrochemical quartz

crystal microbalance method (EQCM), and hence well-behaved $\text{SiW}_{12}\text{O}_{40}^{4-}$ species was considered a good starting point to elucidate the characteristics of ESPR. A freshly prepared 0.2mM solution of $\text{SiW}_{12}\text{O}_{40}^{4-}$ in pH 4 medium (0.1M $\text{NaClO}_4 + \text{HClO}_4$) was chosen as the deposition solution. The solution was subjected to 30 minutes of de-oxygenation using Ar gas bubbling and the experiment was performed under a constant blanket of Ar gas. Pt mesh was employed as counter electrode and Ag/AgCl (3M NaCl) as reference electrode. All potentials are reported as values with respect to a Reversible Hydrogen Electrode (RHE). A potential range of +0.2 V to -0.5 V (vs RHE) was chosen for electrochemical cycling.

Sandwich type structures were then tested using the same set-up under controlled pH and concentration. Freshly prepared solutions of Zn_2POM and Ru_2POM were subjected to electrochemical cycling between +0.4 V to -0.6 V, to determine the nature of electro-adsorption.

5.4.5. Constant Potential Electrodeposition

Two distinct potentials of -0.2V and -0.7V (vs RHE) were chosen for constant potential electrodeposition. The effect of concentration variation from 0.1 μM to 10 μM was also tested under these deposition conditions. The results of the constant potential electrodeposition studies were used as calibration for the sensing surface.

5.5. Results and Discussion

5.5.1 Adsorption of sandwich type polyoxometalates on gold electrodes at open circuit voltage

It has been shown that the most effective means of depositing POMs onto electrode surfaces is by simply soaking the electrode in acidified aqueous POM

solution²⁶. Almost all polyoxometalate species undergo spontaneous adsorption at open circuit potential onto glassy carbon, gold and even platinum surfaces. This particular characteristic has been employed in immobilizing POM species onto traditional porous catalytic substrates such as silica, activated carbon and carbon nanotubes. Despite the promising nature of these POM films in heterogeneous catalysis, especially in the case of electrocatalysis, the monolayer nature of these POMs onto electrode surfaces are not robust enough to provide reliable functional surfaces. Hence there is a need to immobilize these POM species, by electro-adsorption, electrostatic layer by layer deposition or by co-deposition with polymer films. In order to understand the true behavior of the sandwich polyoxometalates in the presence of an electric field, it is important to differentiate between spontaneous adsorption (by physisorption and chemisorption) and electrodeposition. Initially, a flow-through Spreeta™ system was utilized to investigate spontaneous adsorption of POM on gold electrode while simultaneous electrochemical-SPR batch setup (Fig. 5.1) was exploited for electrical potential influence on POM deposition. Control experiments were carried out to ensure no adsorption occurs from electrolytes (0.5M Na₂SO₄).

Fig 5.2a shows the spontaneous adsorption of Ru₂POM to SPR gold surface. Following the introduction of Ru₂POM, an immediate increase in SPR angle was observed which is due to bulk refractive index change followed by gradual adsorption kinetics. Rinsing the surface with Na₂SO₄ removed the bulk refractive index of the solution observed during adsorption process and resulted in 24.3 mdeg change. This could be attributed to the residual film formed on the surface due to spontaneous

adsorption of Ru₂POM. A similar but enhanced mass adsorption (nearly twice) was observed for Zn₂POM species as outlined in fig 5.2b.

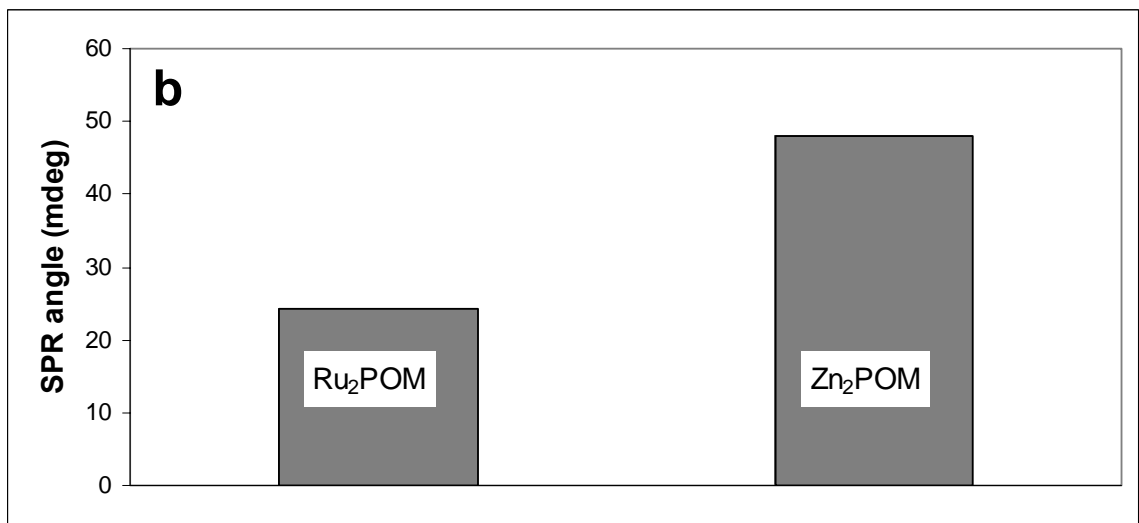
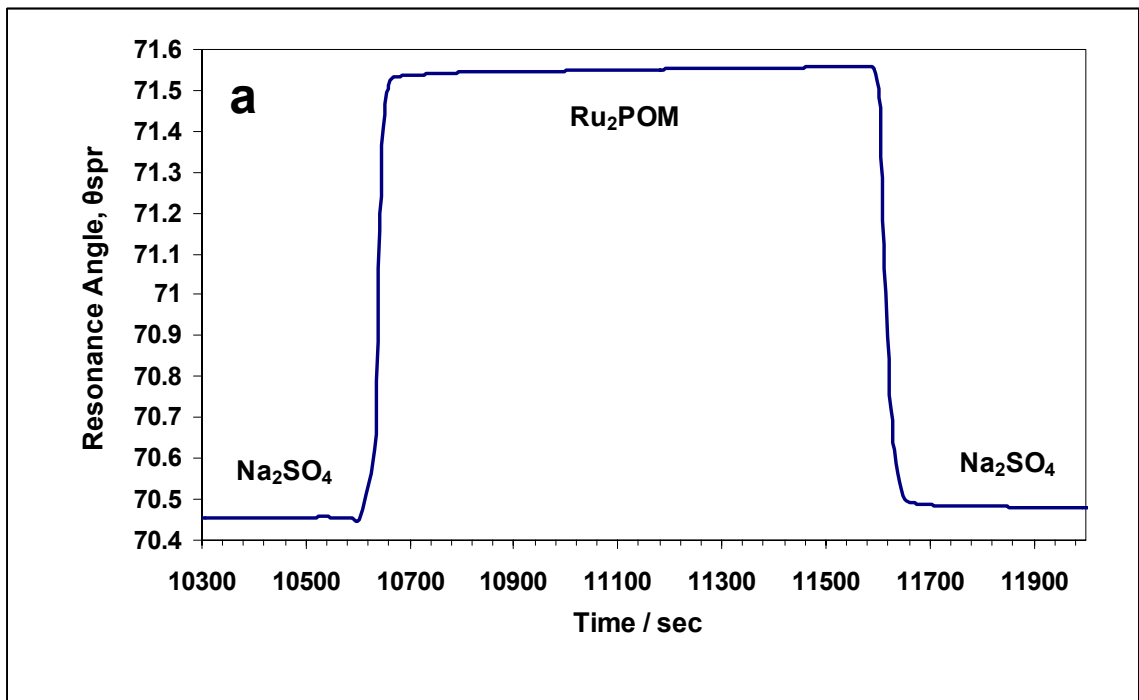


Fig.5.2a. Spontaneous adsorption from a solution of 0.2 mM Ru₂POM in 0.5 M Na₂SO₄.

b. Comparison of SPR response for Ru₂POM and Zn₂POM on gold electrode

5.5.2. Electrodeposition of Sandwich Polyoxometalates

Calibration of Surface Plasmon Resonance in pure 0.1M HClO₄ solution

The ability of the electrochemical-SPR setup to simultaneously monitor the electrode interfacial processes was demonstrated by cyclic voltammetry of 0.1M HClO₄ in the following Fig.5.3. From the studies made by Iwasaki et al²⁷, it has been shown that the scan rate of less than 10mV/s must be chosen for simultaneous measurement of CV and SPR signals.

At low potential regimes (0.0 to 0.95V) corresponding to double-layer charging of the electrode, SPR response increases with the applied potential and this arises due to changes in the surface charge density which is usually indistinguishable in cyclic voltammetry. After electrode double layer charging, gold oxidation starts at 1.05V vs RHE, in our case we see a composite wave in the CV, which has been shown to be comprised of three oxidation peaks (a. deposition of OH in pre-adsorbed anions, b. the place exchange reaction of anions with OH, c. the formation of gold oxide²⁷). There is a single peak in the cathodic part of the scan corresponding to the two electron reduction of gold oxide. These observations validate the electrochemical-SPR setup for simultaneous monitoring of the interfacial processes.

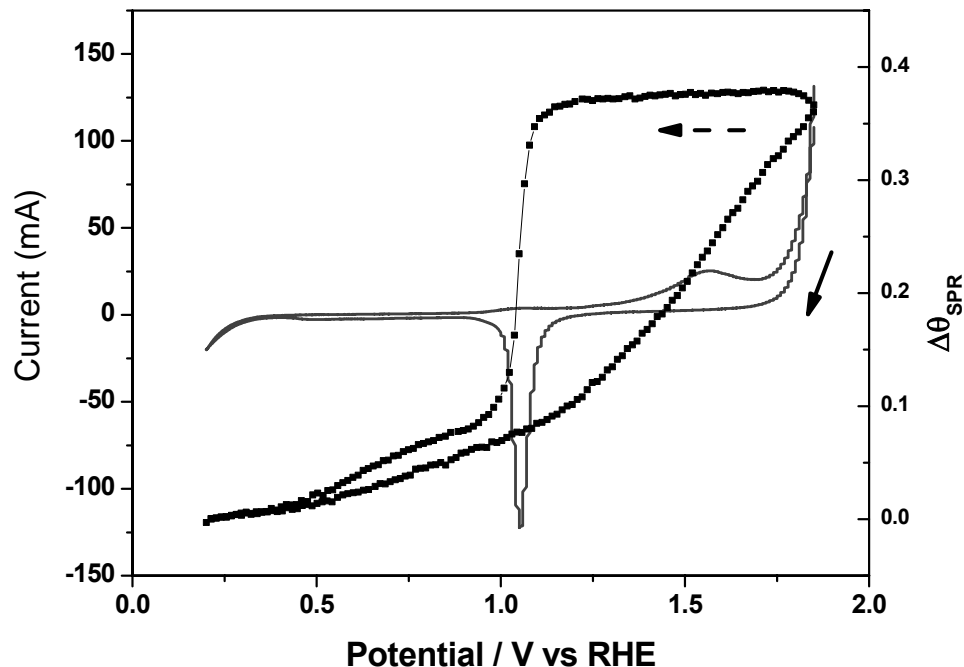


Fig.5. 3 ESPR response in 0.1 M HClO₄ superimposed with the corresponding cyclic voltammetry.

ESPR Response of Keggin type Polyoxometalates in acidic solution

A Keggin solution (0.2 Mm SiW₁₂O₄₀⁴⁻) in a supporting electrolyte of pH 4 was chosen to evaluate the response of the electrochemical surface plasmon resonance (ESPR) to potential cycling. This Keggin based system has already been studied by Keita et al²⁴ using electrochemical quartz crystal microbalance (EQCM) method and hence there is a possibility of comparing the ESPR response to the literature studies. This exercise has been designed to permit the understanding of ESPR response as an indirect method to elucidate mass variations. A potential region from +0.4V to -0.3V has been chosen for our studies as shown in Fig.5.4.

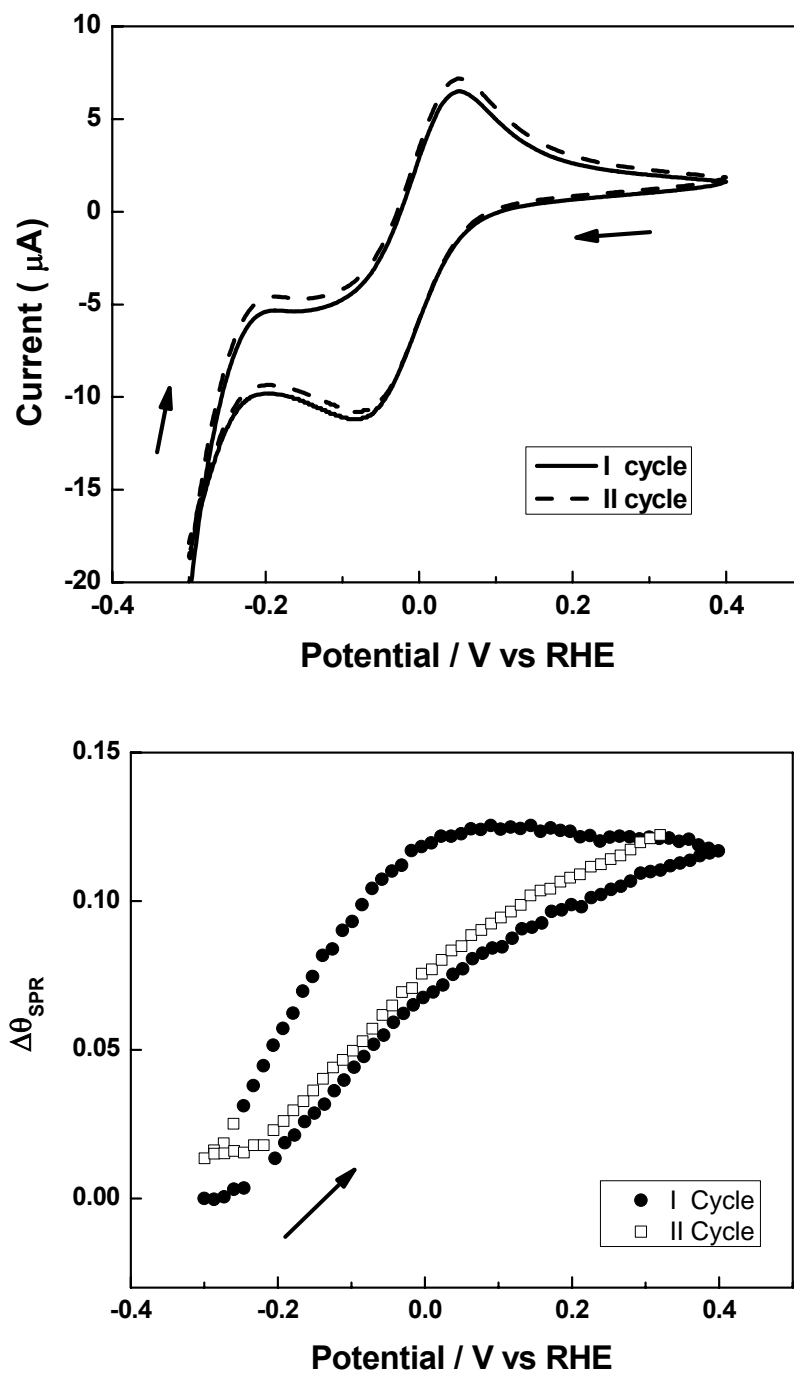


Fig.5. 4 Electrochemical surface plasmon resonance of 0.2mM Keggin ($\text{SiW}_{12}\text{O}_{40}^{4-}$) in pH4 supporting electrolyte (0.1M $\text{NaClO}_4 + \text{HClO}_4$) solution. The upper graph shows cyclic voltammetry behavior and the bottom graph is the corresponding ESPR response.

Initially, the gold electrode is subjected to a pre-treatment in the supporting electrolyte. A potential window from -0.3 to +0.4V was chosen and this corresponds to the region of the first redox couple of $\text{SiW}_{12}\text{O}_{40}^{4-}$. There is no significant change in SPR signal ($\Delta\theta_{\text{SPR}}$) when the electrode is subjected to potential cycling in the pure supporting electrolyte. In the case of $\text{SiW}_{12}\text{O}_{40}^{4-}$, the electrochemical behavior is well-known and at a pH ~ 4 , the first two redox peaks in the negative direction are mono-electronic, corresponding to W (VI) reduction. In Fig.5.4, $\Delta\theta_{\text{SPR}}$ corresponding to this potential cycle reveals a steady increase in signal during the forward scan. This could be correlated to mass increase corresponding to adsorption of oxidized POM. On the reverse scan, the $\Delta\theta_{\text{SPR}}$ shows two domains, a. from +0.4 to +0.05V, the variation is very small; b. from +0.05 to -0.03V, the region where the POM is reduced, a steady decrease is seen in $\Delta\theta_{\text{SPR}}$. This decrease could be due to loss of mass from the surface, corresponding to desorption of reduced species. From the previous study performed on EQCM, a similar response has been reported for the Keggin species, $\text{SiW}_{12}\text{O}_{40}^{4-}$ and hence we can conclude that the SPR response can be correlated to the mass increase in the case of Si Keggin. Keita et al^{2, 24} had concluded that the observed mass increase during oxidative scan is due to adsorption of oxidized species $\text{SiW}_{12}\text{O}_{40}^{4-}$ and the mass decrease is due to desorption of reduced species $\text{SiW}_{12}\text{O}_{40}^{5-}$.

ESPR Response of Sandwich POMs in 0.5M Na_2SO_4

ESPR studies on the electrochemical behavior of sandwich type polyoxometalates have been performed in 0.5 M Na_2SO_4 solution as supporting electrolyte. Initially, the potential window was chosen in order to address the first two redox features of Zn_2POM , as seen in Fig. 5.5.

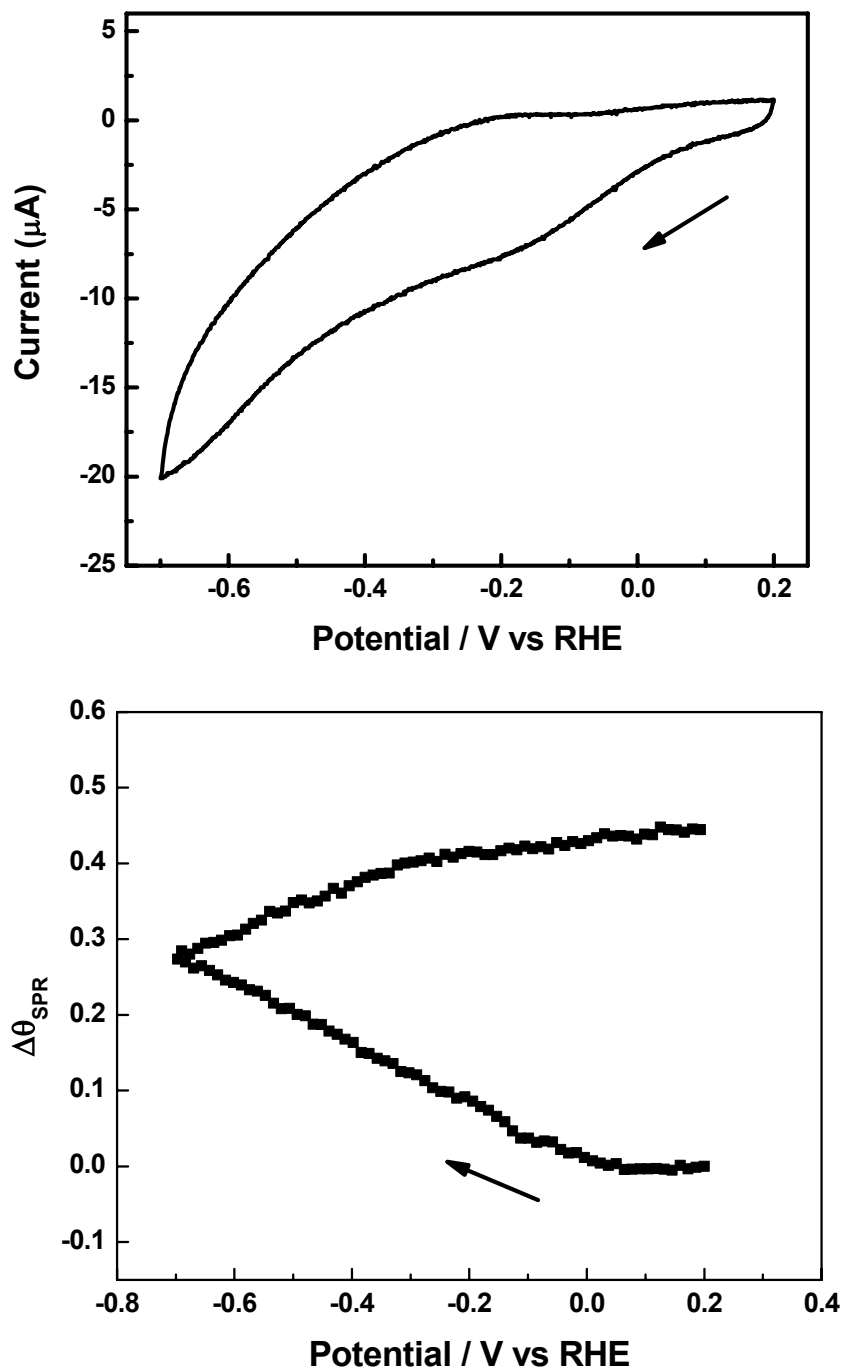


Fig.5. 5 ESPR response corresponding to potential cycling in 0.4mM Zn_2POM . Upper graph shows the cyclic voltammogram and the bottom graph shows the corresponding SPR response curve.

Fig. 5.5 shows the ESPR signal ($\Delta\theta_{\text{SPR}}$) response recorded simultaneously with the voltammogram shown above for 0.4 mM Zn_2POM . The signal increases during the reduction curve and it slows down, but continues during the subsequent positive going scan. On increasing the number of potential scans, SPR signal increased continuously and even when the cycling was stopped, it does not fall back to the initial value. This suggests that there may be an irreversible electro-adsorbed film, which may be stable under open circuit conditions. Since the film is still present in the modifying solution, it will be interesting to observe the film stability in pure supporting electrolyte. One interesting observation in the cyclic voltammetry of Zn_2POM in Au working electrode of ESPR set-up is the decrease of current response with each increasing potential cycle. This behavior suggests the formation of films, which maybe insulating in nature. Previous studies^{5, 25} on electrodeposition of Keggin structures and Wells-Dawson have shown films exhibiting increase in current.

The Ru_2POM compound also exhibited very same growth characteristics, in terms of the potential response, but SPR signal increase corresponding to the mass increase was about half of that seen in Zn_2POM growth.

In order to evaluate the stability of the electro-adsorbed film as a function of potential, a 0.4 mM Ru_2POM solution was subjected to film growth cycling (from +0.2 V to -0.7 V vs RHE) for about 10 minutes (curve not shown), and then subsequently, the potential was scanned from 0 V to +1.2 V and then back to the negative region of -0.7 V.

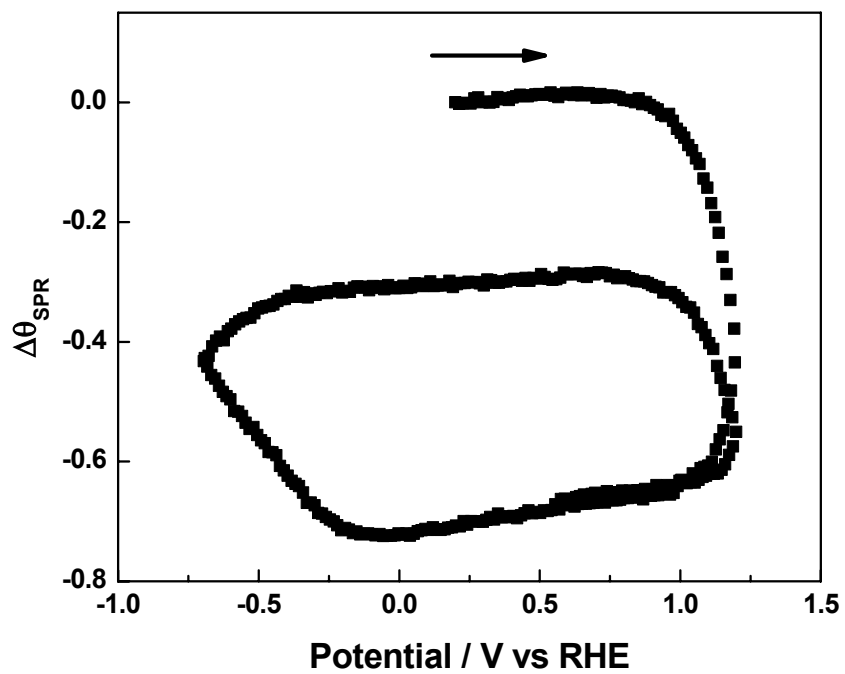
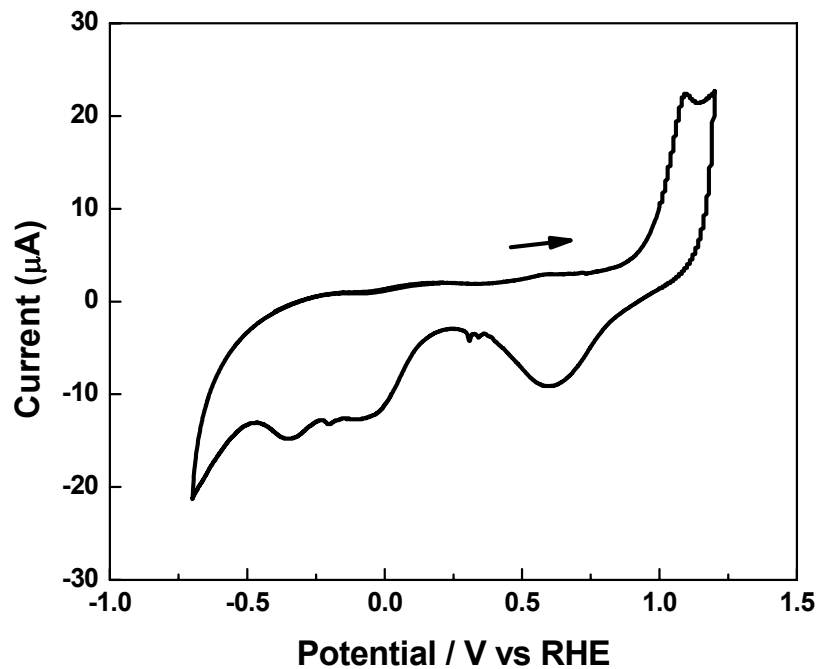


Fig. 5.6. Potential Stability testing of the electro-adsorbed film in 0.4 mM Ru_2POM solution in 0.5 M Na_2SO_4 .

Fig.5.6 shows the SPR response corresponding to the potential scan to extremely positive values of 1.2 V. The potential scan began at 0.0 V, since there is no film growth in this region. On scanning more positive towards the gold oxidation peaks, we see a dramatic fall in the SPR signal, which corresponds to desorption of the electro-adsorbed film. This observation proves that the film formed by cyclic voltammetry and under short time duration (10 minutes), has limitations in terms of potential stability in the gold oxidation region. This behavior has been anticipated and previous workers^{24, 25} have tried to stay away from this region due to the uncertainty of the gold oxide influence in polyanion adsorption. We ventured into this region of high anodic potential to address the possibility of employing these electro-adsorbed films as oxygen generation catalysts at gold electrodes (as a follow-up to studies in chapter 4). The competition due to sulfate anion adsorption in this solution and the effect of different supporting electrolytes could be an interesting direction for future studies.

Conclusions

Electrochemical surface plasmon resonance spectroscopy has been evaluated for polyoxometalate characterization during electrochemical cycling. Interesting insights into the stability of the electro-adsorbed films were obtained. Further, a differentiation between spontaneous adsorption and electro-adsorption has been proved using ESPR.

References

1. Keita, B.; Nadjo, L., *Curr. Top. Electrochem* **1993**, 2, 77.
2. Keita, B.; Nadjo, L.; Belhouari, A.; Constant, R., *J. Electroanal. Chem* **1995**, 381, 243.
3. Keita, B.; Nadjo, L.; Belanger, D.; Wilde, C. P.; Hilaire, M., *Journal of Electroanalytical Chemistry* **1995**, 384, 155-169.

4. Keita, B.; Abdeljalil, E.; Girard, F.; Gerschwiler, S.; Nadjo, L.; Contant, R.; Haut, C., *Journal of Solid State Electrochemistry* **1999**, 3, 446-456.
5. Keita, B.; Contant, R.; Abdeljalil, E.; Girard, F. o.; Nadjo, L., *Electrochemistry Communications* **2000**, 2, 295-300.
6. W.Knoll, *Annual Reviews on physical chemistry* **1998**, 49, 569.
7. A. Tadjeddine; D.M. Kolb; Kotz, R., *Surf. Sci.* **1980**, 101, 277.
8. J.G. Gordon II; Ernst, S., *Surf. Sci.* **1980**, 101, 499.
9. Y. Iwasaki; T. Horiuchi; M. Morita; Niwa, O., *Electroanalysis* **1997**, 9, 1239.
10. Wang, S.; Forzani, E. S.; Tao, N., *Anal. Chem.* **2007**, 79, (12), 4427-4432.
11. S.Balasubramanian; I.B.Sorokulova; V.J.Vodyanoy; A.Simonian, *Biosensors and Bioelectronics* **2007**, 22, 948.
12. R.J.Green; Frazier, R. A.; K.M.Shakesheff; M.C.Davies; C.J.Roberts; S.J.B.Tendler, *Biomaterials* **2000**, 21, 1823.
13. Moon, J.; Kang, T.; Oh, S.; Hong, S.; Yi, J., *Journal of Colloid and Interface Science* **2006**, 298, (2), 543-549.
14. Kang, T.; Moon, J.; Oh, S.; Hong, S.; Chah, S.; Yi, J., *Chemical Communications* **2005**, (18), 2360-2362.
15. Gu, H.; Ng, Z.; Deivaraj, T. C.; Su, X.; Loh, K. P., *Langmuir* **2006**, 22, (8), 3929-3935.
16. Wang, J.; Wang, F.; Zou, X.; Xu, Z.; Dong, S., *Electrochemistry Communications* **2007**, 9, (2), 343-347.
17. Damos, F. S.; de Cássia Silva Luz, R.; Tanaka, A. A.; Kubota, L. T., *Journal of Electroanalytical Chemistry* **2006**, 589, (1), 70-81.

18. Baba, A.; Tian, S.; Stefani, F.; Xia, C.; Wang, Z.; Advincula, R. C.; Johannsmann, D.; Knoll, W., *Journal of Electroanalytical Chemistry* **2004**, 562, (1), 95-103.
19. Kang, X.; Jin, Y.; Cheng, G.; Dong, S., *Langmuir* **2002**, 18, (26), 10305-10310.
20. Keita, B.; Nadjjo, L., *Journal of Electroanalytical Chemistry* **1988**, 243, (1), 87-103.
21. Keita, B.; Nadjjo, L., *Journal of Electroanalytical Chemistry* **1988**, 247, (1-2), 157-172.
22. Keita, B.; Nadjjo, L., *Journal of Electroanalytical Chemistry* **1990**, 287, (1), 149-157.
23. Keita, B.; Nadjjo, L.; Savéant, J. M., *Journal of Electroanalytical Chemistry* **1988**, 243, (1), 105-116.
24. Keita, B.; Nadjjo, L.; Contant, R., *Journal of Electroanalytical Chemistry* **1998**, 443, (2), 168-174.
25. Abdeljalil, E.; Keita, B.; Nadjjo, L.; Contant, R., *Journal of Solid State Electrochemistry* **2001**, 5, (2), 94-106.
26. Sadakane, M.; Steckhan, E., *Chem. Rev* **1998**, 98, 219-237.
27. Iwasaki, Y.; Tsutomotu, H.; Morita, M.; Niwa, O., *Electroanalysis* **1997**, 9, (16), 1239-1241.

CHAPTER 6

POLYOXOMETALATES AS CO-CATALYSTS FOR OXYGEN REDUCTION

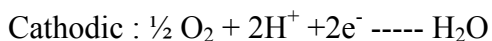
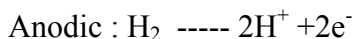
6.1. Introduction

In the field of electrochemistry, oxygen reduction is one of the most important reactions as it plays an important role in the operation of a fuel cell. Fuel cells, most importantly proton exchange membrane fuel cells (PEMFC) are expected to become a major source of environment-friendly energy in the near future. During the operation of a fuel cell, the energy producing reactions are:

Alkaline Fuel cell:



Polymer Electrolyte Fuel cells:



The following efficiency diagram for a fuel cell in operation, deals with the origin of losses during a fuel cell reaction cycle.

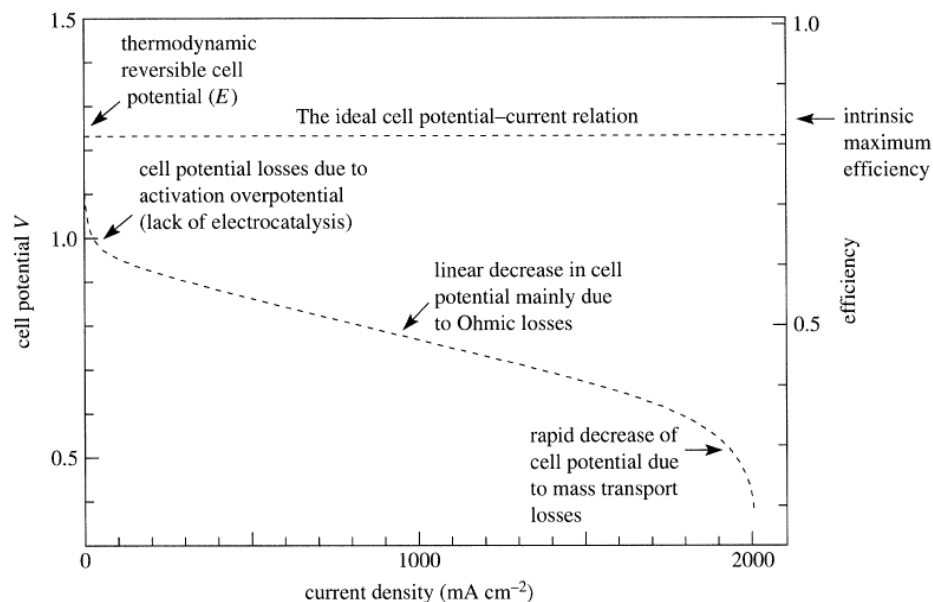
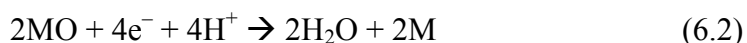


Fig.6. 1 Schematic diagram depicting the efficiency losses observed during the operation of a typical fuel cell.¹

From observing the typical fuel cell performance curves shown in Fig.6.1, we can understand that the deviation from ideal cell potential current response could be caused by three factors: (i) activation overpotential (lack of electrocatalysis) (ii) Ohmic losses and (iii) mass transport losses. Of these three factors, activation overpotential is the region of focus for our group and in particular, the major contributing factor is the oxygen reduction reaction occurring at the cathode.²⁻⁵

Development of electrocatalysts for oxygen reduction reaction (ORR) has reached a new milestone after bimetallic effects⁶⁻¹¹ of improving catalytic properties have been employed. These bimetallic alloys or nanoparticles have been very efficient in improving the activities of the individual metals and to reach the overpotentials observed in platinum electrodes. While the elementary steps of the ORR are not yet firmly established, thermodynamic analyses, such as those published recently by Bard, et al.^{7, 9}

and Balbuena, et al.,^{12, 13} suggest that the ORR can be viewed as consisting of an initial dissociative chemisorption step followed by the four-electron reduction of the oxide to water.



Analysis of thermochemical data for these two reactions spanning a wide range of metals indicates that elements such as W, which form stable bonds to O, perform well for O₂ bond scission and poorly for O atom reduction. Conversely, metals such as Au, which reduce adsorbed O atoms efficiently, are ineffective with respect to O₂ bond scission. Based on these observations, a simple guideline for the development of bimetallic catalysts has been proposed: combine a metal that is good at O-O bond scission with a second metal that reduces adsorbed O atoms efficiently. A possible difficulty with this approach is that, in the case of metals that form stable M-O bonds, there would be a tendency for the O atoms generated in reaction 6.1 to remain adsorbed on the first metal, effectively shutting down reaction 6.2. In practice, a compromise is generally sought, as in the case of bimetallic catalysts such as Co-Pd, where one metal is slightly better at bond scission (Co) and the second is slightly better at reducing adsorbed O atoms (Pd).

Polyoxometalates (POMs) are nanometer sized metal oxygen containing anions that have a wide range of catalytic applications owing to their ability to mediate electron,¹⁴ proton and oxygen atom transfer reactions. These attributes, as well as their ability to catalyze the reduction of hydrogen peroxide¹⁵, make them particularly interesting as oxygen reduction catalysts. Indeed, a number of research groups have explored the catalytic activity of POMs toward the ORR on glassy carbon electrodes as

well as on supported Pt nanoparticles^{16, 17}. There are several other applications of POMs in fuel cells.¹⁸⁻²¹, where they have been employed as electrocatalysts for both cathodes and anodes¹⁸, and as proton conducting component in fuel cell membranes.^{21, 22}

We believe that transition metal substituted POMs adsorbed on the surface of an electrode that is catalytically active for the reduction of adsorbed O atoms (i.e., Au, Pd, Pt) should function in much the same way as a typical bimetallic ORR catalyst. In this contribution, we set out to design POM co-catalysts for Au, Pd and Pt electrodes using the thermodynamic guidelines of Bard's model.

In this work, we have tried to emulate the bimetallic nano-scale effects observed for ORR, in our polyoxometalate mediated electrocatalytic process. The scientific premise happens to be in the following line: A transition metal substituted polyoxometalate (a well characterized molecular entity), acts as an electron mediator between the working electrode (for e.g. Au or Pt) and the substrate to be reduced, i.e., dissolved oxygen. In the interface between the polyoxometalate solution and the working electrode, there is a localized environment, which is very similar to the bimetallic scheme as observed in the nanoparticles. Thus the electrocatalytic properties of the substituted transition metal is coupled with the electrocatalytic property of the substrate metal (working electrode), to accomplish the synergistic electrocatalysis observed in bimetallic alloys and nanoparticles.

A systematic evaluation of the performance of different transition metal substituted polyoxometalates (TMSP) has been performed and an attempt has been made to correlate the overpotential of oxygen reduction reaction (ORR) to the thermodynamic free energy of metal oxygen bond formation. Beginning with the sandwich type

polyoxometalates in near neutral conditions (pH=5, owing to their stability considerations), we have employed the same thermodynamic considerations to further evaluate the performance of mono-transition metal substituted Wells-Dawson structures in acidic conditions (pH=1, 0.1M HClO₄). This exercise has been performed to validate our claims of achieving bimetallic catalysis using polyoxometalate species in polymer electrolyte membrane fuel cells (PEMFC) conditions.

6.2. Materials and Methods

6.2.1. Synthesis of Wells-Dawson type polyoxometalates

Sodium phosphotungstate hydrate, sodium tungstate and phosphoric acid were used as received from Sigma-Aldrich. P₂W₁₈O₆₂⁶⁻ and the corresponding α_2 -monolacunary derivative were prepared using Conant's syntheses.^{15,16} Co-, Fe-, and Ru-substituted Wells-Dawson compounds were prepared according to established literature procedures.¹⁷⁻¹⁹ PCoW₁₁O₃₉⁵⁻ was synthesized from sodium phosphotungstate following the procedure published by Weakley, et al.²⁰ Electrochemical measurements were carried out in a home built three-electrode glass cell with a Pt counter electrode and an Ag|AgCl(sat) reference electrode. The Ag|AgCl(3M NaCl) electrode was isolated from the working electrode using a salt bridge and was calibrated against a reversible hydrogen electrode (RHE); all potentials are referenced to the RHE. The electrochemical circuit was controlled using a BAS Epsilon electrochemical workstation. The supporting electrolyte was 0.10 M HClO₄ prepared using 18.2 M Ω deionized water. Oxygen reduction measurements were carried out in saturated O₂ solutions.

Equipment

Pt electrode is 1.6mm (BAS MF 2013). Au electrode is 1.6mm (BAS MF 2014), Pd electrode is 2.0mm (Alfa Aesar 99.95% metals basis), GC electrode is 3.0mm (BAS MF 2012).

6.3. Results and Discussion

6.3.1 Application of bimetal substituted sandwich type structures for oxygen reduction in pH=5 acetate buffer

From previous chapters, we have observed that the bimetal substituted sandwich type (two trivacant Keggin units connected by a central metal belt), are stable within a pH window of 4 to 8, hence an acetate buffer (pH=5) was chosen as the test electrolyte. Literature results have revealed that in the course of testing electrocatalysts for oxygen reduction, glassy carbon has been chosen as the working electrode of choice, since the base electrode does not have an inherent catalytic activity and has a large potential window to explore the properties of a transition metal catalyst. Oxygen reduction reaction at a pH 5 acetate buffer has been evaluated with the bimetallic substituted sandwich type polyoxometalates, with different transition metals in the central metal belt. The various transition metals are as follows: Ru(III), Ir, Fe, Co, Mn and Zn (Precursor).

Fig. 6.2 reveals the oxygen reduction characteristics for the different transition metal substituted species (TMSP). An analysis of the figure reveals that di-iridium substituted sandwich compound exhibits the most positive overpotential for oxygen reduction reaction (ORR). The positive shift of ORR, from the potential of the bare glassy carbon electrode corresponds to an enhanced electrocatalytic activity due to the presence of the

transition metal substituted POM. The general trend, in terms of ORR activity is as follows: $\text{Ir}_2\text{POM} > \text{Ru}_2\text{POM} > \text{Co}_2\text{POM} > \text{Fe}_2\text{POM} > \text{Zn}_2\text{POM} > \text{Pure GC} > \text{Mn}_2\text{POM}$.

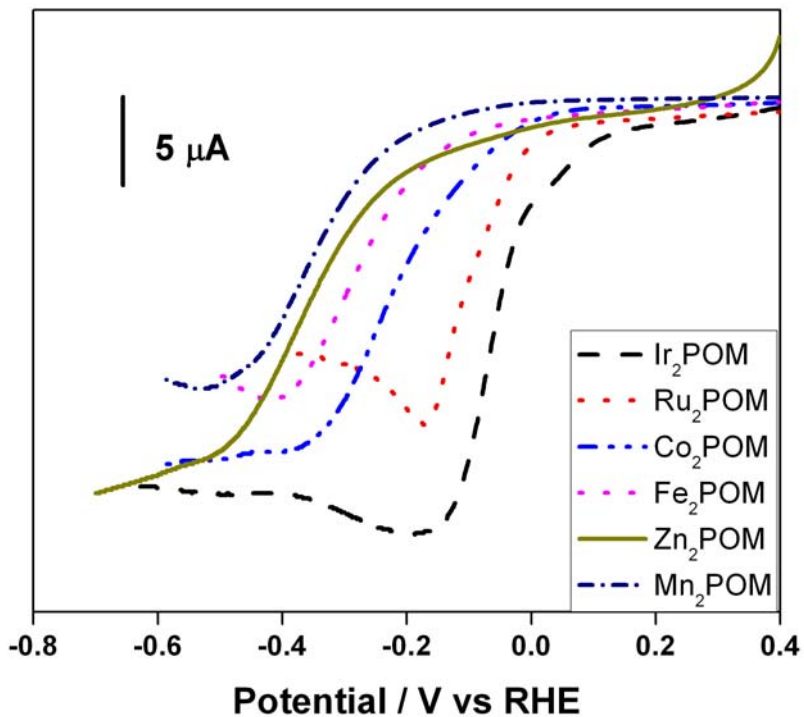


Fig.6. 2 Comparison of polarization curves for the oxygen reduction reaction (ORR) on several transition metal substituted sandwich type polyoxometalates at a glassy carbon electrode (3.0mm Diameter). Supporting electrolyte – pH = 5 acetate buffer, Pt mesh as counter electrode, Ag/AgCl as reference electrode. Scan rate – 10mV/s.

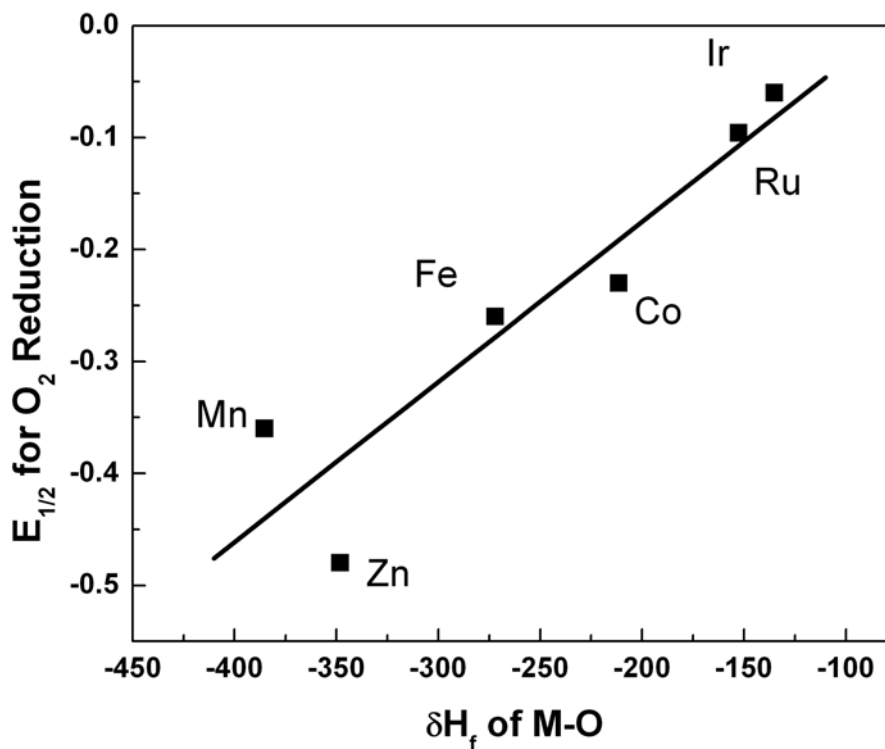


Fig.6. 3 Thermodynamic correlation between the free energy of M-O bond formation and the $E_{1/2}$ for ORR at the transition metal substituted sandwich POM solutions.

From Fig.6.3, we see that there exists a simple correlation between the position of the half wave potentials for oxygen reduction reaction and the enthalpy of metal oxide formation (eqn 6.1). The direct proportionality between the thermodynamic enthalpy of formation of metal oxide and the oxygen reduction wave reveals that the central metal atom plays an important role in this reaction. On the basis of these results, we have explored the opportunity of employing other transition metal substituted POMs in an acidic medium, which is more suited to fuel cell applications. POM structures such as Keggin and Wells-Dawson have been employed for our subsequent studies, because these compounds are more stable than sandwich type structures under the acidic conditions.

6.3.2 Application of mono-metal substituted Wells-Dawson polyoxometalates for oxygen reduction at acidic conditions

Oxygen reduction at glassy carbon electrodes were repeated with mono-substituted Dawson type structures with different transition metal substitution. The choice of electrolyte was 0.1M HClO₄ and a systematic trend seen in the sandwich type structures of the previous study has been observed in this study also. Further studies were performed on noble metal electrodes to elucidate the bimetallic effects

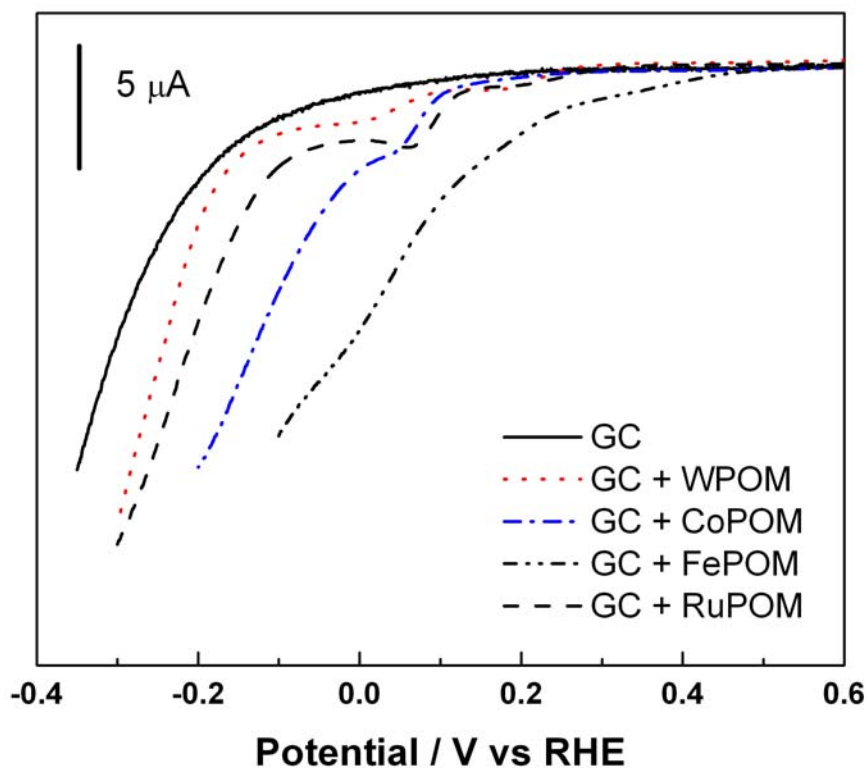


Fig.6. 4 Comparison of polarization curves for ORR at different transition metal substituted Wells-Dawson POM solutions at GC (3.0mM Dia) electrode in 0.1M HClO₄

solution (pH=1). Pt mesh as counter electrode and Ag/AgCl as reference electrode.
(Reported in terms of RHE) Scanrate – 10mV/s.

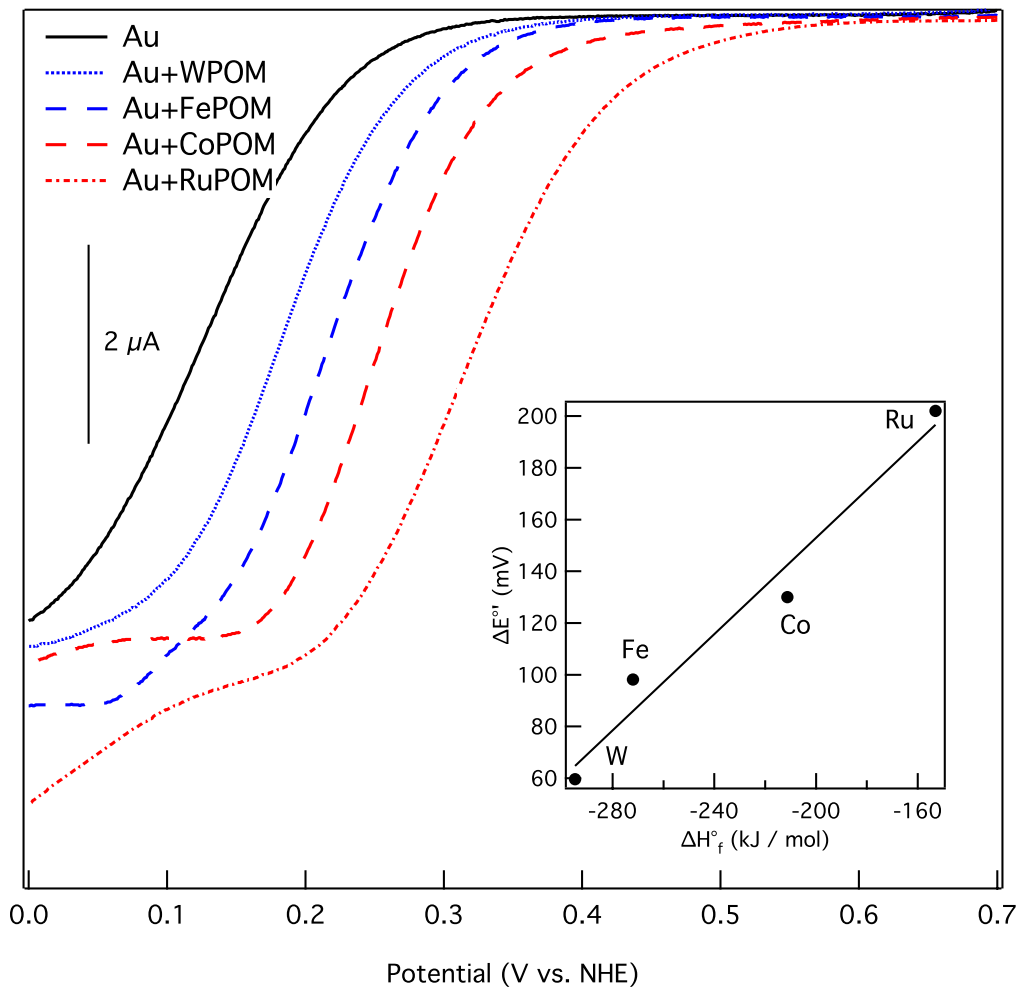


Fig.6. 5 Voltammetric scans at an Au electrode immersed in O₂ saturated 0.1 M HClO₄. POM concentrations were [WPOM] = [FePOM] = [RuPOM] = 0.2 mM and [CoPOM] = 0.2 μM. Scan rate: 10 mV/sec. Inset: Plot of maximum observed ORR potential shift, ΔE° vs. ΔH°_f of the corresponding bulk oxide.

Representative linear sweep voltammograms (scan rate, 10 mV/sec) showing the influence of a series of $P_2W_{17}M^nO_{62}^{(12-n)-}$ POMs on the electrochemical reduction of dioxygen at an Au electrode immersed in 0.10 M $HClO_4$ are presented in Fig.6.5. Au was chosen as the cathode for these measurements because it is not catalytically active for O_2 bond scission as evidenced by an unfavorable free energy change for reaction 6.1. To avoid visual clutter, only the reductive sweeps are shown. The solid black curve shows the ORR behavior of a clean Au electrode in the absence of added POM, and is consistent with previous research on this system. As indicated by the dashed curves, addition of POM to the supporting electrolyte leads to a significant and reproducible positive shift in the O_2 reduction potential ($\Delta E^{o'}$). The concentration of POM added to the supporting electrolyte was optimized separately for each compound to give the maximum shift of the ORR potential in each case. $\Delta E^{o'}$ increases in the order $W < Fe < Co < Ru$, which correlates extremely well with the heats of formation (ΔH_f°) of the corresponding bulk metal oxides (inset to Fig. 6.5).^{21,22} This behavior is in agreement with the predictions of the simple thermodynamic models discussed earlier, namely, that POMs with stronger M-O bonds exhibit a weaker influence on oxygen reduction at Au surfaces (i.e., a less positive shift of the potential) than POMs with weaker M-O bonds.

Next, we investigated the influence of the Wells-Dawson anions on the ORR at Pd, a more catalytically active electrode material. The voltammetric response of a Pd cathode immersed in the series of electrolytes described above is shown in Fig.6.6. Again, we optimized the concentration of each POM with respect to maximum $\Delta E^{o'}$. The behavior of the polycrystalline Pd electrode in the absence of added POM is shown as the

solid black curve for reference, and is consistent with previously published studies. When POM is added to the supporting electrolyte, ΔE° increases, but in a slightly different order ($W < Fe < Ru < Co$) than was seen with the Au electrode. In addition, the ORR potentials are observed to shift both to more positive (red curves) as well as to more negative values (blue curves) relative to pure Pd. The Co- and Ru-substituted Wells-Dawson anions improve the performance of the Pd cathode, while the Fe-substituted POM as well as the un-substituted Wells-Dawson anion (WPOM) shift the ORR potential to significantly more negative potentials (i.e., lead to an increase in the ORR overpotential). In the case of Pt cathodes, addition of W-, Fe- and Ru-containing POMs to the supporting electrolyte resulted in substantial negative potential shifts at all concentrations investigated (data not shown). Negative shifts of the O_2 reduction potential can be rationalized on the basis of site blocking effects that influence the kinetics of the ORR on Pd and Pt electrodes (e.g., by inhibiting the formation of the metal oxide). Similar observations have been reported recently in the case of phosphotungstate and phosphomolybdate anions adsorbed on Pt nanoparticles.¹³

If the negative potential shifts observed for Pd and Pt electrodes are indeed due to surface effects such as active site blocking, changing the concentration of the POM in the supporting electrolyte is expected to influence the magnitude of the shift by altering the adsorption dynamics/equilibrium. Concentration dependent measurements using the Co-substituted Wells-Dawson POM with a Pt cathode strongly support this hypothesis, Fig.6.7. This data set shows the effect of [CoPOM] on the ORR response of a Pt electrode immersed in 0.1 M $HClO_4$. The solid black curve shows the behavior of a naked Pt electrode in the absence of added POM. When the concentration of Co-POM is

increased from about 2 μM to 0.2 mM, the ORR curves shift to more negative values, as illustrated by the dashed blue traces. For POM concentrations below about 2 μM , the trend reverses, and $\Delta E^{\circ'}$ increases slightly as the POM concentration increases, as illustrated by the red curves. The maximum $\Delta E^{\circ'}$ occurs when $[\text{CoPOM}] = 0.2 \mu\text{M}$. Under these experimental conditions, the ORR potential is shifted 21 mV positive of that observed at a naked Pt electrode. A plot of the voltage shift as a function of concentration for the complete data set is shown in the inset to Fig.6.7.

Finally, in an effort to minimize active site blocking effects, we decided to investigate the behavior of Keggin ions as co-catalysts, since we have found them to be less strongly adsorbing on metal surfaces compared to the Wells-Dawson series. Representative voltammetric traces in the ORR potential region are shown in Fig.6.8 for a Pt electrode immersed in a series of POM containing electrolytes. Traces corresponding to unsubstituted $\text{PW}_{12}\text{O}_{40}^{3-}$ are shown in blue, while data corresponding to the Co-substituted Keggin ($\text{PCoW}_{11}\text{O}_{39}^{5-}$) are shown in red. The presence of $\text{PW}_{12}\text{O}_{40}^{3-}$ leads to a negative shift of the ORR potential for all concentrations studied. On the other hand, addition of $\text{PCoW}_{11}\text{O}_{39}^{5-}$ to the background electrolyte leads to substantial positive shifts in the potential. The fact that the optimized $\Delta E^{\circ'}$ value observed for $\text{PCoW}_{11}\text{O}_{39}^{5-}$ (20 μM) is significantly larger (+54 mV) than what was observed in the case of the analogous Wells-Dawson ion is consistent with our hypothesis that site blocking effects are less important for the more weakly adsorbed Keggin ions.

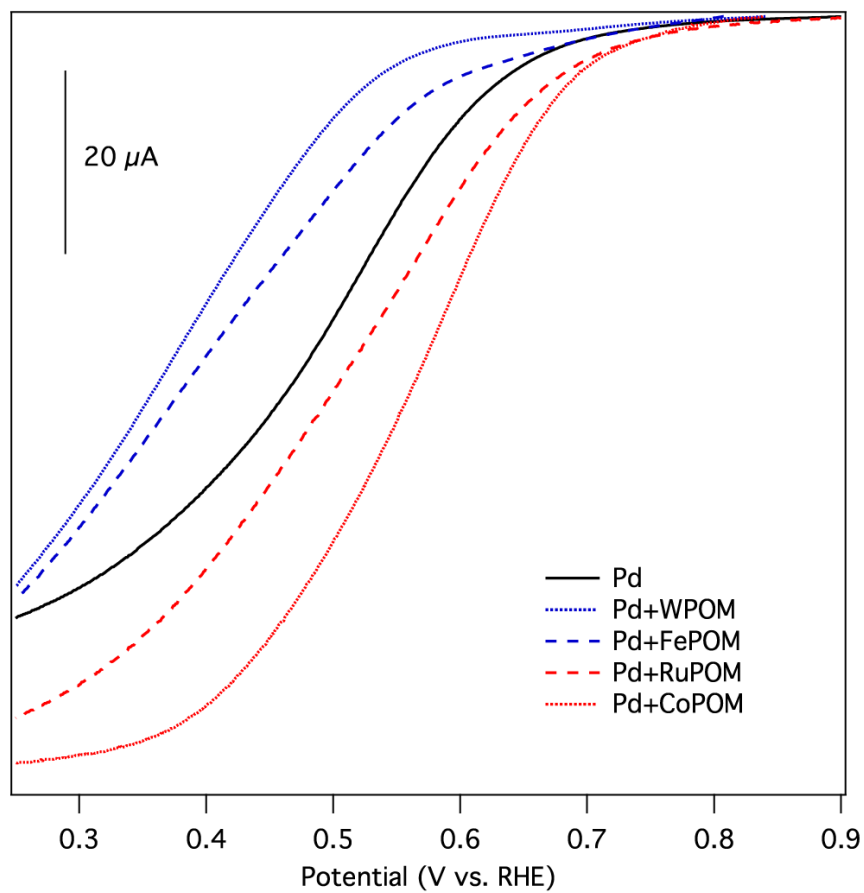


Fig. 6. 6 The voltammetric response of a Pd electrode immersed in O₂ saturated 0.1 M HClO₄. POM concentrations were [WPOM] = [FePOM] = [RuPOM] = 0.2 mM and [CoPOM] = 0.2 μM. Scan rate: 10 mV/sec.

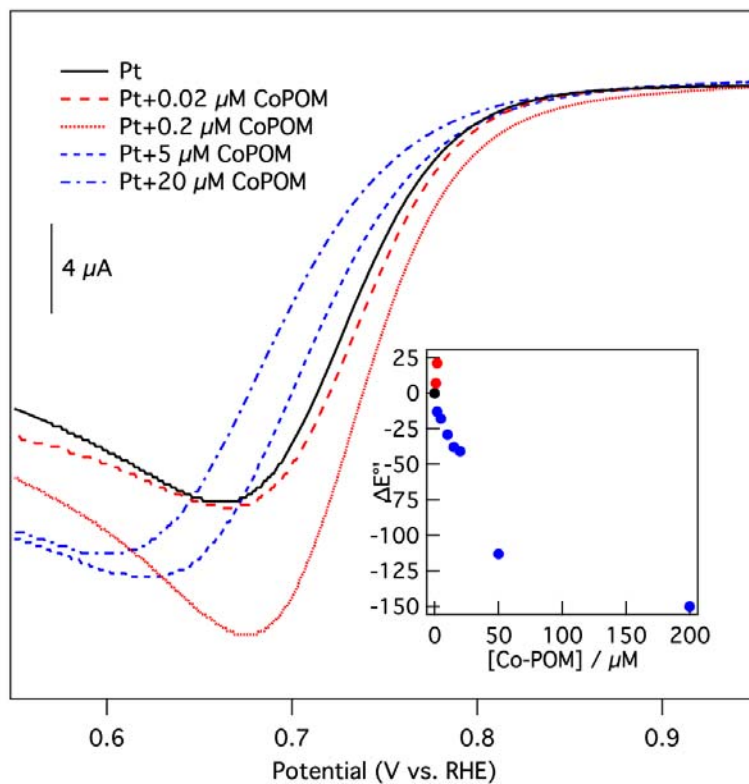


Fig.6. 7 The voltammetric response of a Pt electrode in O₂ saturated 0.1 M HClO₄ as a function of [CoPOM]. Scan rate: 10 mV/sec. Inset: plot of ΔE°' versus [CoPOM].

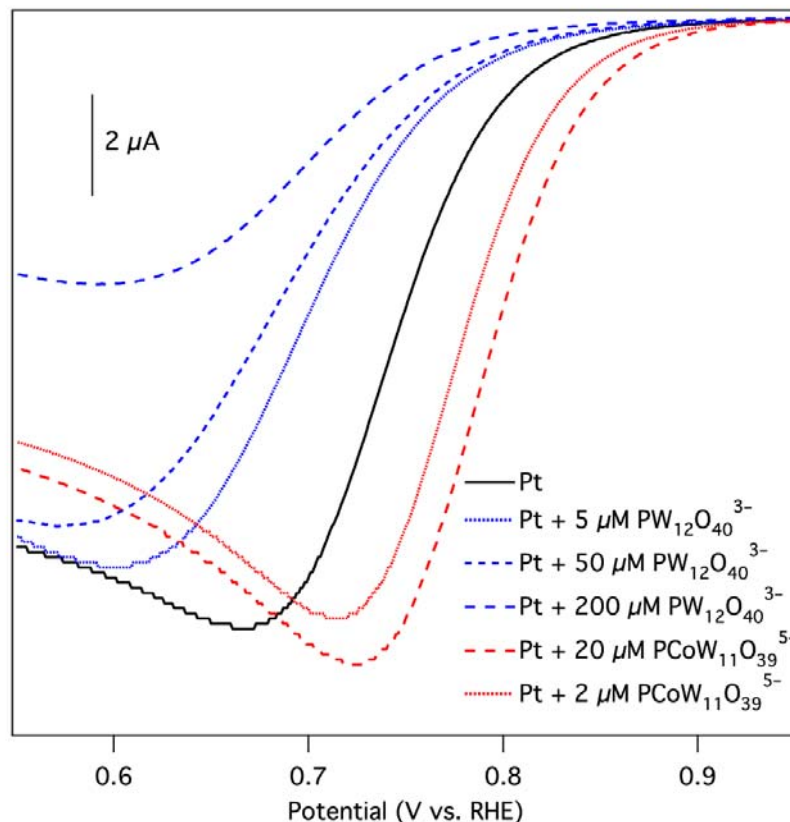


Fig. 6. 8 The voltammetric response of a Pt electrode in O₂ saturated 0.1 M HClO₄ containing the noted concentrations of PW₁₂O₄₀³⁻ and PCoW₁₁O₃₉⁵⁻. Scan rate: 10 mV/sec. Inset: plot of ΔE^{o'} versus [CoPOM].

In conclusion, transition metal substituted Wells-Dawson POMs adsorbed on the surface of Au electrodes lead to positive shifts of the ORR potential by a mechanism analogous to that which has been proposed for bimetallic ORR catalysts. The magnitude of the shift can be quite large (ca. 200 mV), is transition metal dependent, and can be explained using simple thermodynamic concepts. In the case of more active cathode materials such as Pd and Pt, our results indicate that surface effects become increasingly important: there is an optimum concentration of POM for which catalytic activity and site-blocking effects are in balance. In the case of Pd cathodes a maximum ΔE^{o'} of nearly

+100 mV was observed. The best overall cathode performance was achieved using $\text{PCoW}_{11}\text{O}_{39}^{5-}$ in conjunction with a Pt electrode (+54 mV positive shift compared to bare Pt), and this result is comparable to the performance of bimetallic catalysts.³ Finally, the approach to enhancing the performance of oxygen reduction cathodes that we have described is simple to implement and is compatible with existing fuel cell cathode materials.

References

1. Appleby, A. J.; Foulkes, F. R., *Fuel Cell Handbook*. Van Nostrand Reinhold: NY, 1989.
2. Jitianu, M.; Kleisinger, R.; Lopez, M.; Goia, D. V., *Journal of New Materials for Electrochemical Systems* **2007**, 10, (2), 67-74.
3. Mustain, W. E.; Kepler, K.; Prakash, J., *Electrochimica Acta* **2007**, 52, (5), 2102-2108.
4. Travitsky, N.; Ripenbein, T.; Golodnitsky, D.; Rosenberg, Y.; Burshtein, L.; Peled, E., *Journal of Power Sources* **2006**, 161, (2), 782-789.
5. Markovic, N. M.; Ross, P. N., *Surface Science Reports* **2002**, 45, (4-6), 121-229.
6. Fernandez, J. L.; White, J. M.; Sun, Y. M.; Tang, W. J.; Henkelman, G.; Bard, A. J., *Langmuir* **2006**, 22, (25), 10426-10431.
7. Walsh, D. A.; Fernandez, J. L.; Bard, A. J., *Journal of the Electrochemical Society* **2006**, 153, (6), E99-E103.
8. Fernandez, J. L.; Raghuveer, V.; Manthiram, A.; Bard, A. J., *Journal of the American Chemical Society* **2005**, 127, (38), 13100-13101.
9. Fernandez, J. L.; Walsh, D. A.; Bard, A. J., *Journal of the American Chemical Society* **2005**, 127, (1), 357-365.

10. Fernandez, J. L.; Bard, A. J., *Analytical Chemistry* **2003**, 75, (13), 2967-2974.
11. Liu, B.; Bard, A. J., *Journal of Physical Chemistry B* **2002**, 106, (49), 12801-12806.
12. Wang, Y. X.; Balbuena, P. B., *Journal of Physical Chemistry B* **2005**, 109, (40), 18902-18906.
13. Balbuena, P. B.; Altomare, D.; Vadlamani, N.; Bingi, S.; Agapito, L. A.; Seminario, J. M., *Journal of Physical Chemistry A* **2004**, 108, (30), 6378-6384.
14. Keita, B.; Mbomekalle, I. M.; Lu, Y. W.; Nadjo, L.; Berthet, P.; Anderson, T. M.; Hill, C. L., *European Journal of Inorganic Chemistry* **2004**, (17), 3462-3475.
15. Toth, J. E.; Melton, J. D.; Cabelli, D.; Bielski, B. H. J.; Anson, F. C., *Inorganic Chemistry* **1990**, 29, (10), 1952-1957.
16. Chojak, M.; Kolary-Zurowska, A.; Wlodarczyk, R.; Miecznikowski, K.; Karnicka, K.; Palys, B.; Marassi, R.; Kulesza, P. J., *Electrochimica Acta* **2007**, 52, (18), 5574-5581.
17. Wlodarczyk, R.; Kolary-Zurowska, A.; Marassi, R.; Chojak, M.; Kulesza, P. J., *Electrochimica Acta* **2007**, 52, (12), 3958-3964.
18. Limoges, B. R.; Stanis, R. J.; Turner, J. A.; Herring, A. M., *Electrochimica Acta* **2005**, 50, (5), 1169-1179.
19. Geletii, Y. V.; Gueletii, A.; Weinstock, I. A., *Journal of Molecular Catalysis a-Chemical* **2007**, 262, (1-2), 59-66.
20. Justi, E. W. W., E. A., *Kalte Verbrennung-fuel Cells*. Franz Steiner Verlag, Wiesbaden, : 1962; p 248.
21. Kuo, M. C.; Stanis, R. J.; Ferrell, J. R.; Turner, J. A.; Herring, A. M., *Electrochimica Acta* **2007**, 52, (5), 2051-2061.

22. Jennifer, L. M.; Sweikart, M. A.; Horan, J. L.; Turner, J. A.; Herring, A. M., *Journal of Power Sources* **2007**, 172, 83-88.

CHAPTER 7
ANTIBACTERIAL APPLICATIONS OF SANDWICH TYPE
POLYOXOMETALATES

7.1. Introduction

In the course of history, different kinds of epidemics have wreaked havoc on human lives and disease causing microorganisms have been the center of all these turmoil. In recent times, the development of potent antibiotics have been responsible for keeping these organisms at bay, but nature has been silently at work in evolving counter measures. Antibiotics resistant bacterial strains have been discovered in a number of infections and research has been targeted towards development of more effective and non-conventional antibacterial drugs. In this regard, polyoxometalates have been targeted as antibacterial agents against methicillin resistant *Staphylococcus aureus*¹, *Helicobacter pylori*² and several other bacteria. Yamase et al³ have shown that β -lactam resistant bacterial strains can be treated with different polyoxometalate species along with traditional antibiotics. The existence of synergistic effects between traditional antibiotics and polyoxometalates has been established by this group.

In this work, we propose to use our expertise in electrochemical characterization of polyoxometalates to correlate the redox properties of these unique molecules to their observed antibacterial activity. Two distinct types of polyoxometalates, a Keggin structure ($\text{PVW}_{11}\text{O}_{40}$) and a sandwich type $[\text{Na}_{12}\{\text{V}_2\text{Zn}_2(\text{ZnW}_9\text{O}_{34})_2\}]$, have been chosen

as therapeutic agents to be tested on two bacterial species *Listeria monocytogenes* and *Salmonella typhimurium*. These species were chosen because of high level of contamination associated with poultry products.

7.2. Antibacterial Properties of Polyoxometalates

The biological application of POMs were initially demonstrated in France³, when certain POM species [$\text{SiW}_{12}\text{O}_{40}^{4-}$, $\text{Na}(\text{SbW}_7\text{O}_{24})_3(\text{Sb}_3\text{O}_7)_2^{18-}$ and $(\text{AsW}_9\text{O}_{33})_4(\text{WO}_2)_4^{28-}$] were tested for their activity against non-retro RNA and DNA viruses, together with the study of inhibition of Friend leukemia virus using $\text{SiW}_{12}\text{O}_{40}^{4-}$ and other POMs. According to Hill, the antiviral and anti-tumoral activities of POMs have been extensively studied in the pharmaceutical industry, while the third area of antibacterial application is slowly gaining importance. The antibacterial properties of polyoxometalates were serendipitously discovered in the laboratory of Tajima et al⁴ in 1993. Initially the species responsible for enhancing the efficiency of β -lactum antibiotics on methicillin-resistant *Staphylococcus aureus* (MRSA) was thought to be a “Factor T”, which was subsequently found to be the lacunary Keggin species, $\text{PW}_{11}\text{O}_{39}^{7-}$. These Keggin species are known to increase the potency of β -lactum antibiotics on resistant bacterial strains by mainly suppressing penicillinase production and reducing the formation of penicillin-binding protein-2'. It was also shown to cause a metachromatic reaction and to prolong the blood coagulation time, thus providing some evidence of heparin-like polyanion behavior. The same study proposed that since these compounds become inefficient in the presence of polycationic species, an electrostatic charge interaction plays a major role in the antibacterial enhancement process. Based on these observations, several research groups have started evaluations focusing on the redox-active nature of the polyoxometalates to

be part of the driving force in drug-like activities. There are studies showing that these polyoxometalates can non-specifically inhibit several anion-sensitive enzymes – most nucleotide interacting enzymes, but not serum enzymes⁴.

Yamase et al^{1, 3-6} have studied the anti-bacterial activity of antibiotics such as oxacillin or penicillin (β -lactam compounds) in synergy with a variety of polyoxometalates from Keggin, lacunary Keggin, Wells-Dawson, to double Keggin (Sandwich compound)⁶. They have shown that both Gram-positive & Gram-negative bacteria are affected by these compounds. Specifically, they have addressed the enhancement effect of POMs on methicillin resistant *Staphylococcus aureus* (MRSA) and vancomycin resistant *Staphylococcus aureus* (VRSA), which are Gram-positive bacteria. β -lactum resistance in MRSA has been associated with the production of an additional peptidoglycan-synthetic enzyme called the penicillin-binding protein 2' (as mentioned above). This protein is responsible for resistance against β -lactam antibiotics, by forming a protective peptidoglycan layer on the cell wall. Systematic studies using gel-electrophoresis have revealed that polyoxotungstates suppressed the formation of this protein which is essential for cell wall generation during the MRSA growth process. The polyoxotungstates are also shown to reduce the production of penicillinase or β -lactamase, the enzyme produced in the membrane which hydrolyzes β -lactam antibiotics and makes them ineffective. Further studies by the same group have revealed the localization of polytungstate ($P_2W_{18}O_{62}^{6-}$) species at the cell wall of VRSA. (Using TEM images and energy dispersive X-ray analysis)

A particularly interesting phenomenon of biological reduction of polytungstates ($P_2W_{18}O_{62}^{6-}$, $E_{1/2} = +0.058V$ & $SiMo_{12}O_{40}^{4-}$, $E_{1/2} = +0.237V$) has been observed in

MRSA and VRSA cell cultures and this has been claimed as evidence for penetration of POMs through the cell wall to reach the cytoplasmic membrane. Structural integrity of the polyoxotungstates has been shown to be important for enhancement and hence species stable in near neutral physiological conditions are ideal drug candidates.

Other than enhancement of antibiotic activity, there are several instances where the POM species have shown anti-bacterial activity on their own accord. Highly negatively charged polytungstates such as Keggin ($\text{SiVW}_{11}\text{O}_{40}^{5-}$) and other sandwich-type species [$(\text{AsW}_9\text{O}_{33})_4(\text{WO}_2)_4^{28-}$] have been employed against *Helicobacter pylori*⁷ (Gram-negative bacteria)

The redox property of medicinal drugs has been a field of exploration for a long time now. Polyoxometalates with sandwich type structures have good stability in neutral conditions, which is close to the physiological condition and hence these were chosen for our studies in antimicrobial drug development.

7.3. Toxicity

Transition metal based complexes have been employed as therapeutic agents for a long time. For any compound to be successfully tested for clinical trials, toxicity studies play a major role in determining relevance and application. In polyoxometalates, there is evidence for polyoxotungstates to bind with proteins, alkaloids etc and alter their functions and properties. Despite being purely inorganic in nature, tungsten compounds in polyoxometalates are known to have unique biological effects. One study in particular has addressed the effect of lacunary Keggin compounds, phosphotungstate ($\text{PW}_{11}\text{O}_{39}^{7-}$) and silicotungstate ($\text{SiW}_{11}\text{O}_{39}^{8-}$) on stress promoters in *Escherichia coli*⁵. It has been shown that the phosphotungstate produces an osmotic signal at lower concentrations

without increasing ionic strength by inducing the stress promoter gene, *osmY* (which is sensitive to osmotic signals). Silicotungstate was shown to induce gene *clpB*, which is an analog to human heat shock protein.

In terms of practical applications in medicine, Tajima et al⁸ have studied the impact of direct administration of polyoxometalate solutions to animals. Lacunary Silicotungstate ($\text{SiW}_{11}\text{O}_{39}^{8-}$) species were injected into the veins of animals and severe cases of pulmonary embolism have been observed, and this has been attributed to platelet aggregation caused by these POMs. More studies are needed to understand the toxicity effects of POMs. In the case of anti-tumoral activity, these POMs are known to selectively accumulate and attack the diseased cells with very minimal effect on healthy animal cells.

7.4. Materials and Methods

7.4.1. Bacteria

Staphylococcus aureus (ATCC SA), *Salmonella typhimurium* (ATCC 13311 ST) and *Listeria monocytogenes* (ATCC 19115 LM) were obtained from American Type Culture Collection (ATCC, Manassas, VA, USA). These strains were cultured in the respective selective agar culture medium at 35°C for 24 hrs. These agar plate cultures were stored in a refrigerator at 0°C and were employed as stock cultures for all the experiments.

7.4.2. Polyoxometalate and Reagents

Zn_2POM precursor was prepared as described in previous chapter. Vanadium substituted sandwich type POM was prepared by adding vanadyl sulfate solution to Zn_2POM precursor solution in the ratio of 3:1. On continuous stirring at a temperature of 90°C, a greenish brown solution was obtained, which on cooling produced a precipitate of the

same color. On further recrystallization with water and in the presence of a concentrated solution of potassium nitrate, needle like crystals were obtained. Vanadium substituted Keggin structure ($PVW_{11}O_{40}^{5-}$) was also prepared according to literature methods⁹, and was employed as the control species to compare the behavior of sandwich POMs. The bacteriostatic properties of the selected POMs were characterized by monitoring the cell growth in pH7 phosphate buffer media, before employing the generic growth media. All electrochemical experiments were performed in the same pH =7 buffer solution.

7.4.3. Antimicrobial Assay - Qualitative Method:

Spotting or Zone of Inhibition

An initial concentration (10^6 to 10^9 CFU/ml) of bacterial cells was spread on selective culture plate followed by addition of 10 μ L of polyoxometalate on the surface. After incubating for 24 hrs at respective temperatures (LM at 30°C, ST and SA at 37°C) the plates were analyzed for inhibition zones due to POMs bacteriostatic activity. A similar inhibition zone study was carried out using standard microdiscs saturated with POMs. Paper micro discs (Fisher) were saturated with a given concentration of autoclaved polyoxometalate solution and added on top of an agar plate, which were previously plated with bacterial strains. As previously, the plates were incubated at required temperature for about 24 hours and the zone of inhibition was analyzed for each POM species.

7.4.4. Antimicrobial Assay - Quantitative Method:

Time Killing Assay

The bacteriostatic effects of POMs were evaluated by mixing a known concentration of POM to starting bacterial culture. At different time intervals, a 100 μ l of

solution was withdrawn and plated on an agar plate and incubated at respective temperature for 24 hrs. Control experiments were performed from bacterial solution containing no POMs. Finally, number of colonies formed on the plate was counted to quantify the bacteriostatic effect of POMs.

Viability of bacterial cells has been determined by preparing a 10-fold serial dilution of bacterial species in phosphate buffered saline solution and then about 100 μ l aliquot was inoculated onto agar plates. Initially a known concentration of bacterial cells placed in PBS saline and then a known concentration of POM solution (drug) was added. The idea is to identify the nature of bacteriostatic activity and hence the broth is immediately diluted in a successive manner to about 10 orders of magnitude from the initial concentration and each diluted concentration is saved in an individual test-tube. The diluted broth is then plated onto agar culture medium and subjected to incubation for 24-48 hours, to count the colony forming units, as a function of dilution. The diluted broth solutions are themselves placed in an incubator and 100 μ l aliquots are removed as a function of time (every 2hrs) and then plated onto agar culture medium. This method of collecting samples as a function of time and dilution will provide the time killing assay or bacteriostatic curve for each population. The absence or the reduction in number of colonies in drug treated medium implies inhibition of bacterial growth.

7.4.5. Characterization of Redox Activity of Inhibitive Polyoxometalates

Cyclic voltammetry of L-cysteine oxidation was performed in the presence of the different polyoxometalates to provide a simple method to establish oxidation as a route to bacterial inhibition. All experiments were performed with glassy carbon as working electrode, Pt mesh as counter electrode and Ag/AgCl as reference electrode. The

electrolyte solution was a phosphate buffer solution (pH=7) and it was chosen to be consistent with the growth medium used in bacterial cultures.

7.5. Results and Discussion

7.5.1. Electrochemical Characterization

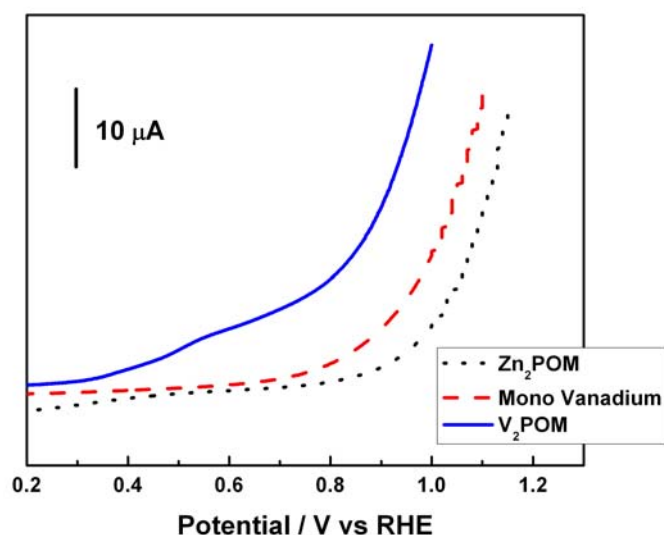


Fig.7. 1 Cyclic voltammetry comparison of L-cysteine oxidation at V keggin, Zn₂POM and V₂POM

The redox capabilities of the three compounds were tested using L-cysteine as the organic substrate. Sweeping the potential from 0 V to the positive direction reveals some interesting behavior in the different POM solutions. A concentration of 0.2 mM was chosen for all three model compounds, V Keggin (monovanadium), Zn₂POM precursor and V₂POM sandwich. L-cysteine oxidation occurs at very high oxidation potential in the glassy carbon electrode employed in the absence of electrocatalyst. In the presence of Zn₂POM, the oxidation peak begins at about 1.05 V. In the presence of V Keggin

structure, the origin of the oxidation peak occurs at 0.7V, which could correspond to some electrocatalysis by the vanadium metal substitution. In the presence of V₂POM, the cysteine oxidation begins more closer to zero, at 0.45 V. An analysis of the oxidation peaks establishes that the V₂POM sandwich exhibits better electrocatalytic property for cysteine oxidation. This electro-organic oxidation can be regarded as a simplistic indication of the potency of the polyoxometalate species with respect to the redox activity.

7.5.2. Qualitative Method

Staphylococcus aureus

Zone of inhibition using paper disc impregnated with POMs was chosen as an initial screening method to establish the bacteriostatic activities of synthesized POMs. Initially, vanadium substituted Keggin (PVW₁₁O₃₉⁵⁻) species was tested with *Staphylococcus aureus* to understand the bacteriostatic activity and compared with reported literature results. Under the given laboratory conditions we were able to repeat the results obtained by Yamase³ for V Keggin structure as shown in Fig.7.2. This experiment proved the validity of our paper microdisc method in achieving the qualitative analysis for the screening of polyoxometalates. Fig.7.2. also reveals the zone of inhibition observed in *Staphylococcus aureus* loaded agar plate, along with three different control samples. Citrate stabilized silver (Ag) nanoparticles were one of the control samples, since Ag has been shown to be bactericidal¹⁰⁻¹² in the nanoparticle regime. The V Keggin saturated microdisc exhibited the largest zone of inhibition compared to V sandwich and Ag nanoparticles. After carefully analyzing literatures^{13, 14}, a concentration of 0.2 mM was selected to test for bacteriostatic activities.

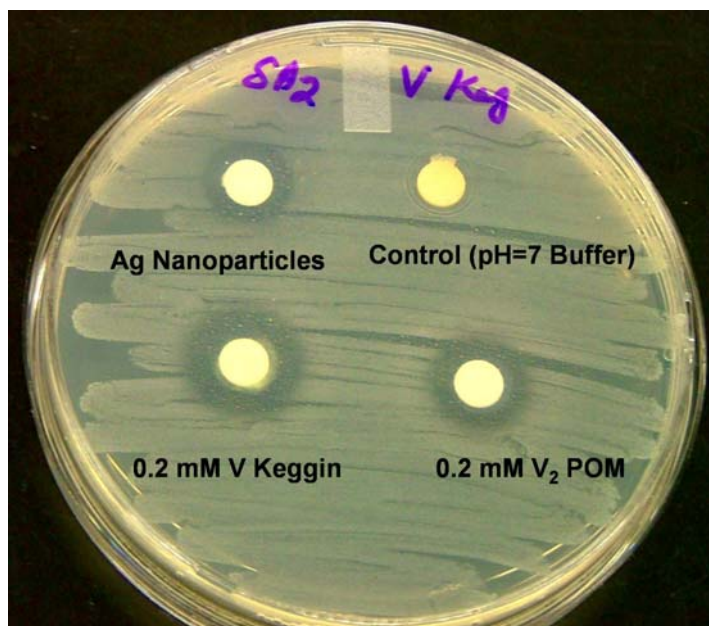


Fig.7.2 Microdisc method of qualitative analysis of bacteriostatic activity for *Staphylococcus aureus* strain in the presence of silver nanoparticles, V Keggin and V sandwich polyoxometalate.

The above testing was repeated with bacterial stains of interest, *Salmonella typhimurium* and *Listeria monocytogenes* using the paper disc method. In order to establish a minimum inhibitory concentration (MIC), the bacteriostatic activity of precursor compound Zn_2POM were tested under different concentrations with *Staphylococcus aureus* and the results were shown in Fig.7.3.



Fig.7. 3 Bacteriostatic activity of the precursor compound Zn₂POM, in an agar medium containing a 10⁵ to 10⁷ CFU/ml of *Staphylococcus aureus* (S.A)

The reasons for choosing the precursor Zn₂POM were two-fold, one to achieve a comparable baseline of bacteriostatic activity for the vanadium substituted sandwich and the other to test the effect of zinc in bacterial systems, as the zinc based compounds are reported to be benign at low concentrations under physiological conditions. The results from Fig.7.3 reveal that the minimum inhibitory concentration for Zn₂POM, is very high, in the range of 2mM to attain a comparable inhibition zone to vanadium Keggin structure in the previous studies shown in Fig.7.2.

Salmonella typhimurium

The Salmonella species have been contributing to increased amounts of morbidity and mortality throughout the world. Further the antibiotic resistant strains have started thriving in the developing countries.

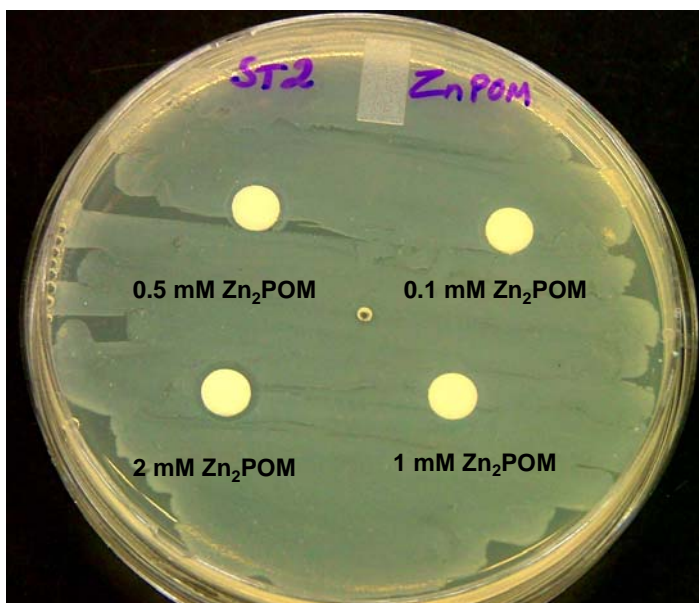


Fig. 7. 4 Microdisc method for the study of bacteriostatic effect of Zn_2POM on *Salmonella typhimurium* (S.T)

The effect of Zn_2POM saturated paper discs at different concentrations were studied as shown in Fig.7.4. Even at a very high concentration of 2 mM, a very small zone of inhibition is observed. The above figure reveals that Zn_2POM cannot be employed as a bactericidal agent in the case of S.T. This finding further reiterates the difference in the mechanism of bacterial cell growth between S.T and S.A.

S.T exhibited a typical growth pattern in the normal control solution as shown in Fig.7.5. In the presence of V sandwich, there was a significant zone of inhibition, when compared to the precursor molecule Zn_2POM . V Keggin on the other hand, did not exhibit very good inhibition, this could be attributed to the different nature of *Salmonella* when compared to *Staphylococcus* species and the presence of two vanadium atoms could be considered as detrimental to the former species. Based on this qualitative

microdisc method, the vanadium di-substituted sandwich compound can be chosen as a suitable candidate to carry out the other quantitative experiments.

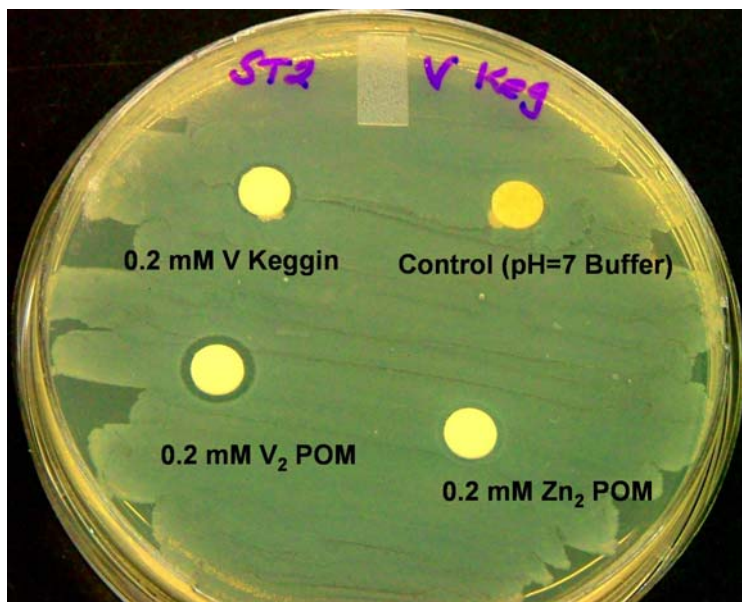


Fig.7. 5 Microdisc method to study the bacteriostatic effect of POMs on 10^5 to 10^7 CFU/ml *Salmonella typhimurium*

Listeria monocytogenes

Listeria monocytogenes is a Gram-positive bacterium, is a significant pathogen contaminating the poultry products. It is one of the primary candidates in causing severe meningitis in infants and has been known to inhabit the human gastrointestinal tracts. Microdisc method studies employing the different concentration of Zn_2POM against this pathogen (Fig.7.6) reveals that there is a significant zone of inhibition observed at both 1mM and 2mM concentration levels. This preliminary response to Zn_2POM could contribute towards more refinement of concentration dependence in the *Listeria monocytogenes* species, in the future.



Fig.7. 6 Microdisc method elucidating the bacteriostatic property of Zn₂POM under different concentrations

Finally, the susceptibility of *Listeria* to different POMs were performed and shown in fig.7.7. Similar to *Salmonella*, only V Keggins and V sandwich compounds exhibit bacteriostatic activity while little to no activity was observed with Zn₂POM.

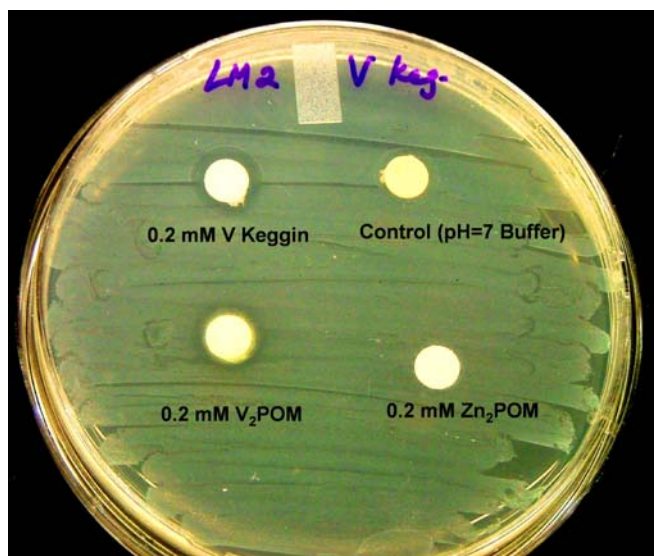


Fig.7. 7 Microdisc method to evaluate the bacteriostatic activity of Vanadium POMs and precursor in *Listeria monocytogenes* agar culture plate

7.5.3. Quantitative method –Time killing assay

The time killing assay in the presence of 0.2mM of polyoxometalate species has been used as the quantitative method of determining the efficacy of bacteriostatic activity. Typically, if an agent exhibits three-orders of log reduction in bacterial population then it is considered as bactericidal in comparison to being bacteriostatic where it would limit the bacterial growth.

Fig.7.8 and 7.9 outlines the susceptibility of *Listeria monocytogenes* and *Salmonella typhimurium* growth in the presence of the same concentration of V Keggin and V sandwich, respectively. Similar to zone-inhibition studies, V Keggin shows the bacteriostatic effect by preventing the growth of both bacteria even after 24 hrs. However, marked differences were observed between V Keggin and V sandwich as the latter compound reduces bacterial concentration by nearly 3 orders of magnitude, demonstrating bactericidal activity. As expected, time-killing assay unambiguously

distinguished bacteriostatic compounds from bactericidal ones which were not prominent in zone-inhibition studies.

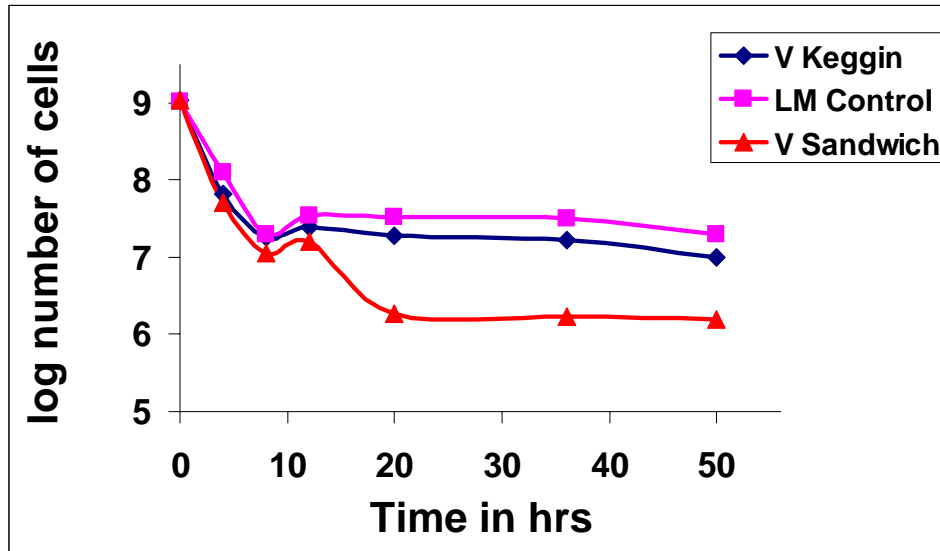


Fig.7.8. Time killing assay analysis of *Listeria monocytogenes* as a function of exposure to V Keggin and V sandwich POMs.

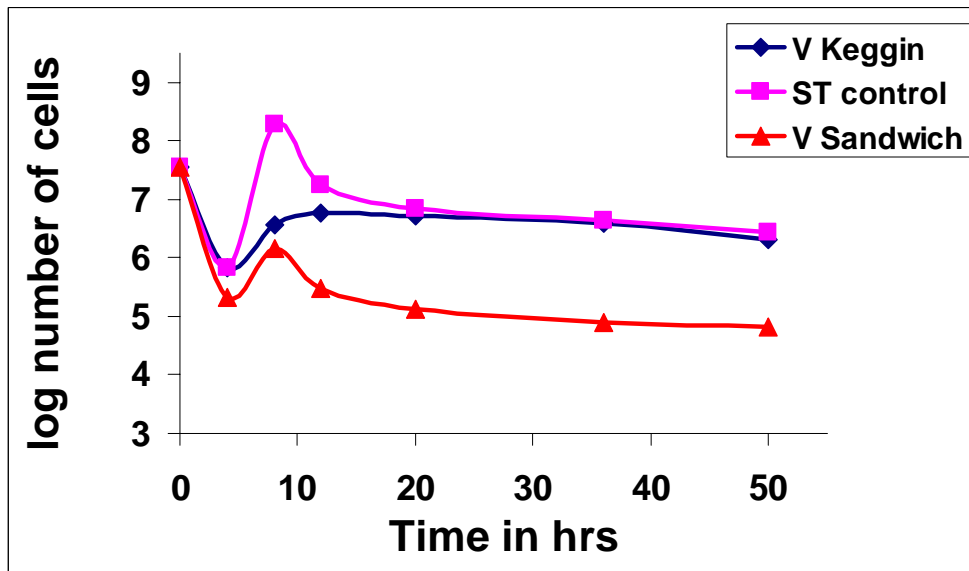


Fig.7.9. Time killing assay analysis of *Salmonella typhimurium* as a function of exposure to V Keggin and V sandwich POMs.

Reasons for Antimicrobial Activity of Polyoxometalates

In this exercise to establish the concept of antibacterial application of sandwich type polyoxometalate, a preliminary effort has been made to provide qualitative information regarding the feasibility of these POMs. From previous chapters, we have seen that the sandwich type polyoxometalates are very good electron transfer mediators and more particularly with respect to oxygen. When a redox active agent such as a POM is chosen as a drug candidate, there are several possibilities for attacking the cellular redox environment of a living cell¹⁵. These redox active sandwich type POMs could act as efficient agents to create reactive oxygen or nitrogen species (ROS, RNS). In addition, these POMs are known to accumulate in cell walls and lead to oxidative stress in the bacterial cell^{1, 3, 13} by producing reactive oxygen species such as superoxides, whose direct products such as H₂O₂, peroxy nitrates and OH· which can disrupt the metabolic pathways by interfering with the intermediates. The biological reduction of polyoxometalates has been observed in bacterial cell cultures and this can be an evidence for the electron transfer mediation of POM in the biochemical system. Despite the fact that detailed study on the mode of action of sandwich type POMs on ST and LM have not been performed, the previous studies have revealed that redox activity could contribute to creating oxidative stress in bacterial cells and could cause cell apoptosis or cell death^{2, 6, 7}. This qualitative investigation of antibacterial activity of sandwich type polyoxometalates can be employed as an effective launching pad for more elaborate mechanistic studies in the future.

References:

1. Yamase, T.; Fukuda, N.; Tajima, Y., *Biological & Pharmaceutical Bulletin* **1996**, 19, (3), 459-465.
2. Miyao, I.; Keiko, S.; Sae, M.; Nobuhiro, M.; Mayumi, O.; Toshihiro, Y., *Journal of inorganic biochemistry* **2005**, 99, (5), 1023-31
3. Yamase, T., *Journal of Materials Chemistry* **2005**, 15, (45), 4773-4782.
4. Y.Tajima; Z.Nagasawa; J.Tadano, *Microbiol. Immunol* **1993**, 37, 695.
5. Y.Tajima, *Journal of inorganic biochemistry* **2003**, 94, 155.
6. T.Yamase; N.Fukudo; Y.Tajima, *Biological & Pharmaceutical Bulletin* **1996**, 19, 459.
7. S.Ikeda; S.Nishiya; A.Yamamoto; T.Yamase; C.Nishimura; Clercq, E. D., *J. Med. Virol* **1993**, 41, 191.
8. Tajima, Y., *Biological & Pharmaceutical Bulletin* **2001**, 24, (9), 1079.
9. Keita, B.; Mbomekalle, I. M.; de Oliveira, P.; Ranjbari, A.; Justum, Y.; Nadjo, L.; Pompon, D., *Journal of Cluster Science* **2006**, 17, (2), 221-233.
10. Pohle, D.; Damm, C.; Neuhof, J.; Rosch, A.; Munstedt, H., *Polymers & Polymer Composites* **2007**, 15, (5), 357-363.
11. Shahverdi, A. R.; Fakhimi, A.; Shahverdi, H. R.; Minaian, S., *Nanomedicine-Nanotechnology Biology and Medicine* **2007**, 3, (2), 168-171.
12. Lee, H. Y.; Park, H. K.; Lee, Y. M.; Kim, K.; Park, S. B., *Chemical Communications* **2007**, (28), 2959-2961.
13. Inoue, M.; Suzuki, T.; Fujita, Y.; Oda, M.; Matsumoto, N.; Yamase, T., *Journal of Inorganic Biochemistry* **2006**, 100, (7), 1225-1233.
14. Kong, Y. M.; Peng, J.; Xue, B.; Pan, L. N.; Xin, Z. F.; Li, L.; Lu, J., *Chemical Journal*

of Chinese Universities-Chinese **2006**, 27, (5), 801-804.

15. Hillard, E. A.; Abreu, F. C. d.; Ferreira, D. C. M.; Jaouen, G.; Goulart, M. O. F.;

Amatore, C., *Chemical Communications* **2008**, (23), 2612-2628.

CHAPTER 8

CONCLUSIONS AND RECOMMENDATIONS FOR FUTURE WORK

The primary objective of this research work was to develop new electrocatalysts using the versatile polyoxometalate structures. We have been successful in synthesis and characterization of transition metal substituted POMs for different applications such as oxygen generation, oxygen reduction and electro-organic oxidation reactions.

In terms of water oxidation, a novel di-ruthenium substituted sandwich type polyoxometalate has been demonstrated to generate oxygen at potentials very close to thermodynamic limits. This is one of the first examples of inorganic ruthenium complexes to provide opportunities for more efficient catalytic systems than existing systems. During the course of electrocatalytic studies, an adsorption phenomenon has been observed for the sandwich type POMs, onto gold and glassy carbon electrodes. This adsorption under the influence of electrochemical potential cycling has been studied using electrochemical surface plasmon resonance. As a result of this study, an elegant method to complement the mass change studies using electrochemical quartz crystal microbalance studies has been proved for POM adsorption. The electrochemical potential stability window for the case of Ru₂POM and Zn₂POM has been obtained using this study. It has also been shown that sandwich type POM undergoes a higher rate of adsorption than Keggin species under the same conditions of concentration and potential window. Future studies are needed to understand the mechanism of oxygen generation

from these diruthenium POM structures and to elucidate the catalytically active species in these reactions. This can be accomplished by the employment of in-situ Raman during electrochemical studies of the interface. These studies could also reveal the nature of the adsorbed species on the electrode surface during electrochemical cycling.

Novel di-iridium substituted sandwich type POMs have been synthesized and characterized for the first time. These structures have been employed for both electrocatalytic oxidation and reduction reactions. The potential for employment of these structures as electrocatalysts for regenerative fuel cells and as sensing electrodes for biological species such as cysteine and ascorbic acid can be explored in the future.

In the direction of oxygen reduction, a simple thermodynamic model proposed for bimetallic electrocatalysis has been shown to exist for polyoxometalate co-catalysts in the presence of noble metal electrodes. A significant improvement was achieved for oxygen reduction potential at palladium electrodes (+100 mV) and platinum electrodes (+54 mV) and these values correspond to the values of the most efficient bimetallic electrocatalysts existing today. Future studies to elucidate the kinetics of electron transfer have been recommended to be performed using rotating disc electrode studies. Further studies should also focus on the immobilization of these homogeneous electrocatalysts onto electrode surfaces to achieve transition onto real-world applications.

Finally, the sandwich type POMs have been demonstrated to exhibit unique anti-bacterial applications on *Salmonella typhimurium* and *Listeria monocytogenes*. These preliminary studies could be extended onto other bacterial species and the nature of the bactericidal action also needs more exploration.